

ALTERATIONS OF THE CLIMATE OF A PRIMITIVE
EQUATIONS MODEL PRODUCED BY FILTERING APPROXIMATIONS
AND SUBSEQUENT TUNING AND STOCHASTIC FORCING

by

ROSS N. HOFFMAN

Sc.B., Brown University (1971)

M.A., Boston University (1975)

SUBMITTED IN PARTIAL FULFILLMENT OF THE
REQUIREMENTS FOR THE DEGREE OF
DOCTOR OF PHILOSOPHY

AT THE

MASSACHUSETTS INSTITUTE OF TECHNOLOGY

January, 1980

© Massachusetts Institute of Technology 1980

Signature of Author
Department of Meteorology, January, 1980

Certified by
Edward N. Lorenz, Thesis Supervisor

Accepted by
Peter H. Stone, Chairman, Departmental Committee on Graduate Students

WITHDRAWN
MASSACHUSETTS INSTITUTE
OF TECHNOLOGY
FEB 29 1980
MIT LIBRARIES
LIBRARIES

Contents

	<u>Page</u>
Preface.	6
1. Introduction	15
2. The model.	32
2a. Governing equations	32
2b. Energy equations.	39
3. Experiments.	46
3a. Numerical procedure	46
3b. Truncation and choice of constants.	48
3c. Initial conditions.	52
3d. Qualitative behavior.	55
4. Gravity waves, digital filtering and data sampling	66
5. Model statistics	69
5a. Description of the statistical methods.	72
5b. Invariance properties and the effect of persistence on the number of independent observations	77
5c. Reliability of the statistics	78
5d. Statistical intercomparisons.	81
6. Model tuning	116
6a. Tuning procedure.	116
6b. Tuning the QG model and results	121
7. Monte Carlo simulation	127
7a. Analysis of the short term prediction errors.	127
7b. Adjustment to conserve energy invariants.	133
7c. Perturbing the QG model and results	136
8. Summary and concluding remarks	141
References	147
Acknowledgements	152

<u>Figures</u>	<u>Page</u>
1. Typical maps of Ψ	58-61
2. Typical evolutions of energy variables	62-63
3. Energy budget of run PE3 decomposed into short and long time scales	105
4. Depiction of short term prediction error	122
5. Energy budget of PQG7.	139

<u>Tables</u>	
1. Wave vector numbering scheme	49
2. List of experiments.	54
3. Variable indexing schemes	70-71
4. Relative uncertainty in σ_x^2 and σ_x^2 / σ_y^2	75
5. Effect of sampling and filtering on model variable statistics.	82-86
6. Intercomparison of model variable statistics	87-94
7. Intercomparison of energy variable statistics.	95-100
8. Intercomparison of maintenance budgets	108-111
9. Tuning the QG model.	124
10. Regression analysis results.	131

ALTERATIONS OF THE CLIMATE OF A PRIMITIVE EQUATIONS MODEL
PRODUCED BY FILTERING APPROXIMATIONS AND
SUBSEQUENT TUNING AND STOCHASTIC FORCING

by

ROSS N. HOFFMAN

Submitted to the Department of Meteorology in January 1980 in partial fulfillment of the requirements for the Degree of Doctor of Philosophy.

ABSTRACT

The simulated climates of nonlinear models based on the primitive equations (PE), balance equations (BE) and quasigeostrophic (QG) equations are compared. The models and numerical procedures are identical in all possible respects. 50 and 26 independent functions of time alone represent respectively the solutions of the PE model and of the filtered models. The models are highly truncated spectral forms of Lorenz's (1960) energy preserving two layer model. It is assumed that the domain of integration is a doubly periodic f-plane, that static stability does not vary horizontally and that linear formulae govern vertical exchanges of heat and momentum. Because of the models' extreme simplicity very long time integrations (greater than 50 years in some cases) are easily effected.

Two levels of the thermal forcing are considered corresponding to radiatively enforced pole to equator temperature contrasts of 100K and 400K. At low forcing ($Ro \sim 0.11$) internal gravity waves in the PE solutions are present only as initial transient disturbances. At high forcing ($Ro \sim 0.33$) internal gravity waves are always present in the PE solution. In the time mean sense the gravity waves obtain their energy from the synoptic scale waves and are frictionally dissipated.

Transports are reasonably well simulated by the QG model at both forcing levels. At the low level of forcing the QG model and at the high level of forcing the BE model are successful at simulating the PE mean states and energy cycles. At high forcing the QG model gives only a qualitatively correct simulation of the PE mean state and energy cycle. The filtered equations always tend to underestimate the time mean gross static stability, energy flows and kinetic energy.

At the high level of forcing two attempts are made to get better simulations of the PE climate within the QG framework - the tuned and perturbed QG models. Both the tuning procedure and the perturbation procedure require some knowledge of the short term ($5f^{-1}$, f = Coriolis parameter) prediction errors caused by the QG assumption. The QG model is tuned to minimize the average squared short term prediction errors. The tuned QG model is better than the untuned version at simulating the PE time mean model state, but the simulated energy cycle and the budgets maintaining the mean state are not improved at all. In the perturbed QG model randomly generated perturbations are added to the model state every $5f^{-1}$. These perturbations are designed so that their statistics, other than those involving time lags, are similar to the statistics of the observed prediction errors. The perturbations are adjusted to conserve the energy invariants of the system thereby ensuring bounded solutions. The perturbed QG model is nearly as successful as the BE model at simulating the PE climate.

Thesis Supervisor: Prof. E.N. Lorenz

Title: Head, Department of Meteorology, M.I.T.

Preface.

The purpose of this preface is to provide background material for those unfamiliar with the concepts discussed here and to provide orientation for assessing the value of the reported results.

Meteorology is based on the belief that the atmosphere uniformly obeys certain basic physical laws. These laws together with some simplifying assumptions allow the deduction of mathematical equations which govern the time evolution of the atmosphere. If we know the exact equations, the exact composition of the atmosphere, the exact state of the boundaries of the atmosphere initially and for all future time and the exact current state of the atmosphere we would in principle be able to predict the evolution of the atmosphere for all future time. In fact our knowledge is and will always be far from exact - consider for example future readers of this page whose every breath must be involved in an exact formulation of the boundary conditions. As our knowledge is inexact our predictions will be inexact. It is expected that as we improve our knowledge (and our numerical skill) our predictions will improve.

It is known that the atmosphere is unstable in the sense that small differences in the initial states generally result in larger differences in the future states. That is to say any errors introduced by our approximations or inadequate observing procedures tend to grow with time. Eventually the true and forecast future states bear no resemblance to each other. Therefore there is a time beyond which our predictions are worthless. However we can still attempt to predict the future climate. We identify the climate with the long time period statistics of the atmosphere. An example of great interest of the various atmospheric

statistics making up the climate is the time averaged pole to equator temperature gradient. This temperature gradient is maintained by three processes - solar heating, infrared cooling to space and the transport of heat by the atmosphere and oceans. The differentially imposed heating drives the atmospheric motions. Besides affecting our comfort directly, the day to day weather transports heat poleward ensuring a relatively moderate pole to equator temperature gradient. If the transports were temporarily suppressed the radiative effects would soon strike a new balance with higher temperatures near the equator and cooler temperatures near the poles. Such a situation, while possible, would be unstable and atmospheric motions, which transport heat poleward, would soon develop.

Since the basic physical laws do not change it is a reasonable guess that the future and past statistics of the atmosphere are identical. This hypothesis will be good to the extent that the boundary conditions and composition of the atmosphere do not vary and to the extent that the climate is independent of the initial state of the atmosphere. Climate theory attempts to predict the atmospheric statistics given the boundary conditions and composition of the atmosphere. If we specify the boundary conditions and composition of the atmosphere and assume that the initial conditions are not relevant then the problem as posed is exact except for our inexact knowledge of the governing equations. Besides being of theoretical interest, the answers to climate questions have important consequences for human existence. How would the climate change if the sun's output decreased slightly? Would an ice age ensue? Would an increase of atmospheric dust be equivalent to a slight decrease in the sun's output? Does overgrazing by cattle induce changes in

Climate? Will the addition of carbon dioxide from burning coal or the addition of fluoro-carbons from spray cans noticeably alter our climate? These questions and others are under current study. Reliable answers to these questions will be necessary if society decides to maintain or improve the quality of the environment. Meteorological studies of the large scale circulation always suffer from an inability to perform real experiments. We are always forced to make do with models, which, no matter how complex, involve some degree of approximation. We must scrutinize our approximations to establish the reliability of our answers.

The advances of modern meteorology are due in large part to systematic approximations based on the introduction of a priori estimates of the scales of the motions of interest. In particular, the theory known as quasigeostrophic (QG) scaling has helped explain the processes controlling the large scale atmospheric motions which influence the day to day weather we experience. Basically it is assumed that the time scale of the motions of interest is long compared to the time scales of the other motions. Let C represent the magnitude of the typical velocities of interest. In a midlatitude storm system C is roughly 50 km/hr. Let L be a typical length. The radius of a midlatitude storm might be 1000 km. During a period of time T , a particle embedded in the flow would move roughly a distance equal to C times T . If we choose a time period equal to L/C the distance traveled will be roughly L . A particle in the center of our typical storm might travel to the edge of the storm in this length of time - approximately one day. This is the time scale of the motions of interest. A convenient measure of this time scale is the Rossby number. The Rossby number (denoted Ro) appears explicitly in the equations which govern all atmospheric motions

when these equations are put in a certain nondimensional form. (Nondimensional form is a standard form in which no references to units of measurement, such as meters, hours or degrees, are present.) The Rossby number is simply a constant (which depends on the latitude of interest) times the ratio of the time of the earth's rotation to the characteristic time scale. For our midlatitude storm the Rossby number is approximately one eighth. For motions which are characterized by faster speeds or shorter lengths the time scale is smaller and the Rossby number is larger. Two types of motions with small time scales present in the atmosphere are sound waves and gravity waves. (An example of gravity waves in a different setting is the ripples on the surface of a pond after a stone is tossed in.) By assuming at the start that the Rossby number is small the equations can be simplified. These simpler equations are called the filtered equations because they filter out the motions with small time scales. There are two commonly used sets of filtered equations, the QG equations and the balance equations (BE). The BE are more accurate and much more complicated mathematically than the QG equations. The original equations, called the primitive equations (PE), are themselves inexact because a number of assumptions must be made in deriving them from the physical laws. However for our purposes they may be considered exact.

The filtered equations have been the basis of many studies of the large scale atmospheric motions. For qualitative understanding of the day to day weather the acoustic and gravity waves are extraneous. The filtered equations isolate the relevant motions. By studying the QG equations we can understand the processes which control the motions and development of typical storm systems.

The filtered equations are also routinely used for predictive purposes. In numerical weather prediction (NWP) the future state of the atmosphere is extrapolated from the observed state of the atmosphere according to the governing equations. To properly describe the motions the extrapolation takes place by a time marching procedure where the time step is smaller than the time scale of the motions. Thus a smaller time step (and hence more computations) are required if the PE are used since short time scales may be present. If we use the PE it is also more difficult to initialize the time marching procedure because small errors in the observations can easily produce large gravity waves in the numerical solution which would not exist in the atmosphere. It was originally felt that the difficulties associated with the PE were insurmountable and the first successful NWP was based on simpler governing equations. While the U.S. National Meteorological Center routinely integrates the PE, the meteorological services of several other nations use various forms of the filtered equations to produce their primary product.

We know that assuming the filtering approximations are correct will introduce some errors over a prediction interval of a day or so but this is acceptable if there are other errors of similar or larger magnitude caused by the uncertainty of the observations and by computational limitations. Thus a NWP model may be labeled "good" if it introduces a negligible error over the short time scale. Such a model may be inappropriate for climate studies since these errors may accumulate and influence the model's statistics over the long time period needed to simulate the climate.

To solve climate problems a wide array of models have been used;

while many employ the QG assumption some of the more complex models are based on the PE. Because of the many differences between the various models and the atmosphere and between the models themselves it is difficult to assess the effects of the QG assumption alone. Will the errors introduced by the QG assumption over the short time scale tend to accumulate or cancel out when we collect statistics? This question is addressed in the present study. We construct models which are completely identical in all respects but one - whether or not one of the filtering assumptions is made. Therefore any differences observed between the behaviors of the models are due to the filtering assumptions. The models are integrated numerically and statistics are collected. For the sake of economy many simplifications are incorporated in the models. This is acceptable since in any comparisons made, both models include the same simplifications. For a low level of the thermal forcing (i.e., the solar heating) the climates simulated by the QG and PE models are nearly identical. At a higher level of the thermal forcing the different models generate quite different climates; that is, the short term errors tend to accumulate. For example, compared to the results of the PE model, the time averaged pole to equator temperature gradient of the QG model is 23% too low, while that of the BE model is 5% too low. However qualitatively the three simulated climates are very similar. Thus the appropriateness of the filtering assumptions for climate studies depends on the values of the external parameters. Generally the filtered equations are suitable for making qualitative climate predictions. The PE should be used whenever a quantitative result is required or when the qualitative results of a filtered equations experiment are not decisive.

It is conceivable that making slight changes to the QG model would improve its ability to simulate the PE model's climate. Most models of the atmosphere contain some adjustable parameters which owe their origin to the parameterization of subgrid scale processes or of physical processes not explicitly represented in the model. Tuning is the process of choosing values for these adjustable parameters. An example of an adjustable parameter is the drag coefficient C_D which appears in the equation for horizontal stress τ_0 in the skin friction formula,

$$\tau_0 = \rho_0 C_D |\underline{u}_0| \underline{u}_0$$

where \underline{u}_0 and ρ_0 are the horizontal velocity and the density at some reference level. This formula is useful for representing the frictional drag of the earth's surface on the atmosphere. Actually the exchange of momentum between the surface and the atmosphere is mediated by molecular collisions so some simplification is necessary. It is possible to obtain values of C_D by measuring the other quantities in the above formula at a particular point and under particular conditions. Empirical values obtained in this manner vary considerably and it is not clear what the single best value is. Further, values valid at particular points are not necessarily appropriate for diagnostic or predictive finite grid calculations. As pointed out by Lorenz (1951) the effects of small hills are not explicitly present in any model but might be included in the calculations of τ_0 by choosing a slightly different value of C_D . In this study we consider whether or not tuning the parameters which appear in the QG model would improve its simulation of the PE climate at the high level of the thermal forcing. In some

respects tuning the QG model leads to an improved simulation. The time averaged pole to equator temperature gradient of the tuned QG model is found to be 7% higher than the PE value. Compared to the error of the original QG model the sign of the error is reversed and the magnitude of the error is considerably less.

Within the framework of a simplified model the short term errors caused by the simplifying assumptions are fundamentally unknowable. However by examining the assumptions it may be possible to estimate the magnitude of the errors. Suppose the statistics of the short term errors are known. Can this knowledge be used to improve the model? Along similar lines, several techniques have been suggested for making use of the statistics of the errors in the initial conditions for predictive purposes. The most straightforward of these, Monte Carlo prediction, is applicable to climate problems. In Monte Carlo prediction the observations are assumed to be known to a certain accuracy and an ensemble (i.e., a collection) of equally possible initial states are chosen. From each of these initial states a prediction is made. The average of the ensemble of final states is generally a better forecast than a prediction made from just one initial state. Furthermore the variability within the ensemble of final states gives an indication of the reliability of the forecast. Part of this procedure was (and possibly is now) actually in operation at the New Zealand Meteorological Office (Trenberth and Neale, 1977). Three alternate forecasts were provided each based on a different analysis of the available data. (In this case, the initial state is only poorly known since New Zealand is surrounded by water and weather ships are expensive to operate.) The difficulty here is that three times as many computations are needed to produce the three forecasts

as are needed for a single forecast. Actually one would prefer an ensemble with more than three members. No extra computation is needed in Monte Carlo climate simulations because we can assume that the climate of each ensemble member is the same. In applying the method we add a small perturbation to the current state of the model after each short term time interval. These perturbations are random but have statistics similar to those of the short term errors. This method was tested on the QG model at the high level of the thermal forcing. The resulting climate agrees much better with that of the PE model. The pole to equator temperature gradient is still in error - the sign of the error is reversed as in the case of the tuned model and the magnitude of the error is now 9%. However nearly perfect knowledge of the short term error statistics did not in this case lead to perfect agreement between the climates. It must be added that the QG statistics are constrained in a way that the PE statistics are not. Therefore perfect agreement is impossible unless the PE statistics satisfy these constraints.

The result that the perturbed QG model out performs the QG model is important because it runs counter to intuition. Offhand one would not expect that a model's response would be improved by adding a random forcing. This technique suffers from one serious drawback - one must know the short term error statistics. Error statistics obtained from comparisons with observations would only be valid under current climate conditions. This problem is left unanswered by the present study, but in cases where the error statistics are known this knowledge should be used.

1. Introduction.

When studying the climate one is faced with the problem of describing the statistics of a system whose time evolution is essentially nonlinear and which is extremely sensitive to initial conditions. A popular plan of attack is to develop a numerical model, integrate it in time and collect statistics. At each time step the current state of the model, which depends on the past history of the model, may be considered the initial conditions for the remainder of the model run. Thus any assumptions introduced in deriving the model may be thought of as introducing errors into the initial conditions. As these errors compound their total effect may be large, although individual errors are small. It has been envisioned (Lorenz, 1970) that eventually super models may provide a solid basis for climate research. However any numerical model must involve some approximation and thus introduce some errors. Although the errors introduced by a particular assumption are unknowable within the context of the model some knowledge of the statistics of the errors may be obtained by comparing short term predictions of the model to either a more complex model or the atmosphere itself. It seems likely to the writer that such information, properly used, would improve the fidelity of the model's simulation of the climate.

Beginning with Phillips (1956) increasingly complex numerical models have been developed for modeling the atmosphere over long time scales. Over time the models have become better at simulating the atmosphere. However important differences exist between the observed climate and the model climates. Even the most complex of the current models involve many assumptions, so it is difficult to determine which assumptions should be relaxed. One method of evaluating a particular assumption is

to compare the model output to that of another model identical in all respects except that the assumption in question is relaxed. This approach is exemplified by the work of Manabe and coworkers at GFDL (Manabe et. al., 1970; Manabe and Terpstra, 1974; Manabe and Wetherald, 1975; Wetherald and Manabe, 1975). Of course the effects of several assumptions are not necessarily additive so the appropriateness of any particular assumption depends upon the "environment" in which it is employed.

In this report we compare the simulated climates of nonlinear models based on the primitive equations (PE), balance equations (BE) and quasigeostrophic (QG) equations. The models and numerical procedures are identical in all possible respects. 50 and 26 independent functions of time alone represent respectively the solutions of the PE model and of the filtered (i.e., QG and BE) models. The models are highly truncated spectral forms of Lorenz's (1960) energy preserving two layer model. We assume that the domain of integration is a doubly periodic f-plane, that static stability does not vary horizontally and that linear formulae govern vertical exchanges of heat and momentum. Because of the models' extreme simplicity very long time integrations (greater than 50 years in some cases) are easily effected. Thus even small differences between the model climates may be determined with high statistical significance. Further, we investigate two means of making use of the information contained in the (presumed) known short term prediction error statistics. The first technique is to tune the adjustable parameters which appear in the model. The second technique is to add perturbations to the model state at regular intervals; these perturbations have carefully designed statistical properties. (Reader beware! In this paper, excluding the portions reviewing previous studies, "perturbation" should connote

neither linearization nor infinitesimally small.)

The results of these experiments may be viewed from two perspectives. First, we may consider the PE model to be the "real" system we wish to simulate. In this light the results are quantitatively correct and differences in (model) climates are due solely to the filtering assumptions. Second, we may extrapolate our results to more complex models of the atmosphere. This is risky; the extrapolated results should be used only as suggestions of the qualitative nature of the errors caused by the filtering assumptions in more complex systems.

Although most suitable for short prediction intervals the QG assumption has proved extremely useful not only in numerical weather prediction and linear stability studies but also in diagnostic and simulation studies and in simple climate models. Surprisingly, until now no direct comparison of the climates of identical PE and QG models has been made. When a model is "improved" and the QG assumption is dropped it is generally easier to reformulate the model from scratch. Then there is a tendency to go "whole hog", relaxing several other assumptions simultaneously. The BE have seen limited use in numerical weather prediction. The long term behavior of BE models has been unknown because the BE are more difficult to integrate than the PE.

Quasigeostrophic theory has by now a long history and many authors have commented on the conditions necessary for its validity. Previous studies of the baroclinic instability problem reveal the effects of the geostrophic assumption on the growth rates and structures of exponentially growing infinitesimal Rossby waves. Of the several studies noted here only one (Simmons and Hoskins, 1976) contains a direct comparison of a PE model and a QG model linearized about the same basic states. A point

to keep in mind when comparing models differing in more than one respect is that it is difficult to assign portions of the error to the different assumptions. It is possible that several assumptions, each of which individually causes a significant error, may together cause only a small total error; the opposite situation of several assumptions each causing small errors which together cause an appreciable total error is also possible. As the principal interest here is in a comparison of nonlinear systems we consider several topics which bear on the applicability of the results of linear theory under nonlinear conditions. Following this, we will review some nonlinear results.

Before reviewing the literature we define two terms. One approach to determine the adequacy of the QG assumption is to study data from actual observations or from a model which does not depend on the QG assumption. Differences from geostrophic balance in the data may then be attributed to effects not included in QG models. These differences may be termed ageostrophic. A second approach, the approach used here, is to compare two models, one of which employs the QG assumption. The total difference between the results of the two models may be partly in geostrophic balance. This total difference has been termed non-quasigeostrophic (Gall, 1977). The first approach provides only a lower bound for the magnitudes of the errors caused by the QG assumption.

The baroclinic instability problem may be stated in brief, as follows. The radiatively enforced or the observed zonally averaged pole to equator temperature gradient might be geostrophically balanced by a zonal thermal wind if the earth's surface were homogeneous and if frictional effects were absent. However, if the temperature gradient exceeds

a critical value such a basic state is baroclinically unstable; that is, small disturbances will grow by releasing some of the available potential energy of the basic state. Those instabilities with the fastest growth rates are seen to correspond in certain respects to the observed disturbances. Although the observed atmospheric disturbances are far from infinitesimal in amplitude, the observed mid-latitude atmospheric structure is basically zonal with superposed perturbations. It is argued that this zonally averaged state is always spawning growing baroclinic disturbances whose growth is ultimately checked by dissipative processes or nonlinearities. As they extract energy from the mean flow these disturbances tend to decrease the pole to equator temperature gradient. This suggests the average state of the atmosphere should be close to neutral stability with respect to these disturbances. The evidence (Stone, 1978) in the extratropical regions supports this contention. For this reason and for analytic convenience many studies have focused on the neutral or nearly neutral case.

To the extent that other processes simply limit their amplitudes the calculated instabilities with the greatest growth rates are valid for parameterizing eddy fluxes for use in simple climate models. For this purpose it is still necessary to determine the amplitudes at which growth stops. Besides this closure problem there are two facts which make it difficult to directly apply the results of baroclinic instability theory. First, the structure of the linear waves and their growth rate spectrum - in particular the wavelength of maximum instability - depend very strongly on the presumed basic state and on the numerical model.

Not constrained by the feedbacks present in a nonlinear system the linear results are very sensitive to modeling assumptions. Second, and partly as a consequence of the previous point, as the waves reach finite amplitude interactions with the mean flow profoundly affect both growth rates and structure. Therefore the concept of the "evolutionary" selection of structures having the greatest linear growth rates must be abandoned or modified to include second order processes. Thus, if we wish to extrapolate comparisons of PE and QG linear instabilities to the nonlinear regime we must choose the "right" basic state and include second order processes in some way. Simmons and Hoskins (1978) observed that in some cases the dependence on the presumed basic state becomes less marked when the wave is allowed to grow to finite amplitude and interact with the mean flow. An analogous result might hold for the dependence on the governing equations. That is, it is possible that finite amplitude perturbations of PE and QG models allowing wave mean flow interactions are more alike in structure than the instabilities of the corresponding strictly linear models.

The earliest studies of baroclinic instability employed the geostrophic approximation. (A succinct review is given by Phillips (1963, Section 3a). A brief historical summary of the problem when geostrophy is assumed and when the zonal wind profile of the basic state is simple, is given by Geisler and Garcia in the introduction to their 1977 paper.) In fact the earliest formal quasigeostrophic scaling argument was motivated by the baroclinic instability problem (Charney, 1947, 1948). More recently the study of this problem has evolved along two paths. One approach is to make enough simplifying assumptions, usually including that of quasigeostrophy, so that analytic

solutions are obtained which explicitly display the dependence of the instabilities on the mean state variables (Saltzman and Tang, 1975; Stone, 1972; and references in these papers). When these results are incorporated into simple climate models the fluxes due to the mean meridional circulation forced by the waves should also be included (Stone, 1972). Along the second path of investigation several of the various assumptions made in the earliest studies have been relaxed and the numerical calculations have increased in complexity. Derome and Dolph (1970) studied higher order effects on the disturbances and found slower growth rates and some differences in the structure of the disturbances. (According to Mak (1978) Derome and Dolph were not careful enough in their consideration of the boundary conditions - the problem they solved is ill-posed and their results are therefore questionable.) Hollingsworth (1975) investigated the differences between the normal modes of several variants of Lorenz's (1960) two layer model (the model used in the present study). On an f -plane channel Hollingsworth found the growth rate spectra of the short waves in the QG model are highly sensitive to whether or not the static stability is allowed to vary. Comparing the results of the QG and BE models with variable static stability he found similar growth rate spectra but indicated that substantial differences in structure exist. On a sphere differences between the two QG models are less pronounced. Warn's (1976) calculated instabilities of two shallow layers on a sphere are significantly ageostrophic. Simons and Hoskins (1976) compared the normal modes of the PE and QG equations on a sphere for three simple zonal flows. In their study the models are identical except for the geostrophic assumption. The modes of the two models are similar;

growth rates and relative amplitudes agree to $O(Ro)$. However agreement in terms second order in amplitude is poorer - when normalized to a constant value of maximum perturbation stream function the eddy meridional fluxes of heat and zonal momentum differ by as much as 25% and 50% respectively. Also the neglect of vertical transports in the QG model leads to poor agreement of the second order changes to the mean state. Gall (1977) calculated the normal modes of an f-plane channel with an idealized zonal flow symmetric about mid-channel. For this geometry and basic state the QG perturbation equations decouple into symmetric and antisymmetric components. Gall used symmetric initial conditions. Therefore any asymmetries which developed in the solutions of the linearized PE must be due to non-quasigeostrophic effects. (This procedure will not detect non-quasigeostrophic effects on the symmetric part of the perturbation.) Gall found that the perturbation fields and meridional heat transports are fairly symmetric but the meridional fluxes of geopotential and zonal momentum are noticeably antisymmetric. As noted by Gall, these results are not surprising as these latter fluxes are covariances of perturbation quantities which are roughly 90° out of phase.

Points relevant to the application of these comparisons to the nonlinear regime are made in several related studies of PE models by Simmons and Hoskins and by Gall and his coworkers. There is some controversy over the wavelength of maximum growth rate in the linear models. Gall (1976a, 1976b, 1976c) found a maximum growth rate for wave numbers 12 through 15 while Simmons and Hoskins (1976, 1977a) found a maximum growth rate for wave number 5 through 9. Some of the difference is due to the assumed basic state (Simmons and Hoskins, 1977b; Gall and Blakeslee, 1977; Staley and Gall, 1977) but the issue is not resolved. It is possible that

details of the model may be crucial. If this is so, application of the linear results to other models or to the atmosphere must be questioned. At any rate, linear growth rate spectra are very sensitive to the basic state. Since the basic state of a nonlinear model or of the atmosphere is constantly changing it is not clear how to apply the linear results. A partial explanation of the sensitive dependence of growth rate spectra on the basic state was noted by Fullmer (1979), using a one dimensional QG model. He found that small changes in the basic state zonal wind can lead to very different growth rate spectra if these small changes in the zonal wind are associated with relatively large changes in the mean profile of the QG potential vorticity gradient, which is the quantity appearing in the stability criterion. In their experiments Simmons and Hoskins found that the meridional flux of zonal momentum is sensitive to the assumed basic state while the meridional heat flux is relatively insensitive.

Most of the calculated normal modes have maximum amplitude near the surface; the shorter the wavelength the more the mode is restricted to lower levels. As a consequence most of the fluxes due to the linear waves are restricted to the surface layer. Gall (1976a) compared the normal modes of the GFDL global circulation model (GCM) to both observational statistics and statistics obtained from the GCM. In contrast to the linear case the most energetic wave numbers in the GCM and in the observations are those less than 9 and these eddies have maximum amplitudes of kinetic energy and momentum transport in the upper troposphere. By allowing growth to finite amplitude and wave mean flow interactions both Gall (1976b) and Simmons and Hoskins (1978) found that the growth of the disturbances ceases at lower levels first allowing

the growth of maximum amplitude at upper levels, thereby favoring the selection of longer wavelengths. In contrast, Simmons (1972), who studied the same problem with a QG model, reported that the finite amplitude wave kinetic energy profiles agreed with those of linear waves.

In summary, baroclinic instability results indicate significant differences between PE and QG linear waves. In particular relatively minor structural differences can result in much larger differences in eddy fluxes. Also indicated is the importance of wave mean flow interactions when the waves reach finite amplitude. The effects of the wave mean flow interactions seem to be as or more important than differences between the PE and QG linear waves. Therefore if a linear theory is acceptable, the errors introduced by the additional assumption of quasi-geostrophy are acceptable. On the other hand it is questionable whether we can extrapolate the comparison of PE and QG linear waves to a non-linear regime.

Heck (1979) calculated the eddy flux of zonal momentum directly from observational data and diagnostically as a residual of the potential temperature and potential vorticity fluxes. If the atmosphere were quasigeostrophic the two calculations should agree. Heck found that the QG assumption causes a relative error of 25% to 60% depending on latitude and season. This is the same order of magnitude as the linear results of Simmons and Hoskins (1976). But it should be noted that they calculated non-quasigeostrophic differences and Heck calculated ageostrophic differences.

Semtner and Holland (1978) compared several QG models with a PE model. Their study shares this objective with the present study but there are major differences in the physical situations considered and in

the models used. Semtner and Holland model a primarily wind driven western North Atlantic circulation using QG models having two or three layers and constant mean stability and a PE model having five layers. The QG models and PE model differ in the details of bottom topography, friction, heating and in other respects. In all, eight QG experiments were performed, demonstrating, among other results, the necessity of including at least simple topography and heating in the QG model to properly simulate the PE model's climate. Semtner and Holland originally felt that the basic QG experiment which includes topography and heating would simulate the PE results best. Qualitatively good agreement is obtained but the eddies in the QG model are too intense; the QG energy levels are approximately 35% higher than the PE energy levels and the QG kinetic energy conversion is too high. Semtner and Holland then tuned the QG model by changing the upper layer thickness from 500m to 200m. This results in good agreement with the PE results. Thus the QG equations are sensitive to vertical discretization. (See also Flierl (1978).) However it is not obvious how good the agreement would be between a QG model and a PE model with identical vertical structure.

Inevitably, as noted earlier, in any numerical model small errors occur at each time step; these errors may amplify, limiting the usefulness of the model for simulation purposes. It seems a reasonable hypothesis that anything decreasing the magnitude of the short term prediction errors will improve the model's ability to simulate the observed climate. A number of empirical methods for decreasing the magnitude of the prediction errors have been proposed - model tuning; the empirical correction method and the empirical dynamical method. (See Leith (1978a) for a review.) These methods are empirical since they require observations

of the real system. (This limitation is discussed in the conclusion.)

Although most models have some adjustable coefficients, tuning is nearly a taboo subject in the meteorological literature. From the discussions which do appear in the literature it appears that tuning is accomplished by rough qualitative argument followed by numerical experimentation. The tuning problem may however be put in the form of an inverse problem if the condition of optimality can be mathematically defined. The single example of this approach we know of for a dynamical system is given by Leith (1974b). Leith chooses λ , a parameter in the long wave correction of a barotropic model by plotting the ensemble averaged root mean square height error of the two day forecasts versus λ and choosing the value of λ corresponding to the minimum error. In geophysical diagnostic studies the inverse problem approach is more popular; for example Olbers et. al. (1976) determined wave spectra from moored array data using inverse techniques.

In Section 6 the QG model is tuned using data obtained from a PE model run to minimize the mean squared short term ($5f^{-1}$) prediction error. In some respects the tuned quasigeostrophic (TQG) model is better able than the untuned model to simulate the PE model's climate.

In Leith's (1974b, 1978a) empirical or climate drift correction method the model equations are altered by adding constant and linear terms to the governing equations. These new terms are statistically determined by requiring that the ensemble mean first and second order statistics are preserved. The tuning procedure is equivalent to an empirical correction method where a special form of the corrections is assumed at the start of the analysis if the terms in the governing

equations containing the adjustable parameters are constant or linear (in the parameters). Faller and coworkers (Faller and Lee, 1975; Faller and Schemm, 1977; Schemm and Faller, 1977) proposed a statistical correction method whereby an empirically determined correction is added to the solution after each time step; they found significantly improved forecasts in experiments with one and two dimensional forms of a modified Burger's equation. Their technique may be considered a finite difference approximation of Leith's empirical correction method.

Presently empirical climate models obtained by inverse techniques are receiving attention from Hasselmann and his coworkers, as outlined by Hasselmann in a series of lectures delivered at Harvard this spring. (A number of papers are in preparation.) For climate simulation purposes Hasselmann suggests seeking agreement between the model and the data in the frequency domain. A technique for accomplishing this was successfully tested by Hartjenstein and Egger (1979) using data from simple two layer model experiments. They sought a constant coefficient linear zonally averaged model which would simulate the zonally averaged behavior of the original model. The model coefficients were found by demanding agreement between the low order Fourier coefficients of the original data and of the solutions generated by the linear model.

The empirical dynamical method uses the results of integrating a dynamical model as predictors of the forecast quantities in an empirical linear (in all studies to date) regression scheme based on observations. This method has been used in creating MOS forecasts (Klein and Glahn, 1974), in studies of a hemispheric barotropic model (Leith, 1974b; Lorenz, 1977) and in the final step of a Monte Carlo prediction study

(Leith, 1974a).

It is not expected that the use of empirical methods will yield a perfect prediction model. Generally a substantial part of the mean squared error remains. The residuals, i.e., the differences between the observed prediction errors and the empirical estimates of the prediction errors, may contain important information. We conjecture that the regular addition to the model state of random perturbations with theoretically or empirically determined statistical properties may improve the model's ability to simulate reality. (In this study the observational data are actually generated by a model, but for the purpose of discussion we will refer to this more complex model as "the real system"; the simpler model involving the additional assumption(s) will be called "the model".)

To illustrate this hypothesis assume that the real system's time evolution may be described by a point moving through a multi-dimensional phase space and that the model's time evolution is described by a point moving on a lower dimensional manifold in the real system's phase space. For predictive purposes we need an initialization procedure; this may be thought of as the projection of the system state on the model manifold. Now consider a point $X(0)$ on the model manifold and the set $\left\{ X_n^i \right\}$ of all points in the phase space which project onto $X(0)$ and which are in the attractor set of the real system. Then the projection of the system state will come arbitrarily close to $X(0)$ as often as desired over a long enough period of time, provided that the set $\left\{ X_n^i \right\}$ is not empty. After a short time T the model state will be $X(T)$ and the points X_n^i will evolve to the points X_n^f . Generally the projection of the set $\left\{ X_n^f \right\}$ will not be a single point and the average of the projections

of the X_n^f will be different from $X(T)$. The statistics of the errors, where the errors are the differences of the projections of X_n^f and $X(T)$, may be determined empirically or by theoretical consideration of the short term behavior of the system. The actual errors are of course unknowable within the context of the model. If the model is to give a good simulation of the system the point $X(0)$ should be in the attractor set of the model. Suppose this is so; then the model state will come arbitrarily close to $X(0)$ as often as desired for a long enough simulation. As the real system evolves every time its projection comes close to $X(0)$ there will be a certain probability that the real system is close to a particular X_n^i . After a time T the projection of the real system will be close to the projection of the corresponding X_n^f with the same probability. The unperturbed model evolution on the other hand is completely determined by $X(0)$. The real system's behavior can be simulated by adding random perturbations to the model state $X(T)$, if the statistical properties of the perturbations are chosen to agree with the statistical properties of the errors. This argument motivates but certainly does not prove our conjecture.

In Section 7 we test our conjecture by perturbing the QG model at regular intervals. The perturbations contain a deterministic component corresponding to a least squares estimate of the prediction error, that is an empirical correction, and a stochastic component having statistical properties similar to those of the residuals of the least squares estimates of the prediction errors.

The addition of randomly generated perturbations to the model state at regular intervals is a finite difference form of adding stochastic forcing to the governing equations. In meteorology, stochastic forcing

has been used previously in stochastic prediction and in linear and non-linear climate modeling.

Since the beginning of modern numerical weather prediction there has been an awareness that predictability is limited by both the uncertainty in the initial conditions and shortcomings in the model (Thompson, 1957). Predictability studies have shown that even with a perfect model the uncertainty in the initial conditions limits the useful forecast range to at most two weeks. Stochastic dynamic prediction has been proposed as an objective way of utilizing our knowledge of the uncertainty in the initial conditions. (Review papers by Leith (1975) and Haltiner and Williams (1975) cover both these topics.) Within the framework of stochastic dynamical prediction it is possible to include stochastic forcing to take into account the effects of model insufficiencies on the forecast (Fleming, 1972; Pitcher, 1977). Because of the nonlinearity of the governing equations most stochastic dynamical prediction models rely on some sort of closure scheme for the higher statistical moments. Leith (1974a) has suggested Monte Carlo methods may be more economical. Besides sidestepping the closure problem Monte Carlo prediction schemes should make it easier to include stochastic forcing.

Recently stochastic climate models have received considerable attention. Hasselmann (1976) suggests that the effect of the short time scale weather phenomena on the long time scale climate system is essentially that of white noise forcing. If a linearized model is adequate it is then possible to evaluate the climate system's frequency response for any given forcing by the weather. This technique has been successfully applied to the forcing by the atmosphere of observed sea surface temperature anomalies (Frankignoul and Hasselmann, 1977; Reynolds, 1978) and of

a β -plane ocean (Frankignoul and Müller, 1979) and to the parameterization of atmospheric eddy heat fluxes in zonally and globally averaged energy climate models (Lemke (1977) and Fraedrich (1978) respectively).

The effects of stochastic forcing on nonlinear (climate) models can in general only be evaluated by numerical means. Robock (1978) included a stochastically forced component in the parameterization of the zonally averaged poleward heat flux in Seller's (1973) time dependent model. The time evolution of the model's annually and globally averaged temperature qualitatively agrees with observations. Williams (1978) incorporated a stochastic energy source in his barotropic model of the Jovian atmosphere, and found the model simulated flow is similar to observations. Without the stochastic forcing both of these models would asymptotically approach a steady or periodic solution for any initial conditions. The present study contains the first report of the response of an aperiodic climate model to stochastic forcing.

2. The model.

2a. Governing equations.

The model presented below is a spectral form of the energy preserving two layer model formulated by Lorenz (1960). For horizontally continuous variables the adiabatic, inviscid governing equations of this model are

$$\begin{aligned} \frac{\partial}{\partial t} \theta &= -J(\Psi, \theta) - J(\mathcal{T}, \sigma) + \nabla \cdot (\sigma \nabla \chi) \\ \frac{\partial}{\partial t} \sigma &= -J(\mathcal{T}, \theta) - J(\Psi, \sigma) + \nabla \theta \cdot \nabla \chi \\ \frac{\partial}{\partial t} \nabla^2 \Psi &= -J(\Psi, \nabla^2 \Psi + f) - J(\mathcal{T}, \nabla^2 \mathcal{T}) \\ &\quad + \delta_B \nabla \cdot (\nabla^2 \mathcal{T} \nabla \chi + \nabla^2 \chi \nabla \mathcal{T}) + \delta_p J(\chi, \nabla^2 \chi) \\ \frac{\partial}{\partial t} \nabla^2 \mathcal{T} &= -J(\Psi, \nabla^2 \mathcal{T}) - J(\mathcal{T}, \nabla^2 \Psi + f) + \nabla \cdot (f \nabla \chi) \\ &\quad + \delta_B \nabla \cdot (\nabla^2 \Psi \nabla \chi) \\ \delta_p \frac{\partial}{\partial t} \nabla^2 \chi &= \nabla^2 c_p b \theta - \nabla \cdot (f \nabla \mathcal{T}) \\ &\quad - \delta_B \left(\nabla \cdot (\nabla^2 \Psi \nabla \mathcal{T} + \nabla^2 \mathcal{T} \nabla \Psi) - \nabla^2 (\nabla \Psi \cdot \nabla \mathcal{T}) \right) \\ &\quad - \delta_p \left(\nabla^2 (J(\Psi, \chi)) + J(\chi, \nabla^2 \Psi + f) \right) \end{aligned}$$

where $\theta + \sigma$ is the potential temperature in the upper layer,
 $\theta - \sigma$ is the potential temperature in the lower layer,
 $\Psi + \mathcal{T}$ is the stream function in the upper layer,
 $\Psi - \mathcal{T}$ is the stream function in the lower layer,
 χ is the velocity potential in the lower layer,

f is the Coriolis parameter,

C_p is the specific heat of air at constant pressure, and

b is a constant approximately equal to 0.124.

J is the Jacobian operator defined by

$$J(A,B) = \nabla A \cdot (\nabla B \times \underline{k})$$

where \underline{k} is the vertical unit vector and

∇ is the horizontal gradient operator. There are two indicator variables distinguishing the three systems of equations.

$$\delta_p = \begin{cases} 0 & \text{for the QG equations and BE} \\ 1 & \text{for the PE} \end{cases}$$

$$\delta_B = \begin{cases} 0 & \text{for the QG equations} \\ 1 & \text{for the BE and PE} \end{cases}$$

For a domain without horizontal boundaries, these equations possess three independent integral invariants which may be taken to be $A+K$, $P+I+K$ and $S-K$. $P+I$, A , K and S are respectively the total potential energy, the available potential energy, the kinetic energy and the gross static stability all averaged over the mass of the atmosphere.

If the further simplifying assumptions that f is constant and that σ does not vary horizontally, and if rectangular coordinates (x,y) and the scaling

$$z : f^{-1} \qquad x, y : L$$

$$\Psi, \tau, \chi : L^2 f \qquad \theta, \sigma : L^2 f^2 (C_p b)^{-1}$$

are introduced then the nondimensional governing equations are

$$\frac{\partial}{\partial t} \theta = -J(\Psi, \theta) + \sigma_0 \nabla^2 \chi$$

$$\begin{aligned} \frac{\partial}{\partial t} \nabla^2 \Psi &= -J(\Psi, \nabla^2 \Psi) - J(\tau, \nabla^2 \tau) \\ &+ \delta_B \nabla \cdot (\nabla^2 \tau \nabla \chi + \nabla^2 \chi \nabla \tau) + \delta_p J(\chi, \nabla^2 \chi) \end{aligned}$$

$$\begin{aligned} \frac{\partial}{\partial t} \nabla^2 \tau &= -J(\Psi, \nabla^2 \tau) - J(\tau, \nabla^2 \Psi) + \nabla^2 \chi \\ &+ \delta_B \nabla \cdot (\nabla^2 \Psi \nabla \chi) \end{aligned}$$

$$\begin{aligned} \delta_p \frac{\partial}{\partial t} \nabla^2 \chi &= \nabla^2 \theta - \nabla^2 \tau \\ &- \delta_B (\nabla \cdot (\nabla^2 \Psi \nabla \tau + \nabla^2 \tau \nabla \Psi) - \nabla^2 (\nabla \Psi \cdot \nabla \tau)) \\ &- \delta_p (\nabla^2 (J(\Psi, \chi)) + J(\chi, \nabla^2 \Psi)) \end{aligned}$$

$$\frac{\partial}{\partial t} \sigma_0 = -\overline{\theta \nabla^2 \chi}$$

$$\frac{\partial}{\partial t} \theta_0 = 0$$

where the overbar and σ_0 and θ_0 represent areal averages and all other variables are deviations from areal averages. With this scaling there are no dimensionless constants in the equations of motion.

An infinite doubly periodic f-plane is chosen as the horizontal domain. Each of θ , Ψ , τ and χ is expanded in a complex Fourier series of the form

$$(1) \quad \zeta(x,y,t) = \sum_{\underline{I}} \zeta_{\underline{I}}(t) F_{\underline{I}}(x,y)$$

where the sum is over all integer wave vectors $\underline{I} = (I_x, I_y)$, excluding $\underline{I} = \underline{0}$ and where I is an ordering of the \underline{I} . (That is, the I (th) wave vector is \underline{I} , the J (th) wave vector is \underline{J} , etc.) In order that ζ be real $\zeta_{-\underline{I}}$, where $-\underline{I}$ is the index of $-\underline{I}$, must be equal to the complex conjugate of $\zeta_{\underline{I}}$ for all \underline{I} and for all ζ .

$$F_{\underline{I}} = \exp(i(I_x x + I_y y))$$

Consequently

$$\overline{F_{\underline{I}} F_{\underline{J}}} = \begin{cases} 0 & \text{if } \underline{I} + \underline{J} \neq \underline{0} \\ 1 & \text{if } \underline{I} + \underline{J} = \underline{0} \end{cases}$$

and
$$\nabla^2 F_{\underline{I}} = (-a_{\underline{I}}^2) F_{\underline{I}}$$

where $a_{\underline{I}}^2 = \underline{I} \cdot \underline{I}$ is positive. Now substitute expressions like (1) into the nondimensional governing equations, multiply by $F_{-\underline{I}}$ and average horizontally. For linear terms

$$\overline{F_{-\underline{I}} \zeta} = \sum_{\underline{J}} \overline{F_{-\underline{I}} F_{\underline{J}}} \zeta_{\underline{J}} = \zeta_{\underline{I}}$$

The quadratic terms all satisfy

$$\begin{aligned} \overline{F_{-I} Q(\zeta, \eta)} &= \overline{F_{-I} Q\left(\sum_J F_J \zeta_J, \sum_K F_K \eta_K\right)} \\ &= \sum_J \sum_K \zeta_J^q \eta_K \end{aligned}$$

where the interaction coefficients

$$q_{IJK} = \overline{F_{-I} Q(F_J, F_K)}$$

are constants. The one term requiring special attention is

$$\overline{\theta \nabla^2 \chi} = \sum_J \sum_K \theta_J (-a_K^2) \chi_K \overline{F_J F_K} = \sum_J \theta_{-J} (-a_J^2) \chi_J$$

The adiabatic inviscid nondimensional equations of motion in spectral form are thus

$$\begin{aligned} \frac{d}{dt} \theta_I &= - \sum_J \Psi_J c_{IJK} \theta_K + \sigma_0 (-a_I^2) \chi_I \\ (2.a) \quad \frac{d}{dt} (-a_I^2) \Psi_I &= - \sum_J \Psi_J c_{IJK} (-a_K^2) \Psi_K - \sum_J \tau_J c_{IJK} (-a_K^2) \tau_K \\ &\quad + \delta_B \left(\sum (-a_J^2) \tau_J d_{IJK} \chi_K + \sum (-a_J^2) \chi_J d_{IJK} \tau_K \right) \\ &\quad + \delta_P \sum_J \chi_J c_{IJK} (-a_K^2) \chi_K \end{aligned}$$

$$\begin{aligned}
 \frac{d}{dt}(-a_I^2) \tau_I &= -\sum \psi_J c_{IJK} (-a_K^2) \tau_K - \sum \tau_J c_{IJK} (-a_K^2) \psi_K \\
 &+ (-a_I^2) \chi_I + \delta_B \sum (-a_J^2) \psi_J d_{IJK} \chi_K \\
 \delta_P \frac{d}{dt}(-a_I^2) \chi_I &= (-a_I^2) \theta_I - (-a_I^2) \tau_I - \delta_B \left(\sum (-a_J^2) \psi_J d_{IJK} \tau_K \right. \\
 &+ \left. \sum (-a_J^2) \tau_J d_{IJK} \psi_K - (-a_I^2) \sum \tau_J e_{IJK} \psi_K \right) \\
 &- \delta_P \left((-a_I^2) \sum \psi_J c_{IJK} \chi_K + \sum \chi_J c_{IJK} (-a_K^2) \psi_K \right) \\
 \frac{d}{dt} \sigma_0 &= -\sum_K (-a_K^2) \theta_{-K} \chi_K \\
 \frac{d}{dt} \theta_0 &= 0
 \end{aligned}$$

where we have written \sum for $\sum_J \sum_K$. The interaction coefficients are

$$\begin{aligned}
 c_{IJK} &= \overline{F_{-I}^J(F_J, F_K)} &= (\underline{K} \times \underline{J}) b_{IJK} \\
 d_{IJK} &= \overline{F_{-I} \nabla \cdot (F_J \nabla F_K)} &= -\frac{1}{2}(\underline{I}^2 + \underline{K}^2 - \underline{J}^2) b_{IJK} \\
 e_{IJK} &= \overline{F_{-I} \nabla F_J \cdot \nabla F_K} &= \frac{1}{2}(\underline{J}^2 + \underline{K}^2 - \underline{I}^2) b_{IJK}
 \end{aligned}$$

where

$$b_{IJK} = \overline{F_{-I} F_J F_K} = \begin{cases} 1 & \text{if } \underline{J} + \underline{K} = \underline{I} \\ 0 & \text{otherwise} \end{cases}$$

These equations conserve the three energy invariants of the original two layer equations. The only requirements for this to hold are that θ , ψ , τ and χ are all expressed in terms of the same expansion functions, and that whenever a wave vector \underline{I} is included in the expansion

so is $\underline{-I}$.

Diabatic and viscous processes must now be specified. Of the many possible parameterizations we choose the simplest. Since the principal interest here is in the differences between two systems of equations having identically parameterized friction and heating it is not expected that these differences will be overly influenced by the choice of parameterizations. Second, simplicity is in keeping with the anticipated severe truncation. Following the approach used by Lorenz (1962, 1963b) in studying QG models, we add to the model surface friction proportional to the velocity in the lower layer, a momentum exchange between the layers proportional to the velocity difference between the layers, a heat exchange between the layers proportional to the potential temperature difference between the layers, heating of the lower layer proportional to the difference between the temperature in the lower layer and an imposed temperature field and heating of the upper layer proportional to the difference between the temperature of the upper layer and an imposed temperature field. These last two effects may be thought of as due to radiative heating and/or boundary layer heating. If the proportionality constants, assumed all non-negative, are respectively $2fk_0$, $\frac{1}{2}f(k_1 - k_0)$, $\frac{1}{2}fh_0$, $f(h_1 + h_2)$ and $f(h_1 - h_2)$ then the scaled spectral equations (2.a) include the additional terms

$$\frac{d}{dt} \Theta_I = \dots - h_1 (\Theta_I - \Theta_I^R)$$

$$(2.b) \quad \frac{d}{dt} (-a_I^2) \Psi_I = \dots - k_0 (-a_I^2) (\Psi_I - T_I)$$

$$\frac{d}{dt} (-a_I^2) \tau_I = \dots - k_1 (-a_I^2) \tau_I + k_0 (-a_I^2) \Psi_I$$

$$\delta_p \frac{d}{dt} (-a_I^2) \chi_I = \dots - \delta_p k_1 (-a_I^2) \chi_I$$

$$\frac{d}{dt} \sigma_0 = \dots - h_0 \sigma_0 - h_1 (\sigma_0 - \sigma_0^R) + h_2 (\theta_0 - \theta_0^R)$$

$$\frac{d}{dt} \theta_0 = -h_1 (\theta_0 - \theta_0^R) + h_2 (\sigma_0 - \sigma_0^R)$$

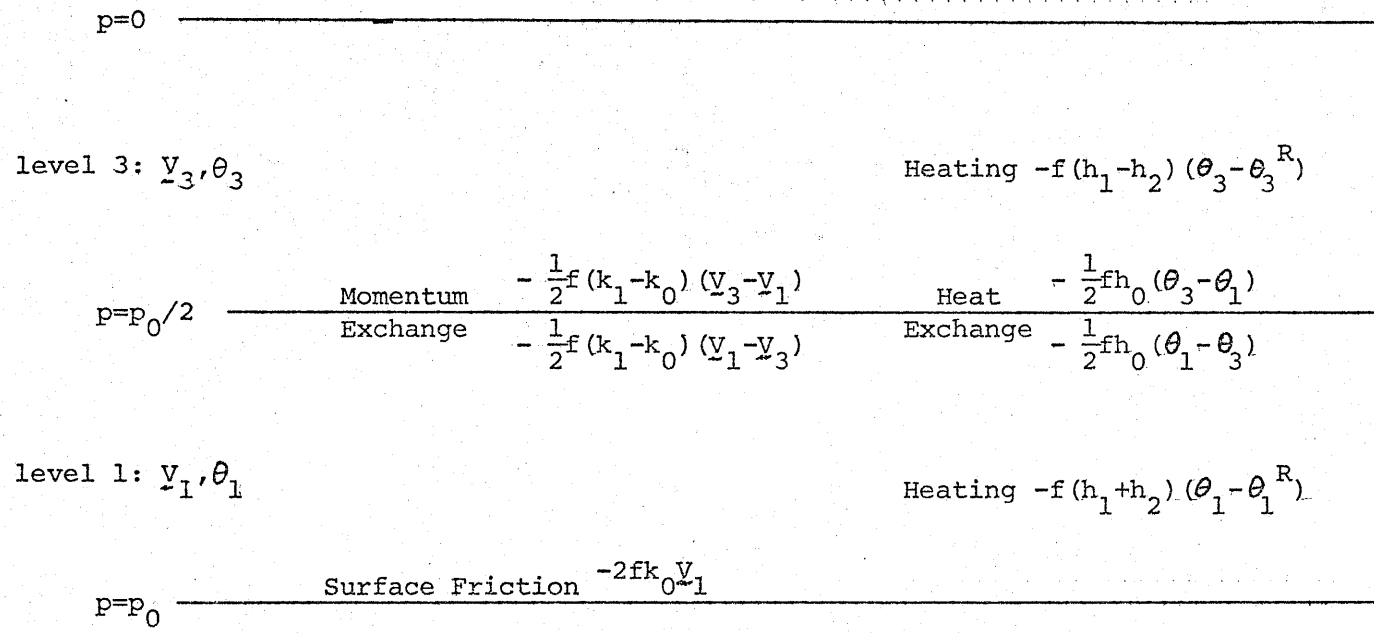
where the superscript R refers to the imposed (radiative) temperature field. The sketch on the next page illustrates the model physics.

2b. Energy equations.

The flow of energy through the system is governed by the usual energy equations,

$$(3) \quad \begin{aligned} \frac{d}{dt} A &= G - C \\ \frac{d}{dt} K &= C - D \\ \frac{d}{dt} A_Z &= G_Z - C_A - C_Z \\ \frac{d}{dt} A_E &= G_E + C_A - C_E \\ \frac{d}{dt} K_Z &= C_Z - C_K - D_Z \\ \frac{d}{dt} K_E &= C_E + C_K - D_E \end{aligned}$$

where A, K, G, C and D represent respectively the available form, kinetic form, generation, conversion and dissipation of energy averaged over the mass of the atmosphere. The subscripts Z, E, A and K denote



Model physics in dimensional form.

respectively zonal, eddy, available and kinetic forms of energy or energy flow. The division into eddy and zonal forms is in the space domain (Oort, 1964). Below the diagnostic equations for the energy variables are presented in terms of the nondimensional horizontally continuous variables. (The scale for energies is $L^2 f^2$.) The notation is more concise and it is easier to follow the derivation in this form; however exactly analogous statements may be made directly in terms of the spectral variables. For example, in terms of the continuous variables the horizontal average of any Jacobian term is zero because of the periodic boundary conditions while in terms of the spectral variables this holds because of the symmetry properties of the interaction coefficients; $c_{IJK} = -c_{-J,-I,K} = -c_{IKJ}$. All calculations reported in the sequel are performed in the spectral domain.

The forms of energy for the two layer model (Lorenz, 1960) are kinetic energy, available energy, gross static stability and total potential energy, which are defined respectively by

$$K = \frac{1}{2} (\overline{\nabla\psi \cdot \nabla\psi} + \overline{\nabla\tau \cdot \nabla\tau} + \delta_p \overline{\nabla\chi \cdot \nabla\chi})$$

$$A = \sigma_m - \sigma_0 = \frac{1}{\sigma_m + \sigma_0} (\overline{\theta^2} + \overline{\sigma^2})$$

$$S = \sigma_0$$

$$P+I = \frac{a}{b} \theta_0 - \sigma_0$$

where an overbar is again an areal average and the unsubscripted variables are deviations from such an average. a/b is a constant, approximately equal to 6.424. σ_m is the maximum value of S for any hypothetical adiabatic rearrangement of the atmosphere. It is equal to $(\sigma_0^2 + \bar{\theta}^2 + \bar{\sigma}^2)^{\frac{1}{2}}$ since mean potential temperature (i.e., θ_0) and mean squared potential temperature (i.e., $\theta_0^2 + \sigma_0^2 + \bar{\theta}^2 + \bar{\sigma}^2$) are conserved by the model under adiabatic conditions. Another energy invariant, that is a quantity conserved by the model in the absence of dissipation and heating, is the total energy $P+I+K$. Therefore $A+K$, $A+S$, $K-S$ and $P+I-A$ are also energy invariants. To divide A and K into zonal and eddy components it is necessary to use the second form of A which, similar to conventional formulations, is the average of the variance of potential temperature divided by a stability factor. Note that the stability factor is a function of time.

Let $[\zeta]$ be the zonal average of ζ and let $\zeta' = \zeta - [\zeta]$ be the deviation from the zonal average. Then

$$K_z = \frac{1}{2} \left(\overline{[\nabla\psi]^2} + \overline{[\nabla\tau]^2} + \delta_p \overline{[\nabla\chi]^2} \right)$$

$$K_e = \frac{1}{2} \left(\overline{(\nabla\psi')^2} + \overline{(\nabla\tau')^2} + \delta_p \overline{(\nabla\chi')^2} \right)$$

As the static stability does not vary horizontally

$$A = (\sigma_m + \sigma_0)^{-1} \overline{\theta^2}$$

and

$$A_z = (\sigma_m + \sigma_0)^{-1} \overline{[\theta]^2}$$

$$A_E = (\sigma_m + \sigma_0)^{-1} \overline{\theta'^2}$$

By deriving the evolution equations of K , K_z , K_E , A , A_z and A_E and identifying the results with (3) the following relationships are obtained.

$$C = -\overline{\chi \nabla^2 \theta}$$

$$C_z = -\overline{[\chi] \nabla^2 [\theta]}$$

$$C_E = -\overline{\chi' \nabla^2 \theta'}$$

$$\begin{aligned} C_K = & \overline{[\Psi] (-J(\Psi, \nabla^2 \Psi) - J(\tau, \nabla^2 \tau))} \\ & + \overline{[\Psi] (\delta_B \nabla \cdot (\nabla^2 \tau \nabla \chi + \nabla^2 \chi \nabla \tau) + \delta_p J(\chi, \nabla^2 \chi))} \\ & + \overline{[\tau] (-J(\Psi, \nabla^2 \tau) - J(\tau, \nabla^2 \Psi) + \delta_B \nabla \cdot (\nabla^2 \Psi \nabla \chi))} \\ & + \overline{[\chi] (-\delta_B (\nabla \cdot (\nabla^2 \Psi \nabla \tau + \nabla^2 \tau \nabla \Psi) - \nabla^2 (\nabla \Psi \cdot \nabla \tau))} \\ & + \overline{[\chi] (-\delta_p (\nabla^2 (J(\Psi, \chi)) + J(\chi, \nabla^2 \Psi))} \end{aligned}$$

$$C_A = \frac{1}{\sigma_m + \sigma_0} (C_E A_Z - C_Z A_E + 2 \overline{[\theta] J(\psi, \theta)})$$

$$D = k_0 \overline{(\nabla\psi - \nabla\tau)^2} + (k_1 - k_0) \overline{(\nabla\tau)^2} + \delta_p k_1 \overline{(\nabla\chi)^2}$$

$$D_Z = k_0 \overline{([\nabla\psi] - [\nabla\tau])^2} + (k_1 - k_0) \overline{[\nabla\tau]^2} + \delta_p k_1 \overline{[\nabla\chi]^2}$$

$$D_E = k_0 \overline{(\nabla\psi' - \nabla\tau')^2} + (k_1 - k_0) \overline{(\nabla\tau')^2} + \delta_p k_1 \overline{(\nabla\chi')^2}$$

$$G = -\frac{A}{\sigma_m} \left(\left. \frac{\partial \sigma_0}{\partial t} \right|_d \right) + \frac{1}{\sigma_m} \overline{\theta \left(\left. \frac{\partial \theta}{\partial t} \right|_d \right)}$$

$$G_Z = -\frac{A_Z}{\sigma_m} \left(\left(\left. \frac{\partial \sigma_0}{\partial t} \right|_d \right) + \frac{1}{\sigma_m + \sigma_0} \overline{\theta \left(\left. \frac{\partial \theta}{\partial t} \right|_d \right)} \right) \\ + \frac{2}{\sigma_m + \sigma_0} \overline{[\theta] \left(\left. \frac{\partial [\theta]}{\partial t} \right|_d \right)}$$

$$G_E = -\frac{A_E}{\sigma_m} \left(\left(\left. \frac{\partial \sigma_0}{\partial t} \right|_d \right) + \frac{1}{\sigma_m + \sigma_0} \overline{\theta \left(\left. \frac{\partial \theta}{\partial t} \right|_d \right)} \right) \\ + \frac{2}{\sigma_m + \sigma_0} \overline{\theta' \left(\left. \frac{\partial \theta'}{\partial t} \right|_d \right)}$$

where $\left. \frac{\partial}{\partial t} () \right|_d$ indicates the diabatic part only of the heating tendency, that is terms corresponding to the terms on the right hand side of (2.b).

The derivation of the above equations is long but straightforward, requiring the repeated use of integration by parts and of the periodic

boundary conditions and the manipulation of the averaging operators. The following example captures the essence of the calculation. Consider the evolution of K_Z for the QG equations; for the barotropic component,

$$\begin{aligned}
 \frac{\partial}{\partial t} \overline{\frac{1}{2}[\nabla\psi]^2} &= \overline{[\nabla\psi] \cdot \frac{\partial}{\partial t} [\nabla\psi]} \\
 &= \overline{[\nabla\psi] \cdot \frac{\partial}{\partial t} \nabla\psi} = \overline{\nabla[\psi] \cdot \nabla \frac{\partial}{\partial t} \psi} \\
 &= \overline{\nabla \cdot ([\psi] \nabla \frac{\partial}{\partial t} \psi)} - \overline{[\psi] \nabla^2 \frac{\partial}{\partial t} \psi} \\
 &= - \overline{[\psi] \nabla^2 \frac{\partial}{\partial t} \psi} \\
 &= - \overline{[\psi] \frac{\partial}{\partial t} \nabla^2 \psi}
 \end{aligned}$$

This argument is also true if τ replaces ψ . Then substitute from the vorticity evolution equations to obtain, under adiabatic inviscid conditions,

$$\begin{aligned}
 \frac{d}{dt} K_Z &= -C_K - \overline{[\tau] \nabla^2 \chi} = -C_K - \overline{[\chi] \nabla^2 [\tau]} \\
 &= -C_K + C_Z
 \end{aligned}$$

since $\nabla^2[\tau] = \nabla^2[\theta]$ for the QG equations.

3. Experiments.

3a. Numerical procedure.

In the integrations reported in the sequel the alternating 4-cycle time marching scheme (Lorenz, 1971) has been used exclusively. This method is essentially fourth order in Δt ; every fourth step the integration error is order $(\Delta t)^5$. (In the N-cycle scheme $\Delta t = N \delta t$, where δt is the small internal time increment.) The computations have been performed in double precision on the GLAS Amdahl computer.

To ensure the solutions remain convectively stable, at each time step a check is made for the condition $\left\{ \sigma_0 \leq \sigma_{0c} \quad \text{and} \quad \frac{d}{dt} \sigma_0 < 0 \right\}$ where σ_{0c} is an assigned constant critical value of mean stability. When this condition obtains $\frac{d}{dt} \sigma_0$ is set equal to zero. This is a parameterization of convection; we assume that whenever σ_0 reaches σ_{0c} convective instability, just enough to offset any further dynamical destabilization, occurs. Actually, with $\sigma_{0c} = 0$, in the experiments reported here the convective adjustment is never needed once equilibration has occurred and we may take the view that the governing equations do not include this process. Unless otherwise stated no adjustment was made during the model integrations.

For PE integrations all the spectral variables are prognostic, while for the filtered equations we have considered σ_0 , θ_0 , Ψ_I and \mathcal{T}_I to be prognostic. Here and below in the text, \mathcal{J}_I without further qualification denotes the set of spectral variables \mathcal{J}_I for all I under consideration. For the QG equations or the BE θ_I is evaluated from the balance condition

$$\theta_I = \tau_I + \delta_0 \left(\sum \psi_J \left(\frac{a_J^2}{a_I^2} d_{IJK} + \frac{a_K^2}{a_I^2} d_{IKJ} - e_{IJK} \right) \tau_K \right)$$

For the BE if θ_I instead of τ_I is chosen to be prognostic, then τ_I is determined by a linear system of equations whose coefficients depend on θ_I and ψ_I . χ_I is found by demanding that the time rate of change of the balance condition holds. The resulting omega equation is of the form

$$(\underline{D} + \underline{A}) \underline{\chi} = \underline{b}$$

where $\underline{\chi}$ is the vector of the χ_I spectral variables and where the diagonal matrix, \underline{D} , corresponding to the QG terms, dominates the full matrix, $\underline{D} + \underline{A}$. \underline{D} depends on σ_0 ; \underline{A} depends on ψ_I and τ_I ; \underline{b} depends on ψ_I , τ_I and θ_I .

In the computations, only variables corresponding to wave vectors in one half of the wave vector plane are actually prognostic since we require that the solution be real; i.e., ζ_{-I} must be equal to the complex conjugate of ζ_I for all I and for all ζ . Another economization results from noting that all interaction coefficients are proportional to b_{IJK} . All the double sums may therefore be collapsed as follows:

$$\sum_J \sum_K \zeta_J q_{IJK} \tau_K = \sum_J \zeta_J q_{I,J,I-J} \tau_{I-J}$$

3b. Truncation and choice of constants.

In simulation studies one is always faced with a trade off between the model resolution and the length of the model generated time history. Truncation errors due to the space and time finite differencing schemes are proportional to some power of the grid increment. To minimize truncation error one would like the highest resolution possible, but the higher the resolution the higher the computational burden. On the other hand, the computational burden is also increased by the long time histories one would like in order to make statistical inferences.

In this study highly truncated models are used so that long time histories may be easily obtained. Highly truncated models have proved useful in a variety of studies (Lorenz, 1963a). In the comparisons to follow we may assert that the truncated PE model is the real system we wish to model. In this context the choice of extreme truncation in the filtered equations models is appropriate. The 12 wave vectors kept are represented below by the x's in the I plane,

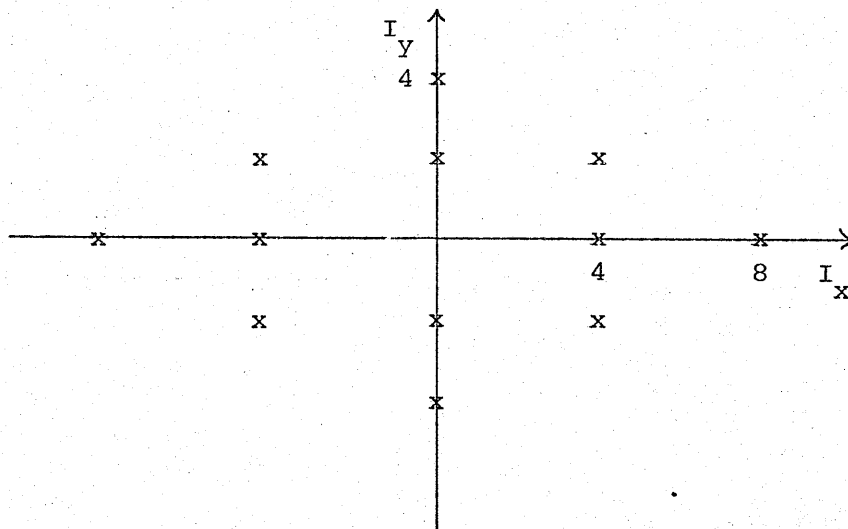


Table 1. Wave vector ordering scheme.

<u>Wave number</u> <u>(I)</u>	<u>Wave vector</u> <u>(I_x , I_y)</u>
0	(0 , 0)
1	(0 , 2)
2	(0 , 4)
3	(-4 , 2)
4	(4 , 2)
5	(4 , 0)
6	(8 , 0)

The wave vectors in one half of the \underline{I} plane are ordered in Table 1, thereby ordering the spectral variables.

It is known (Lorenz, 1963a) that highly truncated models may exhibit a variety of types of solution depending on the values of the constants appearing in the parameterizations of friction and heating. In preliminary experiments the evolution of the energy variables was constant, periodic or irregular for different choices of the constants and truncation. For the purposes of this study values which yield irregular solutions exhibiting several time scales are desired. To limit the number of free parameters we assume that

$$2k_0 = k_1 = k$$

$$h_0 = h_1 = h_2 = h$$

$$\theta_0^R = -10 \sigma_0^R = 10 \theta^*$$

$$\theta_I^R = \begin{cases} \theta^* & \text{if } \underline{I} = (0,2) \text{ or } (0,-2) \\ 0 & \text{otherwise} \end{cases}$$

so that once the truncation is fixed only k , h and θ^* are free. These assumptions correspond to no diabatic heating of the upper layer and an imposed temperature field in the lower layer of

$$\theta^R(x,y,t) = \theta^* (11 + 2 \cos (2y))$$

The governing equations might have been written without reference to θ_0^R by substituting $\theta_0' + \theta_0^R$ for θ_0 , noting that θ_0^R does not vary and then dropping the prime notation. Therefore θ_0^R might have been chosen quite arbitrarily; it affects only the unavailable

potential energy of the model. The average of $\left| \frac{\partial \theta^R}{\partial y} \right|$ is $\frac{8}{\pi} \theta^*$. Two values of θ^* have been considered: $\theta^* = 0.008$, which will be called the low thermal forcing case and $\theta^* = 0.032$, the high thermal forcing case. If the length scale l is taken to be the radius of the earth then these values of θ^* are dimensionally 25K and 100K respectively. In the absence of other effects the constants of proportionality listed in the previous section are reciprocals of e-folding decay times for the velocity in the lower layer, the velocity difference between the layers, the potential temperature difference between the layers and the differences of the temperature from the imposed temperature in the lower layer and the upper layer respectively. The above assumptions imply that the parameterized exchanges of heat and momentum between the surface and the lower layer are four times stronger than the corresponding exchanges between the two layers. In this study, except for the tuning experiments in Section 6, $k = 0.016$ and $h = 0.018$. For these values and for $f = (3 \text{ hours})^{-1}$ the first four of the above e-folding times are 7.81, 31.25, 13.89 and 3.47 days. Admittedly these are not optimal estimates of decay times for these processes in the atmosphere, however choosing values based on atmospheric observations would not necessarily ensure atmospheric (i.e., irregular) behavior in this simple model.

To complete the model specification Δt must be chosen. As noted earlier, in determining the size of Δt the two conflicting criteria of accuracy and economy must be satisfied. For the purpose of comparing the models, time stepping errors should be insignificant compared to the difference between the evolutions of the models from the same initial conditions. For the purpose of computing statistics of an irregularly

evolving system it is reasonable to choose Δt as large as is compatible with computational stability, since for any Δt which is numerically stable the variables will be positively correlated for lags of several Δt . Thus the effective number of independent observations will always be less than the actual number of observations. Secondly, when the initial conditions for the problem are arbitrary the statistics identified with the climate of the model are an average over time and initial conditions. If the time stepping procedure is accurate for only M steps then every M (th) data point may be considered a new set of initial conditions. With these thoughts in mind we have performed a series of test integrations and (conservatively) chosen $\Delta t = 1.0$ and 0.5 for the low and high thermal forcing cases respectively. These values are appropriate for PE integrations once the model is equilibrated and these values are used universally so that the models are computationally identical. Larger values of Δt could be used for the QG and BE models.

3c. Initial conditions.

The initial conditions for the experiments are zonal steady state solutions of the appropriate governing equations. If all the variables associated with nonzero I_x are initially zero they remain zero. If the equations are integrated from the initial conditions $\theta_0 = 10 \theta^*$, $\sigma_0 = 0$, all other variables with $I_x = 0$ equal to a small value and all variables with $I_x \neq 0$ equal to zero, then for the first few hundred time units the convective adjustment is on. Subsequently the solutions asymptotically approach steady states which have positive σ_0 .

The final states obtained in this manner plus small perturbations are the initial conditions for the long time integrations.

It is possible to analytically solve the zonal steady state QG equations. Since the Jacobian terms vanish

$$\psi_I = \tau_I = \theta_I = \frac{2}{k} \chi_I$$

for all I and

$$\theta_0 - \theta_0^R = \sigma_0 - \sigma_0^R$$

The evolution equation for each θ_I then reduces to

$$(a_I^2 \frac{k}{2} \sigma_0 + h) \tau_I = h \theta_I^R$$

Now restrict \underline{I} to the positive I_y axis. For the forced mode

$-I = F - \tau_F$ cannot be zero; therefore

$$\sigma_0 = \frac{2h}{a_F^2 k} \left(\frac{\theta_F^R}{\tau_F} - 1 \right)$$

For the other modes two possibilities exist; either $\tau_I = 0$ for all $I \neq F$ or $\tau_I = 0$ for all $I \neq F, J$ and $\tau_J \neq 0$. The second case leads to a contradiction. For the first case the σ_0 evolution equation implies

Table 2. Experiments

<u>Run</u>	<u>Governing Equation</u>	<u>Run Name</u>	<u>θ^*</u>	<u>Length of Integration</u>	<u>Comments</u>
1	PE	PE1	0.008	102500	
2	QG	QG2	0.008	102500	
3	PE	PE3	0.032	202500	
4	BE	BE4	0.032	52500	
5	QG	QG5	0.032	202500	
6	Tuned QG	TQG6	0.032035	102500	h,k altered
7	Perturbed QG	PQG7	0.032	102500	Perturbations added every 5 time units

$$|\tilde{\gamma}_F|^2 = 2 \left(\frac{h}{a_F^2 k} \right)^2 \left(\frac{\theta_F^R}{\tau_F} - 1 \right)$$

Since the left hand side is real and positive, if $x = \tau_F / \theta_F^R$, then $x \in (0,1)$ and satisfies

$$f(x) \equiv x^3 + b^2(x-1) = 0$$

where

$$b^2 = \frac{2}{|\theta_F^R|^2} \left(\frac{h}{a_F^2 k} \right)^2 \gg 1$$

As $f'(x) > 0$ for all real x only a single solution exists. An asymptotic expression for x is

$$x = 1 - b^{-2} + 3b^{-4} + O(b^{-6})$$

3d. Qualitative behavior.

The basic experiments performed are listed as runs 1-5 in Table 2. For a given value of θ^* the qualitative behaviors in these runs are the same. It is possible to select instantaneous states or short evolutions from the various experiments (with the same value of θ^*) which are either very much alike or significantly different. To avoid either prejudice, typical results from the PE runs only are presented here; similar results could be chosen from the filtered equations experiments.

The maps of Ψ , the midlevel streamfunction (Figure 1) show that in spite of the severe truncation a variety of situations are possible. As an aid to visualization slightly more than one wavelength in x is shown in Figure 1. Figure 1a depicts Ψ at a time during run PE1 when the kinetic energy is relatively low while Figure 1b shows Ψ at a slightly later time immediately after a relatively high peak in kinetic energy. Figures 1c-d are similar plots from run PE3. Note the change in contour interval. The Ψ field in the high thermal forcing experiments is roughly three times as intense as that in the low thermal forcing experiments. (Therefore the kinetic energy levels differ by approximately one order of magnitude.) Because there is no β -effect, that is since f is constant, the features on the maps tend to intensify and decay in place.

The time evolutions of the energy variables provide good visualizations of the time behavior of the model. Plotted in Figure 2 are the time evolutions of K , $K-S$ and $A+K$ for experiments 1 and 3. The time intervals contain the times of the maps in Figure 1. In Figure 2 the zero point for $A+K$ is different from the zero point of K and $K-S$ but the scales for the three quantities are identical. Comparing the plots in Figure 2, the low thermal forcing case has longer time scales than the high thermal forcing case and the magnitude of A is several times the magnitude of K in the low thermal forcing case while A and K are roughly the same size in the high thermal forcing case. $K-S$ and $A+K$ are controlled solely by the slowly acting dissipative processes; compared to K , most of the variance of $A+K$ and $K-S$ is associated with the longer time scales. $\left| \frac{d}{dt}(K-S) \right|$ and $|K-S|$ tend to be small compared to $\left| \frac{d}{dt}K \right|$ and $|K|$ respectively. In part this behavior is

connected with our choice of the parameters h and k . In the tuning experiment, for another choice of the parameters, $K-S$ still has less variance and longer time scales than K but does not have a mean close to zero. A partial explanation of this behavior is that whenever there is conversion between A and K both K and S increase by a similar amount; thus K and S should be positively correlated. If K and S are strongly correlated with similar variances - as observed in this system - then the variance of $K-S$ will be small compared to the variance of K .

The sign of $K-S$ is a convenient indicator of the two regimes evident in longer plots like Figure 2. When $K-S$ is positive K tends to be high - roughly 15% above the overall average - and the variances of K and $\frac{d}{dt}K$ are larger than when $K-S$ is negative. Usually the transition to the high K regime occurs during a rapid conversion of A into K following a buildup of A (e.g. near time 5800 in Figure 2a). The transition to the low K regime is generally preceded by a decay in $A+K$ (e.g. near time 56100 in Figure 2b). These regimes tend to persist for long periods of time as can be seen in Figure 2.

Figure 2 suggests and longer plots show that the system is bounded and in particular that σ_0 is bounded away from zero. While we can prove that the system is bounded we cannot prove that σ_0 must be positive. Physically we expect the system to be bounded as long as the drag coefficients - h and k - are positive. That is, both friction and heating tend to drive the system towards finite states - the states of no motion and radiative equilibrium respectively. We expect the system to remain in the neighborhood of these states. Budget constraints

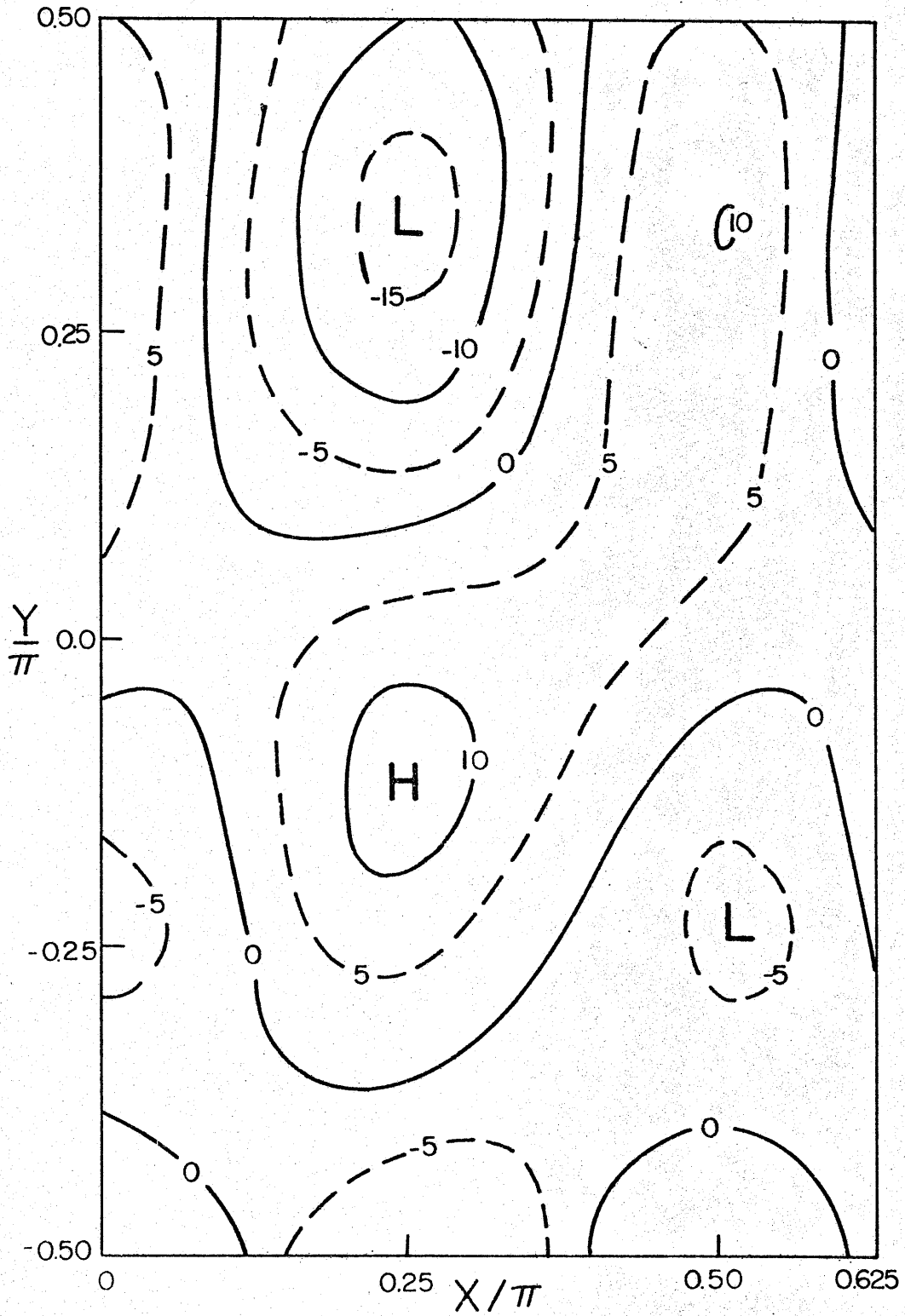


Figure 1a. Map of ψ ($\times 10^3$) at time 5670. Run PE1.

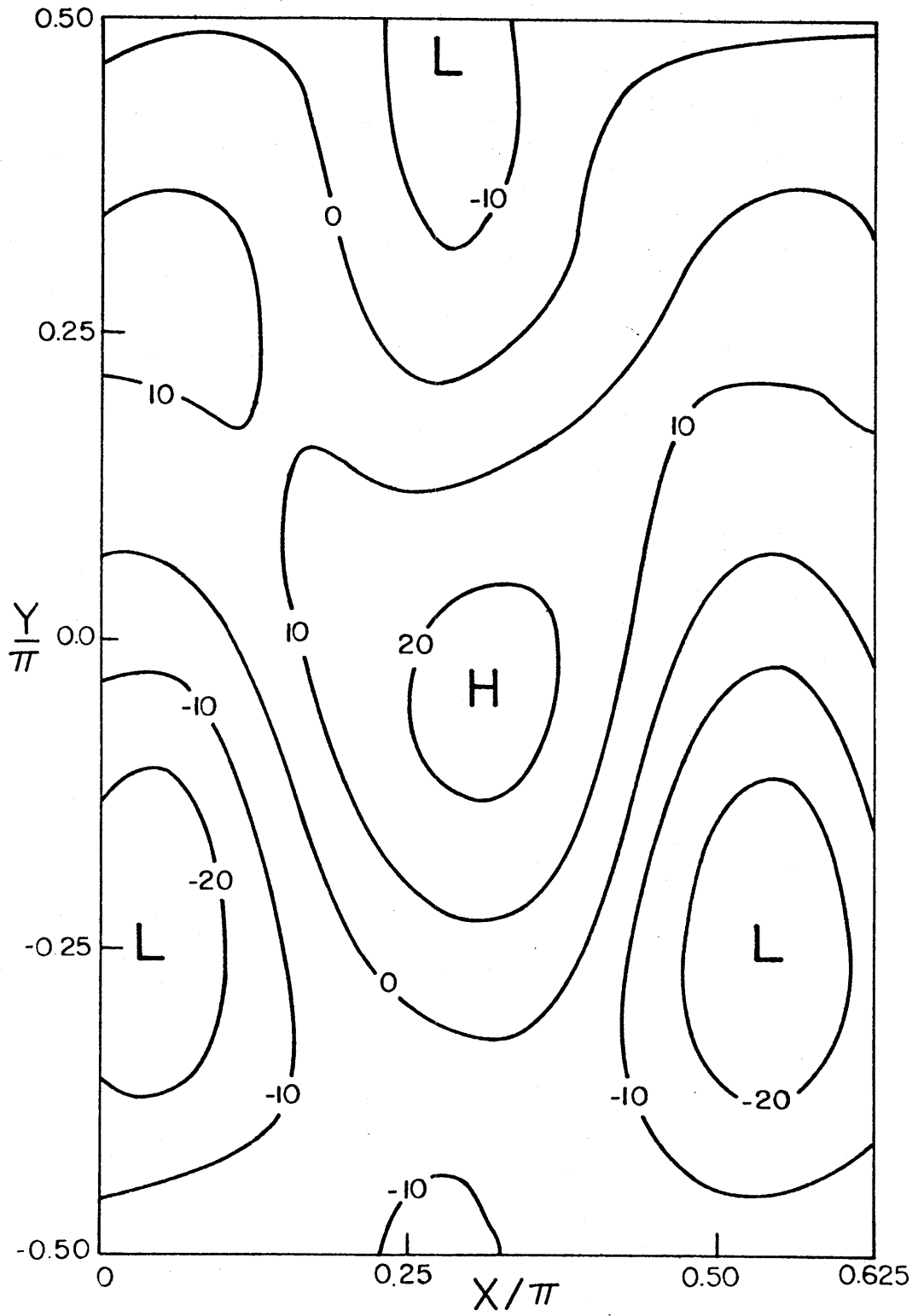


Figure 1b. Map of ψ ($\times 10^3$) at time 5795. Run PE1.

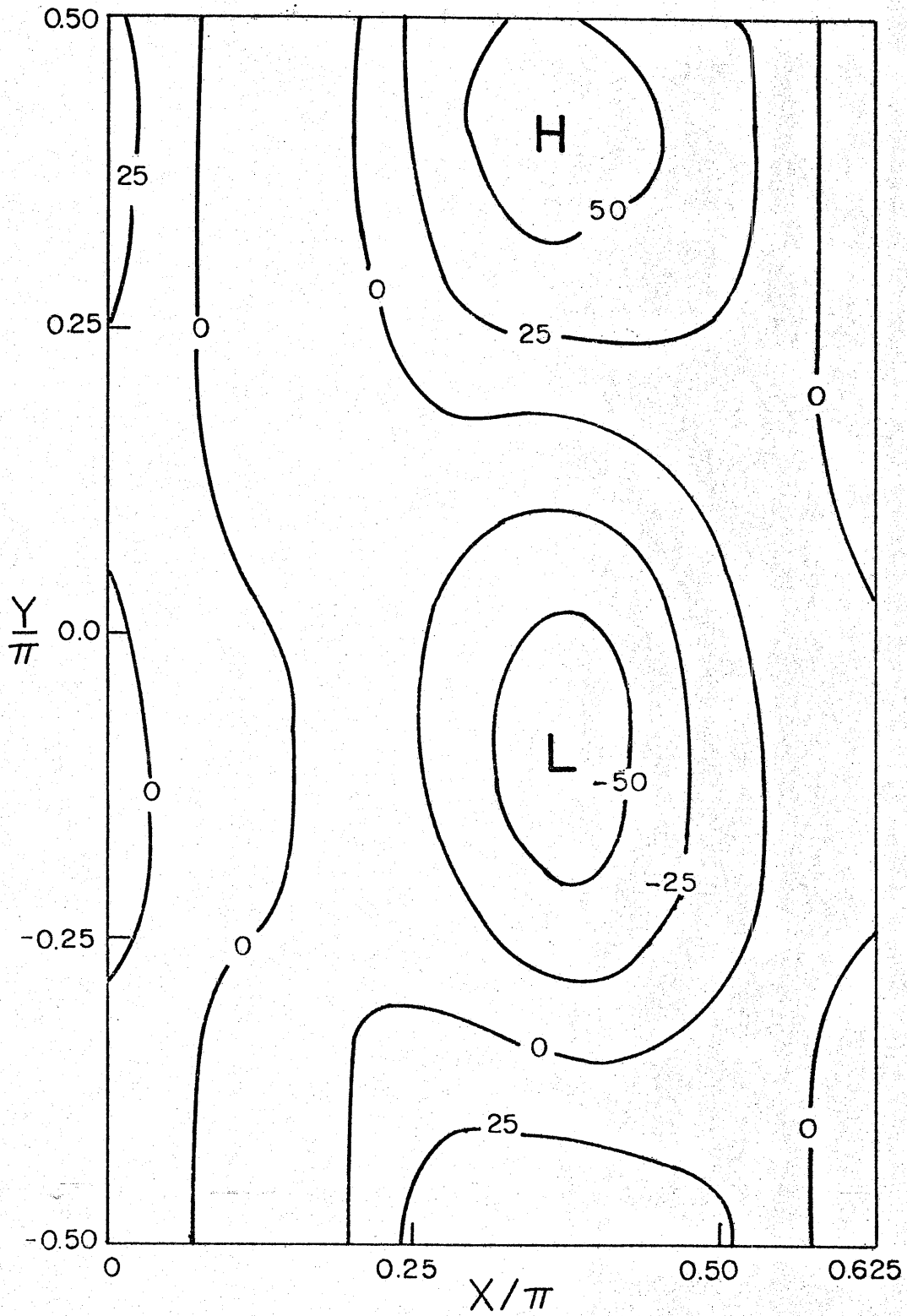


Figure 1c. Map of Ψ ($\times 10^3$) at time 56135. Run PE3.

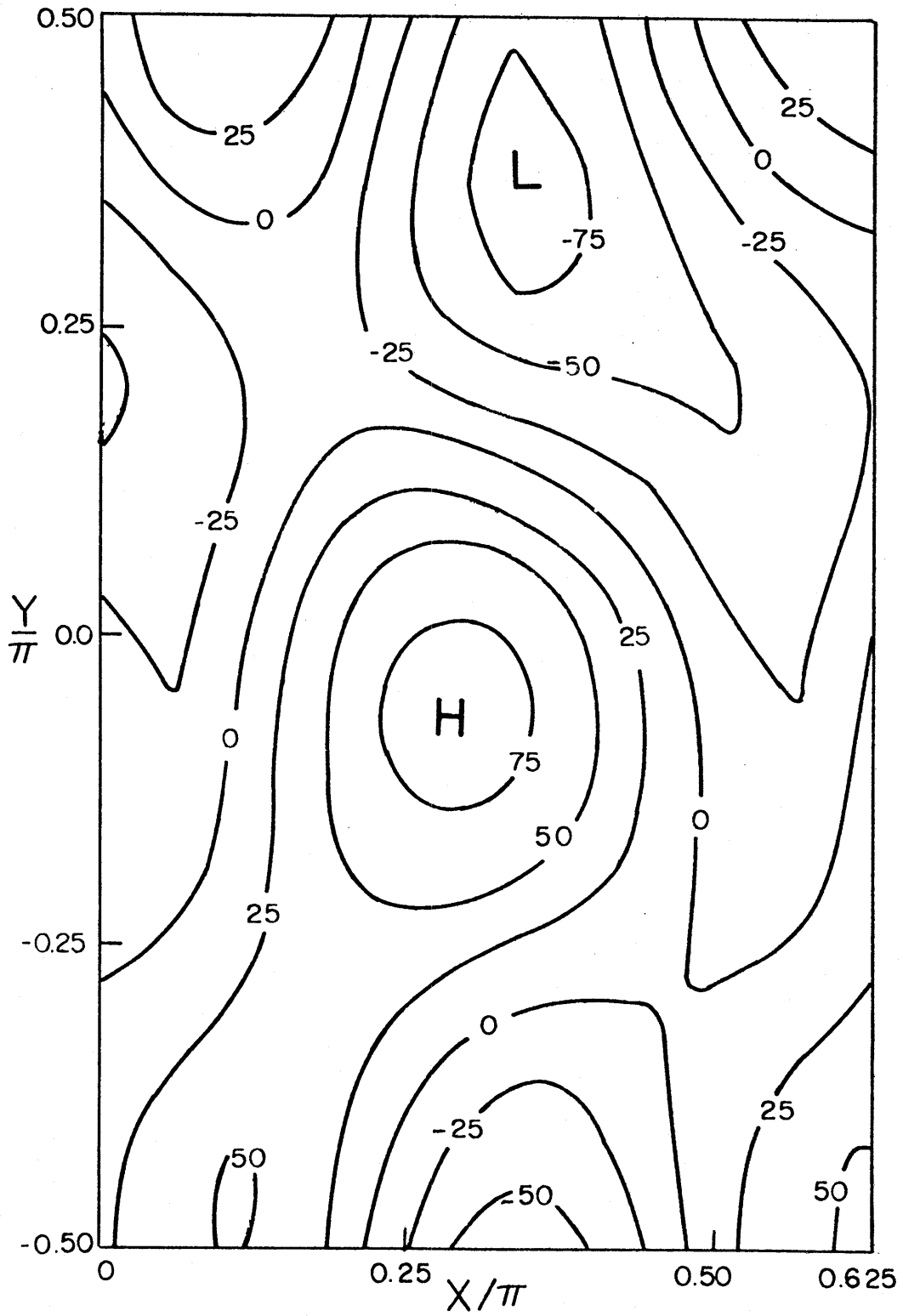


Figure 1d. Map of Ψ ($\times 10^3$) at time 56425. Run PE3.

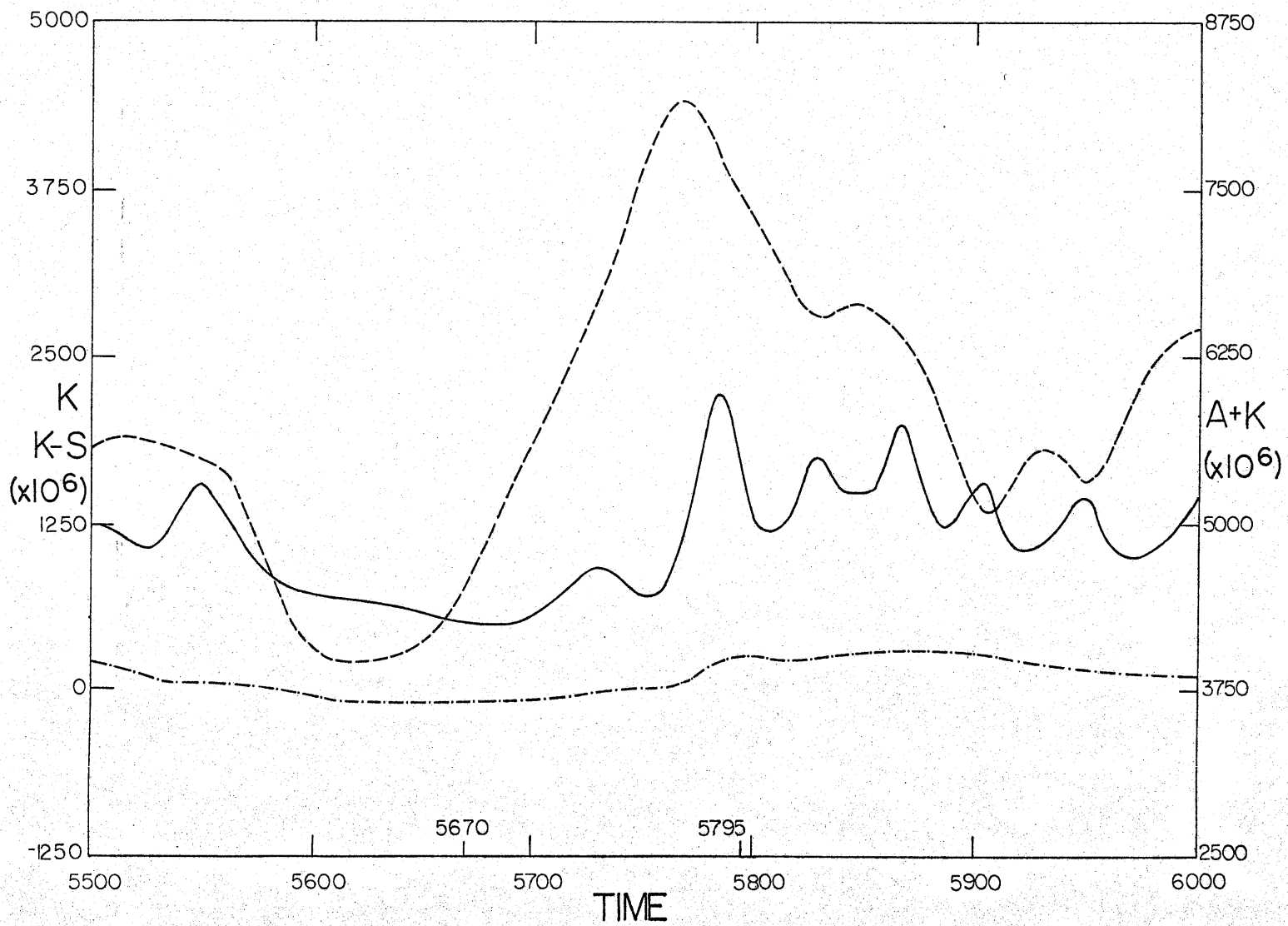


Figure 2a. Time evolution of K (————), A+K (-----) and K-S (-·-·-·-·). Run PE1. Scale for A+K is on right.

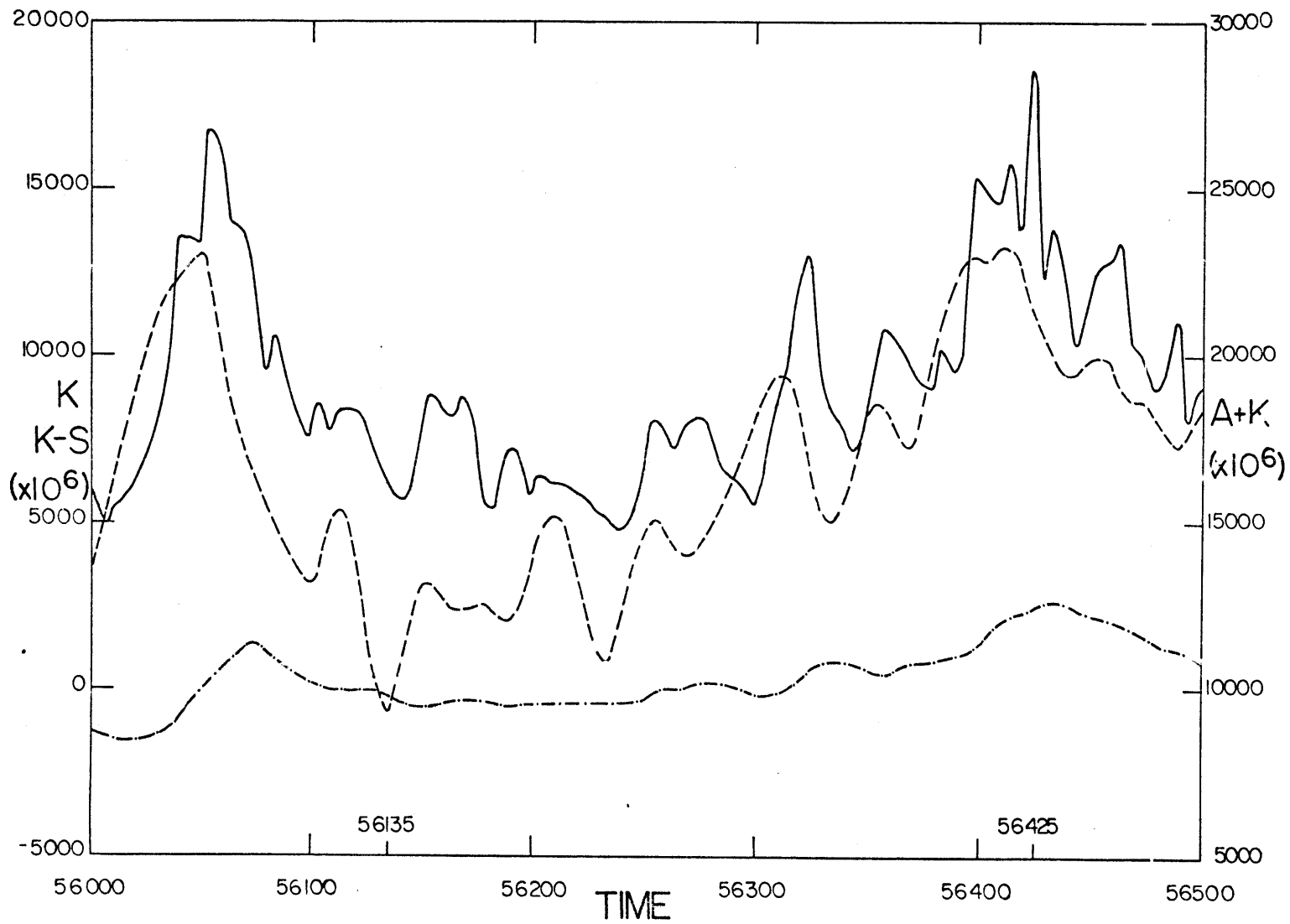


Figure 2b. Time evolution of K (—), $A+K$ (-----) and $K-S$ (-·-·-·-). Run PE3. Scale for $A+K$ is on right.

(see Section 5) imply that the time average of σ_0 is positive but do not ensure that σ_0 is always positive.

To prove that the system is bounded we seek a quadratic positive definite quantity, Q^2 , which is conserved in the absence of friction and heating. If the friction and heating are linear then $\frac{d}{dt}Q^2$ will be constant on (generalized) conic sections in phase space. For this system an appropriate choice is

$$\begin{aligned} Q^2 &= 2bK + \sum_I |\theta_I|^2 + (\theta_0' - a)^2 + (\sigma_0 - b)^2 \\ &= 2b(K - \sigma_0) + (\theta_0'^2 + \sigma_0^2 + \sum_I |\theta_I|^2) \\ &\quad - 2a\theta_0' + (a^2 + b^2) \end{aligned}$$

where $\theta_0' = \theta_0 - \theta_0^R$, a is an arbitrary constant and b is an arbitrary constant greater than zero. Since $(\theta_0'^2 + \sigma_0^2 + \bar{\theta}^2)$,

θ_0' and $(K - \sigma_0)$ are conserved in the absence of friction and heating so is Q^2 . The evolution of Q^2 is governed by

$$\begin{aligned} \frac{d}{dt}Q^2 &= -h \sum_I |\theta_I - \theta_I^R/2|^2 - bD - h(\theta_0' - \sigma_0 + \frac{c}{2})^2 \\ &\quad - h(\sigma_0 - \frac{b}{2})^2 + h\left(\frac{\theta_0'^2}{2} + \frac{b^2}{4} + (\theta_0' + \frac{c}{2})^2\right) \end{aligned}$$

where $c = b - a - \theta^*$. $\frac{d}{dt}Q^2 = 0$ defines an ellipsoid, E , in phase space, where the phase space is defined by the real and imaginary parts of the

spectral variables, excluding χ_I in the QG and BE cases. Within E, $\frac{d}{dt}Q^2 > 0$, while outside of E $\frac{d}{dt}Q^2 < 0$. Once transients die out Q^2 is bounded by the maximum of Q^2 on E. Thus the system is bounded.

Note that one point on E is

$$\psi_x = \tau_x = \chi_x = \theta_x - \frac{\theta_x^R}{2} = \theta_0' - \sigma_0 + \frac{c}{2} = 0$$

and

$$\sigma_0 = \frac{b}{2} - \left(\left(\frac{b}{2}\right)^2 + \frac{\theta^{*2}}{2} + \left(\theta^* + \frac{c}{2}\right)^2 \right)^{1/2} < 0$$

Thus this analysis fails to show that σ_0 is bounded away from zero.

4. Gravity waves, digital filtering and data sampling.

The prescribed boundary conditions - the vanishing of the vertical velocity in pressure coordinates at the top and bottom of the model domain - prohibit external gravity waves. The adiabatic inviscid equations possess a solution of no motion in which σ_0 and θ_0 are constants and all other variables are zero. Linearizing about this basic state and assuming a time dependence of the form $e^{-i\gamma t}$ two solutions are found. The first, the geostrophic mode with $\gamma = 0$, is found for the QG, balance and primitive equations. The second solution represents (internal) gravity waves and is present only in the PE case; the frequency dispersion relationship is

$$(4) \quad \gamma^2 = \sigma_0 a_I^2 + 1$$

For σ_0 positive the gravity wave modes are neutrally stable.

For the low thermal forcing case, estimating the size of σ_0 as 10^{-3} gives γ in the interval 1.0 to 1.064 for the retained wave vectors. Discrete Fourier transforms of some time series of the χ_I evolving according to the PE were calculated. Using initial conditions obtained from the final state of a PE model integration no evidence of gravity waves was found. Using the same initial conditions but setting the dissipative constants k and h equal to zero, gravity waves developed almost immediately. Using initial conditions obtained from the final state of a QG model run and integrating the PE, gravity waves which dissipated with a time scale of 100 were present. We conclude gravity waves are not present in the PE model once transients die out when the thermal forcing is low.

When the thermal forcing is high gravity waves are always present in the PE solution. Frequency spectra of the nonlinear QG model solutions are flat and have little amplitude for ν greater than about 0.35, while the nonlinear PE model solutions of χ_I and τ_I exhibit peaks in the frequency range 0.62 to 1.96, corresponding to periods from 3.2 to 10.0. Most of the power is concentrated in periods from 5.5 to 8.2. Estimating σ_0 as 10^{-2} , (4) gives ν in the interval 1.0 to 1.64. Another family of linear gravity waves develops during the growth of disturbances from the zonal steady state solutions. During these experiments the PE model χ_I exhibit spectral peaks for $\nu = 0.57$ to 0.79, corresponding to periods from 8.0 to 11.0.

In making the QG or balance assumption the possibility of gravity wave behavior is eliminated. Therefore we evaluate the success or failure of the QG model in terms of how well it simulates the behavior of the PE model on time scales longer than the gravity wave time scale. For the low thermal forcing case this presents no problem; gravity waves are not present. The statistics presented in the next section are calculated from the model output sampled every 5 time units. For the high thermal forcing case the time series of the PE spectral variables are filtered to eliminate the gravity waves. The digital filter used is one of Kaiser's (1974) I_0 -sinh window nonrecursive (i.e., moving average) filters. It is a low pass filter with a total length of 128 time units and a transition band, in terms of period, from 9.0 to 11.0 time units. A small correction is added to each filter coefficient to force a unit response at zero frequency. The maximum response error outside the transition band is 0.5%. The filter uses data every time unit as input and is applied to the original time series every 5 time units. Since the

filter removes frequencies higher than the Nyquist frequency of this sampling rate, an adequate representation is obtained. The effects of the digital filter on the output of the filtered equations models are small (order 1%) and the effects on the filtered equations models' statistics are small compared to sampling errors. However to avoid any possible bias the filter is used to sample the spectral variables of all the runs excluding the low thermal forcing runs.

Gravity waves affect the model statistics directly and indirectly. Second moment and higher moment statistics, as for example variances, are directly affected by the presence of gravity waves. Mean values will not be directly affected except possibly through sampling errors. Indirectly, through nonlinear interactions, the presence of gravity waves may affect any of the statistics. Comparing the statistics obtained from filtered and unfiltered PE model time series isolates the direct effect of the gravity waves. Comparing the statistics of the filtered PE model time series with the BE model statistics isolates the indirect effect of the gravity waves. This last comparison is only approximate since besides eliminating the gravity waves, the BE neglect some of the dynamics. A final motivation for filtering is to eliminate the high frequencies before evaluating the short term error statistics. When verifying QG model predictions it seems reasonable to use the filtered PE time series as the true initial and final conditions.

5. Model statistics.

We describe and compare the climates simulated by the models governed by (2) primarily through the sample means and variances of the model and energy variables. Covariances or equivalently correlations are also of interest and some of these are discussed below when the budgets which maintain the mean state are considered. However the invariance properties (see Section 5b) and the dynamics of the system constrain the statistics so that it is not desirable (and in any case it is certainly not possible) to consider every possible statistic.

In the remainder of this paper we find it convenient to refer to the variables appearing in the governing equations in several ways. To avoid confusion the conventions followed are detailed here. As before the "continuous variables" refer to the variables appearing in the non-dimensional horizontally continuous governing equations and the "spectral variables" refer to the variables appearing in (2), the spectral governing equations. "Model variables" will mean the set of real and imaginary parts of the spectral variables. The " ζ_I variables" will denote the set of real and imaginary parts of the corresponding spectral variables ζ_I for all I in the truncation not equal to 0. The " ζ_n variables", where n is a particular integer will denote $\text{Re } \zeta_n$ and $\text{Im } \zeta_n$.

For convenience in constructing tables the model and energy variables have been numbered. (See Table 3.) Although the model state is most appropriately described by a vector of the 50 or the first 26 model variables, each of the model variables will be considered a scalar function of (discrete) time in most of the statistical comparisons reported here. Tables 5-7 display some of the sample statistics. The

Table 3a. Model variables indexing scheme.

<u>Variable</u>	<u>Index of</u>	
	<u>Real part</u>	<u>Imaginary part</u>
σ_0	1	
θ_0	2	
ψ_1	3	4
ψ_2	5	6
ψ_3	7	8
ψ_4	9	10
ψ_5	11	12
ψ_6	13	14
τ_1	15	16
τ_2	17	18
τ_3	19	20
τ_4	21	22
τ_5	23	24
τ_6	25	26
χ_1	27	28
χ_2	29	30
χ_3	31	32
χ_4	33	34
χ_5	35	36
χ_6	37	38
θ_1	39	40
θ_2	41	42
θ_3	43	44
θ_4	45	46
θ_5	47	48
θ_6	49	50

Table 3b. Energy variables indexing scheme.

<u>Variable</u>	<u>Index</u>
A_Z	1
A_E	2
K_Z	3
K_E	4
C_Z	5
C_E	6
G_Z	7
G_E	8
D_Z	9
D_E	10
C_A	11
C_K	12
$\frac{d}{dt} A_Z$	13
$\frac{d}{dt} A_E$	14
$\frac{d}{dt} K_Z$	15
$\frac{d}{dt} K_E$	16

time interval between observations is 5. All samples begin with time 2000; by time 2000 any transient behavior associated with the initial conditions has died out. The statistics are calculated from the filtered data except for runs PE1 and QG2 and in those cases when an asterisk is appended to the name of a run (e.g. QG5*). In each of these tables the numerical entries in the first column, identifying the rows, are the energy or model variable indices. The row labeled D.F. is the number of degrees of freedom of the sample. Exponentiation is denoted by ** and subscripts are not lowered but are enclosed in parentheses.

5a. Description of the statistical methods.

A brief description of the sample statistics used is now presented. Suppose there are N_x observations of a scalar quantity x . The sample mean is \bar{x} , where the averaging operator is defined by

$$\bar{x} = \frac{1}{N_x} \sum_I^N x_i$$

Here and below the overbar will be used to denote both time and sample averages; all time averages are in fact calculated as sample averages.

The sample variance is

$$s_x^2 = \overline{x^2} - \bar{x}^2$$

and s_x is the standard deviation of x . N_x' , the effective number of observations, i.e., the number of degrees of freedom, is defined by

$$\sigma^2(\bar{x}) = \sigma_x^2 / N_x'$$

where σ_x^2 is the population variance and $\sigma^2(\bar{x})$ is the variance of the sample mean determined from N_x observations. Laurmann and Gates (1977) show that

$$(5) \quad \frac{N_x}{N_x'} = 1 + 2 \sum_{m=1}^{N_x-1} r_{mx}$$

where

$$(6) \quad r_{mx} = \frac{\left\{ \sum_{i=1}^{N_x-m} (x_i - \mu_x)(x_{i+m} - \mu_x) \right\}}{\left\{ \sum_{i=1}^{N_x} (x_i - \mu_x)^2 \right\}}$$

μ_x , the population mean, is generally unknown.

Under the assumption that the true population has certain ideal features and in the limit of large N_x' ,

$$\bar{x} \sim N(\mu_x, s_x^2/N_x')$$

$$N_x' \frac{s_x^2}{\sigma_x^2} \sim \chi^2(N_x') \sim N(N_x', 2N_x')$$

where the symbols $A \sim N(\mu, \sigma^2)$ means that A is a normally distributed random variable with mean μ and variance σ^2 , and $B \sim \chi^2(\nu)$ means that B is a chi-squared random variable with ν degrees of freedom. The above relationships imply

$$\mu_x = \bar{x} \left(1 \pm \frac{1}{t_x} \right)$$

$$\sigma_x^2 = s_x^2 \left(1 \pm \left(\frac{2}{N_x'} \right)^{\frac{1}{2}} \right)$$

where

$$t_x = \bar{x} \left(\frac{s_x^2}{N_x'} \right)^{-\frac{1}{2}}$$

is a statistic similar to Student's t-statistic. (Selected values of $\left(\frac{2}{N_x'} \right)^{\frac{1}{2}}$ are presented in Table 4a.) Here and below "±" will indicate a 0.68 (or 68%) confidence interval. If "±" is replaced with "±α" for any $\alpha > 0$, then the confidence level is one minus twice the probability that $z > \alpha$, where $z \sim N(0,1)$.

Suppose there is also a control sample of N_y observations of an independent quantity y , which has population mean and variance equal to μ_y and σ_y^2 . Let

$$t_{xy} = (\bar{x} - \bar{y}) \left(\frac{s_x^2}{N_x'} + \frac{s_y^2}{N_y'} \right)^{-\frac{1}{2}}$$

and

$$F_{xy} = s_x^2 / s_y^2$$

For ideal populations and in the limit of large N_x' and N_y'

Table 4a. Relative uncertainty in σ_x^2 expressed as a percentage.

N_x'	$100 \left(\frac{2}{N_x'} \right)^{\frac{1}{2}}$
250	8.9
500	6.3
1000	4.5
2000	3.2

Table 4b. Relative uncertainty in σ_x^2/σ_y^2 expressed as a percentage.

N_x'	N_y'	$100 \left(\frac{2(N_x' + N_y')}{N_x' N_y'} \right)^{\frac{1}{2}}$
250	1000	10.0
500	1000	7.7
1000	1000	6.3
250	2000	9.5
500	2000	7.1
1000	2000	5.5
2000	2000	4.5

$$(\bar{x} - \bar{y}) \sim N(\mu_x - \mu_y, \frac{s_x^2}{N_x'} + \frac{s_y^2}{N_y'})$$

$$F_{xy} \frac{\sigma_y^2}{\sigma_x^2} \sim N(1, \frac{2(N_x' + N_y')}{N_x' N_y'})$$

Thus

$$(\mu_x - \mu_y) = (\bar{x} - \bar{y}) (1 \pm \frac{1}{t_{xy}})$$

$$\sigma_x^2 / \sigma_y^2 = F_{xy} (1 \pm (\frac{2(N_x' + N_y')}{N_x' N_y'})^{1/2})$$

(Selected values of $(\frac{2(N_x' + N_y')}{N_x' N_y'})^{1/2}$ are presented in Table 4b.)

The difference in means may be written in terms of a percentage of the observed control sample mean, i.e.,

$$\frac{100}{\bar{y}} (\mu_x - \mu_y) = \frac{100}{\bar{y}} (\bar{x} - \bar{y}) (1 \pm \frac{1}{t_{xy}}) = p (1 \pm \frac{1}{t_{xy}})$$

thus defining the statistic p . Comparing two model runs yields a series of M t_{xy} and F_{xy} statistics: t_{xy}^m , F_{xy}^m , $m=1, \dots, M$.

Convenient summary statistics are

$$T^2 = \sum_{1}^M (t_{xy}^m)^2$$

and

$$F^2 = \frac{N_x' N_y'}{2(N_x' + N_y')} \sum_{I=1}^M (F_{xy}^m - 1)^2$$

For large N_x' and N_y' , under the null hypothesis that the two simulated climates are identical and that the t_{xy}^m and F_{xy}^m statistics are independent, T^2 and F^2 have $\chi^2(M)$ distributions.

5b. Invariance properties and the effect of persistence on the number of independent observations.

In the specific problem considered here the population mean, μ , is zero for most model variables. Since the model is invariant with respect to a change in x origin, each solution is a member of a family of solutions differing only in x origin. If we identify the model climate with an average over initial conditions it is proper to average over such families of solutions. In particular, given any one solution we may average it with the solution having x shifted by π/I_x , before averaging over the entire family. Therefore $\mu = 0$ for all model variables associated with nonzero values of I_x . This shows that the ensemble mean state is zonal. Since the model is also invariant with respect to a rotation of 180° the same argument implies that the ensemble zonal mean state is symmetric about $y = 0$. Therefore $\mu = 0$ for the imaginary parts of the model variables associated with zero values of I_x .

For those model variables for which the invariance properties imply $\mu = 0$, N_x/N_x' has been calculated using (5) and (6) with $\mu_x = 0$.

The time between independent observations, T_0 , is equal to N_x/N_x' times the time interval between observations. T_0 varies from variable to variable and from sample to sample. The most persistent model variables are those associated with $\underline{I} = (8,0)$. The evolution of these variables as well as those associated with $\underline{I} = (0,4)$ is primarily controlled by dissipative processes as there are only limited interactions with variables associated with other wave vectors. The model variables associated with $\underline{I} = (0,4)$ or $\underline{I} = (8,0)$ will be called corner variables because these \underline{I} are at the corners of the truncation. T_0 is typically 100 to 200 for the corner variables, but may be an order of magnitude larger. Excluding the corner variables the average of the values of T_0 calculated is approximately 40 for the high thermal forcing case and 60 for the low thermal forcing case. Since the evolution equations couple all variables (strongly, except the corner variables and energy invariants) and since there is essentially one scale of motion, we expect there to be a single value of T_0 characterizing the entire system. For the purpose of discussion we will take $T_0 = 100$ as a conservative estimate applicable to all variables and models. Thus N_x' is simply the sample length divided by 100.

5c. Reliability of the statistics.

The statistical methods assume ideal populations which are normally distributed and an unbiased sampling procedure which yields independent observations. These assumptions present difficulties when these methods are applied. Variables such as energies which are non-negative cannot be normally distributed since there is zero probability of a value being less than zero. In fact since all the variables are bounded, once

transients die out, none of the variables can be normally distributed. It is observed that while many of the model variables are approximately normally distributed an equal number are distinctly not normally distributed. Typically members of this second group have distributions which are too highly peaked; a few of these distributions are noticeably skewed. The statistical tests are fairly robust with respect to non-normality, especially for large samples. Of greater importance is the non-independence of the observations. Assuming the sample size is N_x' instead of N_x is an attempt to bypass this difficulty. Neither normality nor independence is necessary to assure the validity of the point estimates \bar{x} and s_x^2 , but if these assumptions do not hold then the levels of significance and confidence intervals reported will differ from the true levels of significance and the true confidence intervals. The estimates of error we give will all be approximate. Strictly T_0 should be different for each variable and model run. Choosing T_0 larger than necessary avoids making unexpected Type I errors, e.g., concluding the means of two samples are different when in fact they are the same. However the larger T_0 is chosen the larger will be the confidence intervals for a given significance level, so there is a greater risk of making Type II errors, e.g., concluding the means of two samples are the same when in fact they are different. Since the present concern is to identify the most significant differences between model statistics this approach is adequate. Another sort of difficulty arises when comparing several statistics at once. If $\mu_x = 0$ at the 90% confidence level and also if $\mu_y = 0$ at the 90% confidence level then the compound statement that $\mu_x = \mu_y = 0$ will usually be associated with a lower confidence level. Finally, although we generally ignore the fact that

the variables are coupled dynamically, this is a powerful tool, as is evident in the discussion of the budgets below.

To illustrate the effects of the invariance properties and of sampling and filtering the model variable statistics of run QG5 are displayed for different samples and before and after digital filtering. Tables 5a-e display respectively the sample means, standard deviations and the t_x , t_{xy} and F_{xy} statistics. In the latter two tables the control sample is the filtered sample of length 200000. Unless otherwise noted the results discussed below apply equally to all the runs.

Because all samples begin with time 2000, the samples used in Table 5 are not independent and the uncertainties of $(\mu_x - \mu_y)$ and of σ_x^2 / σ_y^2 are smaller than indicated by the previous discussion. Provided T_0 is chosen properly, the t_{xy} and F_{xy} statistics comparing different samples must show the population means and variances are the same. These statistics are useful for comparing the relative effects of filtering and sampling.

The means and t_x statistics (Table 5a and Table 5c) show that all the model variable means which should be zero because of the invariance properties are in fact not significantly different from zero. Of these variables, the corner variables tend to have t_x statistics with the largest absolute magnitudes implying that the corner variables have the longest persistence times. There is a circular argument here since T_0 is chosen to insure the first result. The magnitudes of the t_x statistics are a check showing that the choice of T_0 is appropriate.

Changes in means due to changing the sample length are, as expected, small compared to their respective standard deviations (Table 5d). The corner variables exhibit the comparatively largest changes. The means

of the energy variables (excluding 13-16, which are effectively zero) typically change by 1% for the low thermal forcing experiments when the sample length is doubled from 50000 to 100000 and by 2% for the high thermal forcing experiments when the sample length is doubled from 100000 to 200000. The variances of the model variables typically change 2 to 4% when the sample length is doubled from 50000 to 100000 or from 100000 to 200000. (See Table 5b and Table 5d.) Variances of the energy variables change even less under these conditions.

The columns in Table 5 labeled QG5* contain statistics obtained from the unfiltered data of run QG5. Similar results are expected to hold for all the runs excluding PE3 because none of these runs have significant amplitude in the high frequency part of their discrete Fourier transforms. Comparing the differences in statistics between samples of the same length of filtered and unfiltered data to the differences in statistics between samples of different lengths, it is clear that the effect of filtering is negligible compared to the effect of sampling. Changes to the means due to filtering are $O(10^{-6})$ for both model and energy variables. Variances of model variables are always decreased by filtering but the changes are small compared to sampling changes. Changes to the variances of the energy variables due to filtering are the same size or smaller than changes due to sampling.

5d. Statistical intercomparisons.

The statistics of the model variables are compared in Tables 6a-f which display respectively the means, standard deviations and t_x , t_{xy} , F_{xy} and p statistics. In these tables, the control run for the low thermal forcing experiments is PE1; the control run for all other

TABLE 5A. MEANS OF MODEL VARIABLES (X10**6)

RUN	QG5	QG5	QG5	QG5	QG5*
D.F.	2000	1000	500	250	2000
1	6017.67	5970.83	5905.68	5884.01	6017.69
2	358017.59	357971.39	357907.78	357886.11	358017.59
3	1006.85	942.07	918.09	892.77	1006.86
4	-58.25	-220.21	-215.77	-171.12	-58.25
5	21.82	-8.51	-136.70	-3.94	21.82
6	-9.51	-35.61	6.70	26.88	-9.51
7	6.02	91.96	-106.64	65.31	6.01
8	-79.00	-107.50	-423.67	-482.22	-79.01
9	116.73	272.88	247.68	198.24	116.73
10	-34.71	-183.37	-278.63	-312.70	-34.73
11	15.28	28.04	43.59	128.08	15.27
12	43.39	97.68	50.10	-43.84	43.38
13	-11.69	4.14	19.90	-46.76	-11.69
14	-4.26	-51.29	54.23	70.36	-4.26
15	3694.04	3663.94	3653.43	3674.71	3694.04
16	-3.25	4.47	-80.71	-134.47	-3.25
17	21.06	-9.08	-137.51	-6.99	21.05
18	-8.86	-34.26	9.85	34.73	-8.86
19	-3.78	18.00	-19.48	-18.69	-3.77
20	-0.99	-3.09	-41.56	-30.99	-1.00
21	28.66	36.06	33.82	58.52	28.64
22	11.39	1.71	-37.27	-31.22	11.40
23	6.91	-2.13	-83.00	-32.58	6.91
24	58.56	105.39	216.17	199.90	58.57
25	-11.89	4.08	15.33	-49.56	-11.89
26	-4.00	-51.80	53.86	68.30	-4.00
27	-38.92	-40.07	-45.14	-52.28	-38.91
28	1.01	3.73	-2.34	-12.82	1.01
29	0.16	-0.11	-1.12	0.03	0.16
30	-0.06	-0.22	0.19	0.52	-0.05
31	3.21	4.48	4.26	-20.97	3.20
32	9.85	14.56	7.55	10.15	9.85
33	-2.72	-2.44	-8.47	-8.91	-2.71
34	-4.87	-6.05	-7.31	-4.90	-4.86
35	-1.67	-4.70	-12.35	-13.24	-1.68
36	2.85	4.09	11.60	13.16	2.85

TABLE 5B. STANDARD DEVIATIONS OF MODEL VARIABLES

(x10**6)

RUN	QG5	QG5	QG5	QG5	QG5*
D.F.	2000	1000	500	250	2000
1	1813.52	1797.49	1801.67	1808.78	1816.08
2	967.28	940.62	959.41	974.19	967.59
3	5550.84	5520.34	5513.56	5520.49	5552.35
4	6406.85	6338.39	6286.73	6220.17	6407.45
5	855.75	824.68	824.96	817.60	855.87
6	749.53	761.74	771.99	767.20	749.65
7	6516.62	6477.34	6321.70	6352.34	6520.20
8	6408.77	6369.09	6216.19	6194.35	6412.26
9	6496.19	6462.68	6492.45	6491.35	6499.69
10	6468.03	6440.85	6510.08	6430.15	6471.58
11	6256.97	6206.00	6025.89	6066.50	6258.99
12	6094.85	6092.02	6180.37	6103.74	6096.62
13	601.02	584.29	572.80	552.30	601.11
14	584.73	586.06	598.06	593.35	584.82
15	3191.18	3203.62	3261.47	3283.75	3191.69
16	2959.27	2962.37	2950.86	2993.98	2959.81
17	2319.39	2300.43	2306.93	2303.15	2320.15
18	2236.03	2209.12	2223.17	2224.12	2237.06
19	2629.95	2621.57	2567.73	2548.36	2630.79
20	2581.92	2581.74	2576.56	2595.47	2582.95
21	2622.96	2593.95	2583.43	2617.34	2623.91
22	2584.12	2584.17	2597.67	2532.34	2585.04
23	3007.41	2987.20	3000.72	3041.89	3008.66
24	2924.89	2931.86	2960.43	3007.49	2926.10
25	2200.79	2183.68	2134.90	2150.22	2201.03
26	2160.80	2161.61	2155.81	2103.96	2161.15
27	591.01	586.73	592.67	597.64	591.20
28	563.82	560.85	561.59	563.56	564.10
29	395.24	392.17	392.00	392.26	396.55
30	398.37	390.52	390.68	392.69	399.65
31	651.50	645.36	642.21	622.18	652.06
32	657.18	650.36	650.66	652.03	657.81
33	653.02	644.58	631.63	633.53	653.69
34	652.21	645.58	633.50	622.84	652.75
35	581.10	573.03	561.83	563.25	581.29
36	572.38	565.24	572.08	572.05	572.59

TABLE 5C. T(X)-STATISTICS OF MODEL VARIABLES

RUN	QG5	QG5	QG5	QG5	QG5*
D.F.	2000	1000	500	250	2000
1	148.396	105.043	73.296	51.435	148.187
2	16552.613	12034.725	8341.616	5808.572	16547.312
3	8.112	5.397	3.723	2.557	8.110
4	-0.407	-1.099	-0.767	-0.435	-0.407
5	1.140	-0.326	-3.705	-0.076	1.140
6	-0.567	-1.478	0.194	0.554	-0.567
7	0.041	0.449	-0.377	0.163	0.041
8	-0.551	-0.534	-1.524	-1.231	-0.551
9	0.804	1.335	0.853	0.483	0.803
10	-0.240	-0.900	-0.957	-0.769	-0.240
11	0.109	0.143	0.162	0.334	0.109
12	0.318	0.507	0.181	-0.114	0.318
13	-0.870	0.224	0.777	-1.339	-0.869
14	-0.325	-2.767	2.028	1.875	-0.325
15	51.769	36.167	25.048	17.694	51.760
16	-0.049	0.048	-0.612	-0.710	-0.049
17	0.406	-0.125	-1.333	-0.048	0.406
18	-0.177	-0.490	0.099	0.247	-0.177
19	-0.064	0.217	-0.170	-0.116	-0.064
20	-0.017	-0.038	-0.361	-0.189	-0.017
21	0.489	0.440	0.293	0.354	0.488
22	0.197	0.021	-0.321	-0.195	0.197
23	0.103	-0.023	-0.619	-0.169	0.103
24	0.895	1.137	1.633	1.051	0.895
25	-0.242	0.059	0.161	-0.364	-0.242
26	-0.083	-0.758	0.559	0.513	-0.083
27	-2.945	-2.160	-1.703	-1.383	-2.944
28	0.080	0.210	-0.093	-0.360	0.080
29	0.018	-0.008	-0.064	0.001	0.018
30	-0.007	-0.018	0.011	0.021	-0.005
31	0.220	0.219	0.148	-0.533	0.220
32	0.670	0.708	0.259	0.246	0.670
33	-0.186	-0.120	-0.300	-0.222	-0.185
34	-0.334	-0.296	-0.258	-0.124	-0.333
35	-0.129	-0.259	-0.492	-0.372	-0.129
36	0.223	0.229	0.453	0.364	0.223

TABLE 5D. T(X,Y)-STATISTICS OF MODEL VARIABLES

RUN	QG5	QG5	QG5	QG5	QG5*
D-F.	2000	1000	500	250	2000
1	0.0	-0.671	-1.242	-1.101	0.000
2	0.0	-1.256	-2.285	-2.013	-0.000
3	0.0	-0.302	-0.322	-0.308	0.000
4	0.0	-0.657	-0.499	-0.270	-0.000
5	0.0	-0.938	-3.814	-0.467	-0.000
6	0.0	-0.890	0.422	0.709	-0.000
7	0.0	0.342	-0.354	0.139	-0.000
8	0.0	-0.115	-1.102	-0.967	-0.000
9	0.0	0.623	0.403	0.187	-0.000
10	0.0	-0.595	-0.750	-0.644	-0.000
11	0.0	0.053	0.093	0.276	-0.000
12	0.0	0.230	0.022	-0.213	-0.000
13	0.0	0.693	1.092	-0.937	0.000
14	0.0	-2.074	1.965	1.878	0.000
15	0.0	-0.243	-0.250	-0.088	-0.000
16	0.0	0.067	-0.525	-0.654	-0.000
17	0.0	-0.337	-1.373	-0.181	-0.000
18	0.0	-0.296	0.168	0.292	-0.000
19	0.0	0.214	-0.122	-0.087	0.000
20	0.0	-0.021	-0.315	-0.172	-0.000
21	0.0	0.073	0.040	0.170	-0.000
22	0.0	-0.097	-0.375	-0.250	0.000
23	0.0	-0.078	-0.599	-0.194	-0.000
24	0.0	0.413	1.067	0.703	0.000
25	0.0	0.188	0.253	-0.260	-0.000
26	0.0	-0.571	0.537	0.511	0.000
27	0.0	-0.051	-0.210	-0.334	0.000
28	0.0	0.125	-0.119	-0.366	-0.000
29	0.0	-0.017	-0.065	-0.005	0.000
30	0.0	-0.010	0.013	0.022	0.001
31	0.0	0.051	0.033	-0.576	-0.000
32	0.0	0.186	-0.071	0.007	0.000
33	0.0	0.011	-0.181	-0.145	0.000
34	0.0	-0.047	-0.077	-0.001	0.000
35	0.0	-0.136	-0.377	-0.305	-0.000
36	0.0	0.056	0.306	0.269	0.000
T**2	0.	11.	34.	14.	0.

TABLE 5E. F(X,Y)-STATISTICS OF MODEL VARIABLES

RUN	QG5	QG5	QG5	QG5	QG5*
D.F.	2000	1000	500	250	2000
1	1.000	0.982	0.987	0.995	1.003
2	1.000	0.946	0.984	1.014	1.001
3	1.000	0.989	0.987	0.989	1.001
4	1.000	0.979	0.963	0.943	1.000
5	1.000	0.929	0.929	0.913	1.000
6	1.000	1.033	1.061	1.048	1.000
7	1.000	0.988	0.941	0.950	1.001
8	1.000	0.988	0.941	0.934	1.001
9	1.000	0.990	0.999	0.999	1.001
10	1.000	0.992	1.013	0.988	1.001
11	1.000	0.984	0.927	0.940	1.001
12	1.000	0.999	1.028	1.003	1.001
13	1.000	0.945	0.908	0.844	1.000
14	1.000	1.005	1.046	1.030	1.000
15	1.000	1.008	1.045	1.059	1.000
16	1.000	1.002	0.994	1.024	1.000
17	1.000	0.984	0.989	0.986	1.001
18	1.000	0.976	0.989	0.989	1.001
19	1.000	0.994	0.953	0.939	1.001
20	1.000	1.000	0.996	1.011	1.001
21	1.000	0.978	0.970	0.996	1.001
22	1.000	1.000	1.011	0.960	1.001
23	1.000	0.987	0.996	1.023	1.001
24	1.000	1.005	1.024	1.057	1.001
25	1.000	0.985	0.941	0.955	1.000
26	1.000	1.001	0.995	0.948	1.000
27	1.000	0.986	1.006	1.023	1.001
28	1.000	0.989	0.992	0.999	1.001
29	1.000	0.985	0.984	0.985	1.007
30	1.000	0.961	0.962	0.972	1.006
31	1.000	0.981	0.972	0.912	1.002
32	1.000	0.979	0.980	0.984	1.002
33	1.000	0.974	0.936	0.941	1.002
34	1.000	0.980	0.943	0.912	1.002
35	1.000	0.972	0.935	0.940	1.001
36	1.000	0.975	0.999	0.999	1.001
F**2	0.	7.	12.	10.	0.

TABLE 6A. MEANS OF MODEL VARIABLES (X10**6)

RUN	PE1	QG2	PE3	BE4	QG5	TQG6	PQG7	PE3*
D.F.	1000	1000	2000	500	2000	1000	1000	2000
1	1010.43	957.67	9479.66	8211.33	6017.67	9000.49	8029.66	9480.90
2	89010.28	88957.85	361479.63	360208.61	358017.59	361384.60	360057.40	361479.63
3	824.79	457.57	1575.94	1829.19	1006.85	907.97	1642.30	1575.52
5	366.34	-15.85	1598.20	1758.72	21.82	47.52	1648.52	1598.04
15	2399.66	2376.60	6082.79	4966.08	3694.04	5114.10	5195.40	6082.13
17	10.79	-16.44	121.76	307.23	21.06	48.52	207.89	111.46
27	28.11	29.37	153.19	91.25	-38.92	149.47	16.02	163.44
29	-4.22	-0.15	-16.08	-18.77	0.16	1.03	-4.39	-14.67
39	2327.30	2376.60	4781.38	4547.35	3694.04	5114.10	5195.40	4781.54
41	47.86	-16.44	128.07	305.35	21.06	48.52	207.89	129.79

TABLE 6B. STANDARD DEVIATIONS OF MODEL VARIABLES (X10**6)

RUN	PE1	QG2	PE3	BE4	QG5	TQG6	PQG7	PE3*
D.F.	1000	1000	2000	500	2000	1000	1000	2000
1	292.60	300.46	2691.26	2408.32	1813.52	1827.59	1933.78	2711.48
2	159.73	169.01	1809.03	1480.72	267.28	953.97	1070.54	1809.41
3	1909.03	1632.53	7264.26	6795.46	5550.84	4599.12	7457.57	7270.66
4	2421.96	2335.24	7945.94	7449.03	6406.85	5449.50	8200.47	7952.88
5	457.90	392.58	2668.41	2880.78	855.75	1052.65	2454.85	2674.52
6	445.44	279.17	2941.98	3079.42	749.53	907.12	2757.65	2946.90
7	2416.48	2370.43	6792.08	6947.83	6516.62	5805.95	6596.33	6796.09
8	2401.33	2422.28	6889.13	6937.73	6408.77	5787.40	6566.09	6895.12
9	2347.94	2381.02	6735.87	6793.90	6496.19	5746.28	6296.94	6741.32
10	2309.75	2469.10	6753.82	6886.62	6468.03	5826.17	6288.82	6756.39
11	2267.43	2301.06	6803.58	6523.52	6256.97	5625.59	6642.03	6807.73
12	2361.83	2161.14	6741.22	6585.80	6094.85	5495.62	6831.50	6746.16
13	688.66	339.83	2764.63	3008.77	601.02	1064.18	2884.02	2768.36
14	683.17	340.26	2838.22	2897.09	584.73	1108.10	2841.25	2841.88
15	1105.14	1151.24	4825.25	4019.95	3191.18	3323.33	3675.63	5256.70
16	1028.01	1096.13	4200.15	3597.83	2959.27	2859.13	3405.79	4615.33
17	834.63	720.99	3198.10	3063.60	2319.39	2114.84	2797.43	3298.01
18	757.07	704.13	3161.05	3043.70	2236.03	1985.87	2754.38	3263.06
19	979.56	1034.22	3257.38	3232.88	2629.95	2975.15	2727.13	3340.92
20	1019.04	994.64	3254.33	3221.92	2581.92	2929.61	2691.38	3332.30
21	1080.93	1031.88	3292.76	3123.00	2622.96	3020.93	2967.94	3382.76
22	1092.85	983.40	3265.87	3219.17	2584.12	2934.30	2983.94	3362.21
23	1247.55	1283.51	3075.05	3176.17	3007.41	3440.19	3161.07	3185.24
24	1263.76	1233.68	3082.82	3198.92	2924.89	3401.26	3092.83	3192.29
25	1004.08	972.92	2021.66	2067.25	2200.79	1992.73	2024.20	2049.52
26	1024.49	1038.04	2020.71	2075.37	2160.80	2008.18	2018.51	2053.20

TABLE 6B. STANDARD DEVIATIONS OF MODEL VARIABLES (X10**6)

(CONT.)

27	93.47	97.68	1037.94	822.64	591.01	658.17	663.25	2233.02
28	93.04	88.93	990.30	801.35	563.82	611.48	630.12	2161.54
29	59.02	47.26	630.59	572.82	395.24	325.86	465.01	1049.30
30	62.29	54.54	626.54	579.40	398.37	325.20	466.74	1050.26
31	133.86	127.14	1179.10	1141.52	651.50	597.33	895.44	1424.96
32	139.87	125.57	1104.08	1147.18	657.18	584.73	892.89	1429.38
33	137.72	130.09	1256.90	1170.99	653.02	597.36	890.41	1546.64
34	135.09	120.40	1243.37	1187.85	652.21	595.99	879.23	1531.12
35	127.18	112.81	1266.21	1132.50	581.10	724.86	907.86	1580.76
36	126.21	107.04	1253.22	1092.52	572.38	715.12	903.24	1570.14
37	68.26	60.71	390.02	397.09	348.38	260.32	343.89	565.69
38	67.03	66.34	391.32	405.35	341.54	260.93	342.17	572.62
39	1074.75	1151.24	3229.26	3263.13	3191.18	3323.33	3675.63	3232.42
40	978.69	1096.13	2771.20	2922.60	2959.27	2859.13	3405.79	2775.14
41	802.25	720.99	2434.84	2439.30	2319.39	2114.84	2797.43	2442.85
42	739.99	704.13	2406.12	2401.85	2236.03	1985.87	2754.38	2413.53
43	983.83	1034.22	2626.16	2779.78	2629.95	2975.15	2727.13	2636.54
44	1027.44	994.64	2615.66	2746.99	2581.92	2929.61	2691.38	2628.30
45	1039.83	1031.88	2451.55	2550.12	2622.96	3020.93	2967.94	2466.24
46	1054.18	983.40	2455.22	2591.86	2584.12	2934.30	2983.94	2468.44
47	1259.23	1283.51	2875.65	3035.97	3007.41	3440.19	3161.07	2883.23
48	1257.50	1233.68	2882.57	3081.72	2924.89	3401.26	3092.83	2891.14
49	983.90	972.92	1829.09	1981.95	2200.79	1992.73	2024.20	1847.01
50	1003.07	1038.04	1825.26	1982.81	2160.80	2008.18	2018.51	1841.18

TABLE 6C. T(X)-STATISTICS OF MODEL VARIABLES

RUN	PE1	QG2	PE3	BE4	QG5	TQG6	PQG7	PE3*
D.F.	1000	1000	2000	500	2000	1000	1000	2000
1	109.203	100.794	157.526	76.240	148.396	155.736	131.307	156.372
2	17622.233	16644.321	8936.210	5439.576	16552.613	11979.455	10635.793	8934.317
3	13.662	8.863	9.702	6.019	8.112	6.243	6.964	9.691
5	25.299	-1.277	26.785	13.651	1.140	1.428	21.236	26.721
15	68.665	65.281	56.376	27.624	51.769	48.663	44.698	51.744
17	0.409	-0.721	1.703	2.242	0.406	0.725	2.350	1.511
27	9.511	9.507	6.600	2.480	-2.945	7.181	0.764	3.273
29	-2.264	-0.102	-1.141	-0.733	0.018	0.100	-0.298	-0.625
39	68.477	65.281	66.216	31.161	51.769	48.663	44.698	66.154
41	1.887	-0.721	2.352	2.799	0.406	0.725	2.350	2.376

TABLE 6D. T(X,Y)-STATISTICS OF MODEL VARIABLES

RUN	PE1	QG2	PE3	BE4	QG5	TQG6	PQG7	PE3*
D.F.	1000	1000	2000	500	2000	1000	1000	2000
1	0.0	-3.978	0.0	-10.280	-47.708	-5.743	-16.901	0.015
2	0.0	-7.123	0.0	-16.380	-75.474	-1.883	-26.963	0.000
3	0.0	-4.623	0.0	0.735	-2.784	-3.064	0.232	-0.002
5	0.0	-20.038	0.0	1.131	-25.157	-22.696	0.514	-0.002
15	0.0	-0.457	0.0	-5.326	-18.466	-6.431	-5.595	-0.004
17	0.0	-0.781	0.0	1.200	-1.140	-0.748	0.757	-0.100
27	0.0	0.294	0.0	-1.424	-7.193	-0.119	-4.385	0.186
29	0.0	1.703	0.0	-0.092	0.976	0.980	0.574	0.052
39	0.0	0.990	0.0	-1.437	-10.711	2.609	3.026	0.002
41	0.0	-1.885	0.0	1.454	-1.423	-0.922	0.768	0.022
T**2	0.	498.	0.	412.	9125.	612.	1074.	0.

TABLE 6E. F(X,Y)-STATISTICS OF MODEL VARIABLES

RUN	PE1	QG2	PE3	BE4	QG5	TQG6	PQG7	PE3*
D.F.	1000	1000	2000	500	2000	1000	1000	2000
1	1.000	1.054	1.000	0.801	0.454	0.461	0.516	1.015
2	1.000	1.120	1.000	0.670	0.286	0.278	0.350	1.000
3	1.000	0.731	1.000	0.875	0.584	0.401	1.054	1.002
4	1.000	0.930	1.000	0.879	0.650	0.470	1.065	1.002
5	1.000	0.735	1.000	1.166	0.103	0.156	0.846	1.005
6	1.000	0.393	1.000	1.096	0.065	0.095	0.879	1.003
7	1.000	0.962	1.000	1.046	0.921	0.731	0.943	1.001
8	1.000	1.018	1.000	1.014	0.865	0.706	0.908	1.002
9	1.000	1.028	1.000	1.017	0.930	0.728	0.874	1.002
10	1.000	1.143	1.000	1.040	0.917	0.744	0.867	1.001
11	1.000	1.030	1.000	0.919	0.846	0.684	0.953	1.001
12	1.000	0.837	1.000	0.954	0.817	0.665	1.027	1.001
13	1.000	0.244	1.000	1.184	0.047	0.148	1.088	1.003
14	1.000	0.248	1.000	1.042	0.042	0.152	1.002	1.003
15	1.000	1.085	1.000	0.694	0.437	0.474	0.580	1.187
16	1.000	1.137	1.000	0.734	0.496	0.463	0.658	1.207
17	1.000	0.746	1.000	0.918	0.526	0.437	0.765	1.063
18	1.000	0.865	1.000	0.927	0.500	0.395	0.759	1.066
19	1.000	1.115	1.000	0.985	0.652	0.834	0.701	1.052
20	1.000	0.953	1.000	0.980	0.629	0.810	0.684	1.048
21	1.000	0.911	1.000	0.900	0.635	0.842	0.812	1.055
22	1.000	0.810	1.000	0.972	0.626	0.807	0.835	1.060
23	1.000	1.058	1.000	1.067	0.956	1.252	1.057	1.073
24	1.000	0.953	1.000	1.077	0.900	1.217	1.007	1.072
25	1.000	0.939	1.000	1.046	1.185	0.972	1.003	1.028
26	1.000	1.027	1.000	1.055	1.143	0.988	0.998	1.032

TABLE 6E. F(X,Y)-STATISTICS OF MODEL VARIABLES

(CONT.)

27	1.000	1.092	1.000	0.628	0.324	0.402	0.408	4.629
28	1.000	0.914	1.000	0.655	0.324	0.381	0.405	4.764
29	1.000	0.641	1.000	0.825	0.393	0.267	0.544	2.769
30	1.000	0.767	1.000	0.855	0.404	0.269	0.555	2.810
31	1.000	0.902	1.000	0.937	0.305	0.257	0.577	1.461
32	1.000	0.806	1.000	0.939	0.308	0.244	0.569	1.457
33	1.000	0.892	1.000	0.868	0.270	0.226	0.502	1.514
34	1.000	0.794	1.000	0.913	0.275	0.230	0.500	1.516
35	1.000	0.787	1.000	0.800	0.211	0.328	0.514	1.559
36	1.000	0.719	1.000	0.760	0.209	0.326	0.519	1.570
37	1.000	0.791	1.000	1.037	0.798	0.445	0.777	2.104
38	1.000	0.979	1.000	1.073	0.762	0.445	0.765	2.141
39	1.000	1.147	1.000	1.021	0.977	1.059	1.296	1.002
40	1.000	1.254	1.000	1.112	1.140	1.064	1.510	1.003
41	1.000	0.808	1.000	1.004	0.907	0.754	1.320	1.007
42	1.000	0.905	1.000	0.996	0.864	0.681	1.310	1.006
43	1.000	1.105	1.000	1.120	1.003	1.283	1.078	1.008
44	1.000	0.937	1.000	1.103	0.974	1.254	1.059	1.010
45	1.000	0.985	1.000	1.082	1.145	1.518	1.466	1.012
46	1.000	0.870	1.000	1.114	1.108	1.428	1.477	1.011
47	1.000	1.073	1.000	1.115	1.094	1.431	1.208	1.005
48	1.000	0.962	1.000	1.143	1.030	1.392	1.151	1.006
49	1.000	0.978	1.000	1.174	1.448	1.187	1.225	1.020
50	1.000	1.071	1.000	1.180	1.401	1.210	1.223	1.018
F**2	0.	636.	0.	214.	5900.	4420.	1711.	18981.

TABLE 6F. P-STATISTICS OF MODEL VARIABLES

RUN	PE1	QG2	PE3	BE4	QG5	TQG6	PQG7	PE3*
D.F.	1000	1000	2000	500	2000	1000	1000	2000
1	0.0	-5.22	0.0	-13.38	-36.52	-5.05	-15.30	0.0
2	0.0	-0.05	0.0	-0.35	-0.96	0.0	-0.39	0.0
3	0.0	-44.52	0.0	0.0	-36.11	-42.39	0.0	0.0
5	0.0	-104.33	0.0	0.0	-98.63	-97.03	0.0	0.0
15	0.0	0.0	0.0	-18.36	-39.27	-15.93	-14.59	0.0
17	0.0	0.0	0.0	0.0	0.0	0.0	0.0	0.0
27	0.0	0.0	0.0	0.0	-125.40	0.0	-89.54	0.0
29	0.0	0.0	0.0	0.0	0.0	0.0	0.0	0.0
39	0.0	0.0	0.0	0.0	-22.74	6.96	8.66	0.0
41	0.0	0.0	0.0	0.0	0.0	0.0	0.0	0.0

TABLE 7A. MEANS OF ENERGY VARIABLES (X10**6)

RUN	PE1	QG2	PE3	BE4	QG5	TQG6	PQG7	PE3*
D.F.	1000	1000	2000	500	2000	1000	1000	2000
1	2388.87	2510.24	3836.41	4012.21	3915.15	3905.27	5080.69	3841.01
2	2619.99	2604.69	3699.99	4380.15	5010.22	4888.14	4560.79	3729.90
3	102.11	86.00	1423.39	1269.26	608.65	553.82	1219.53	1531.06
4	953.49	901.66	8034.03	7993.84	6051.00	5414.61	7305.65	8235.83
5	1.53	1.63	15.83	8.75	10.68	24.24	6.41	15.63
6	16.66	15.61	155.67	139.43	97.64	194.85	186.63	154.29
7	101.56	99.52	279.70	276.79	255.34	409.72	283.98	279.28
8	-83.38	-82.28	-107.74	-128.44	-146.92	-190.48	-133.85	-103.58
9	2.00	1.74	29.52	24.79	12.55	27.16	23.12	32.95
10	16.19	15.50	131.10	122.71	95.69	191.85	119.87	137.29
11	100.01	97.91	263.71	267.95	244.51	385.29	395.38	264.54
12	-0.47	-0.11	-16.27	-16.25	-1.87	-2.93	-3.88	-17.99
13	0.02	-0.02	0.15	0.10	0.16	0.19	-117.81	-0.89
14	-0.03	0.02	0.29	0.07	-0.05	-0.03	74.89	1.67
15	0.00	-0.00	2.58	0.20	-0.01	0.01	-12.83	0.66
16	-0.00	0.00	8.31	0.48	0.09	0.07	62.88	-0.98

TABLE 7B. STANDARD DEVIATIONS OF ENERGY VARIABLES (X10**6)

RUN	PE1	QG2	PE3	BE4	QG5	TQG6	PQG7	PE3*
D.F.	1000	1000	2000	500	2000	1000	1000	2000
1	1337.96	1403.99	2432.60	2531.20	2518.14	2733.76	2811.25	2435.03
2	922.43	992.08	1648.01	1936.74	1683.84	1594.31	1847.08	1654.90
3	45.71	43.70	694.53	637.94	335.32	292.58	588.66	780.42
4	340.94	349.97	2680.91	2861.97	2083.92	1727.54	2249.89	2808.51
5	2.94	2.67	96.70	89.15	50.30	47.08	68.42	175.58
6	27.63	28.03	347.34	341.18	304.75	275.20	302.99	438.02
7	32.70	35.32	180.26	198.97	236.63	235.17	219.24	180.38
8	21.71	22.23	49.52	55.82	52.36	53.77	52.86	40.89
9	1.02	0.98	17.02	14.56	8.22	15.64	12.69	19.99
10	6.79	7.14	50.61	47.34	38.98	77.56	42.51	54.40
11	98.04	102.56	481.39	551.91	515.95	495.20	618.29	486.72
12	2.96	3.17	96.70	95.16	59.54	46.07	65.83	143.39
13	89.10	93.86	404.94	465.71	429.90	406.81	516.23	431.20
14	77.82	78.27	357.18	425.71	358.64	321.56	430.44	431.82
15	3.20	3.39	113.61	105.50	65.57	44.14	81.28	233.13
16	26.56	27.38	354.42	353.11	316.38	254.89	296.65	454.25

TABLE 7C. T(X)-STATISTICS OF ENERGY VARIABLES

RUN	PE1	QG2	PE3	BE4	QG5	TQG6	PQG7	PE3*
D.F.	1000	1000	2000	500	2000	1000	1000	2000
1	56.461	56.539	70.529	35.444	69.532	45.174	57.151	70.543
2	89.818	83.025	100.405	53.325	133.067	96.955	78.083	100.796
3	70.650	62.229	91.654	44.489	81.174	59.859	65.513	87.736
4	88.439	81.472	134.019	62.456	129.855	99.115	102.683	131.143
5	16.457	19.247	7.323	2.194	9.492	16.279	2.962	3.980
6	19.066	17.613	20.043	9.138	14.329	22.390	19.479	15.753
7	98.223	89.089	69.390	31.106	48.257	55.094	40.962	69.242
8	-121.471	-117.055	-97.297	-51.449	-125.474	-112.015	-80.076	-97.339
9	61.904	55.980	77.556	38.079	68.270	54.921	57.608	73.701
10	75.398	68.684	115.851	57.957	109.780	78.221	89.167	112.872
11	32.260	30.190	24.499	10.856	21.193	24.604	20.222	24.307
12	-5.007	-1.077	-7.523	-3.818	-1.401	-2.011	-1.865	-5.610
13	0.007	-0.006	0.017	0.005	0.017	0.015	-7.216	-0.093
14	-0.010	0.007	0.037	0.004	-0.007	-0.003	5.502	0.173
15	0.003	-0.001	1.017	0.042	-0.007	0.008	-4.992	0.127
16	-0.001	0.005	1.048	0.030	0.012	0.009	6.703	-0.097

TABLE 7D. T(X,Y)-STATISTICS OF ENERGY VARIABLES

RUN	PE1	QG2	PE3	BE4	QG5	TQG6	PQG7	PE3*
D.F.	1000	1000	2000	500	2000	1000	1000	2000
1	0.0	1.979	0.0	1.400	1.006	0.674	11.939	0.060
2	0.0	-0.357	0.0	7.555	24.869	19.026	12.464	0.573
3	0.0	-8.060	0.0	-4.745	-47.244	-48.103	-8.409	4.609
4	0.0	-3.355	0.0	-0.284	-26.117	-32.297	-7.829	2.324
5	0.0	0.791	0.0	-1.562	-2.116	3.201	-3.081	-0.046
6	0.0	-0.843	0.0	-0.948	-5.616	3.359	2.510	-0.110
7	0.0	-1.343	0.0	-0.297	-3.661	15.372	0.534	-0.073
8	0.0	1.117	0.0	-7.579	-24.308	-40.770	-13.020	-0.534
9	0.0	-5.833	0.0	-6.264	-40.141	-3.784	-11.562	5.848
10	0.0	-2.230	0.0	-3.493	-24.789	22.491	-6.389	3.729
11	0.0	-0.469	0.0	0.157	-1.217	6.398	5.899	0.054
12	0.0	2.631	0.0	0.005	5.672	5.116	4.126	-0.444
13	0.0	-0.009	0.0	-0.002	0.001	0.003	-6.319	-0.079
14	0.0	0.012	0.0	-0.011	-0.031	-0.025	4.727	0.109
15	0.0	-0.003	0.0	-0.445	-0.884	-0.887	-4.265	-0.331
16	0.0	0.005	0.0	-0.443	-0.774	-0.729	4.444	-0.721
T**2	0.	131.	0.	194.	6435.	6228.	942.	76.

TABLE 7E. F(X,Y)-STATISTICS OF ENERGY VARIABLES

RUN	PE1	QG2	PE3	BE4	QG5	TQG6	PQG7	PE3*
D.F.	1000	1000	2000	500	2000	1000	1000	2000
1	1.000	1.101	1.000	1.083	1.072	1.263	1.336	1.002
2	1.000	1.157	1.000	1.242	1.044	0.936	1.256	1.008
3	1.000	0.914	1.000	0.844	0.233	0.177	0.718	1.263
4	1.000	1.054	1.000	1.140	0.604	0.415	0.704	1.097
5	1.000	0.829	1.000	0.850	0.271	0.237	0.501	3.297
6	1.000	1.029	1.000	0.965	0.770	0.628	0.762	1.590
7	1.000	1.167	1.000	1.218	1.723	1.702	1.479	1.001
8	1.000	1.049	1.000	1.271	1.118	1.179	1.139	1.015
9	1.000	0.924	1.000	0.732	0.233	0.844	0.556	1.380
10	1.000	1.104	1.000	0.875	0.593	2.349	0.706	1.155
11	1.000	1.094	1.000	1.314	1.149	1.058	1.656	1.022
12	1.000	1.145	1.000	0.968	0.379	0.227	0.463	2.199
13	1.000	1.110	1.000	1.323	1.127	1.009	1.625	1.134
14	1.000	1.012	1.000	1.421	1.008	0.811	1.452	1.462
15	1.000	1.121	1.000	0.862	0.333	0.151	0.512	4.211
16	1.000	1.063	1.000	0.993	0.797	0.517	0.701	1.643
F**2	0.	46.	0.	148.	1769.	1924.	939.	9132.

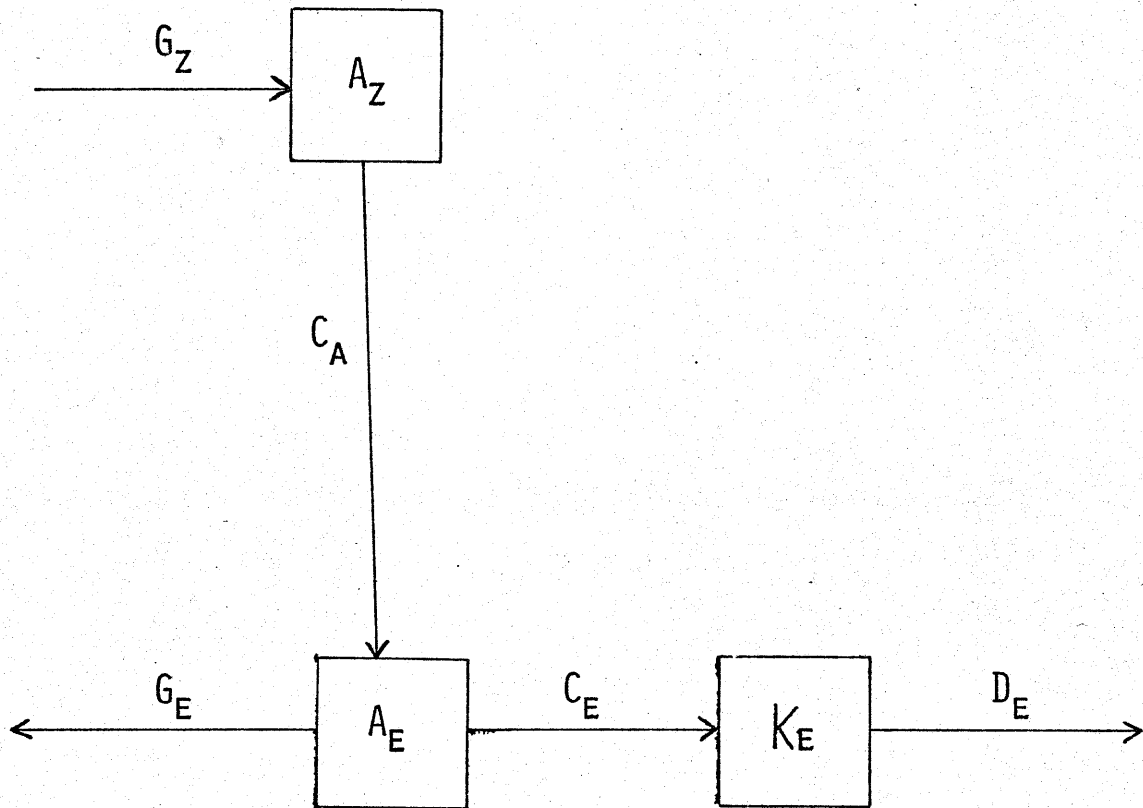
TABLE 7F. P-STATISTICS OF ENERGY VARIABLES

RUN	PE1	QG2	PE3	BE4	QG5	TQG6	PQG7	PE3*
D.F.	1000	1000	2000	500	2000	1000	1000	2000
1	0.0	0.0	0.0	0.0	0.0	0.0	32.43	0.0
2	0.0	0.0	0.0	18.38	35.41	32.11	23.27	0.0
3	0.0	-15.78	0.0	-10.83	-57.24	-61.09	-14.32	7.56
4	0.0	-5.44	0.0	0.0	-24.68	-32.60	-9.07	2.51
5	0.0	0.0	0.0	0.0	-32.57	53.08	-59.52	0.0
6	0.0	0.0	0.0	0.0	-37.28	25.17	19.89	0.0
7	0.0	0.0	0.0	0.0	-8.71	46.49	0.0	0.0
8	0.0	0.0	0.0	19.21	36.36	76.79	24.23	0.0
9	0.0	-13.07	0.0	-16.00	-57.48	-8.00	-21.67	11.63
10	0.0	-4.29	0.0	-6.40	-27.01	46.34	-8.56	4.73
11	0.0	0.0	0.0	0.0	0.0	46.10	49.93	0.0
12	0.0	-76.97	0.0	0.0	-88.53	-81.99	-76.13	0.0
13	0.0	0.0	0.0	0.0	0.0	0.0	-77492.27	0.0
14	0.0	0.0	0.0	0.0	0.0	0.0	25300.70	0.0
15	0.0	0.0	0.0	0.0	0.0	0.0	-596.68	0.0
16	0.0	0.0	0.0	0.0	0.0	0.0	656.99	0.0

experiments is PE3. The means of the model variables which the invariance arguments show should be zero are not displayed. Neither are the corresponding t_x , t_{xy} and p statistics, which depend on the means. Entries in the table of p statistics are zero if the difference in means is judged to be insignificant at the 95% confidence level (that is, if $t_{xy}^2 < 4$). Of the variables associated with wave vector (0,4) only $\text{Re } \overline{\Psi_2}$ is definitely different from zero and only for runs PE1, PE3 and BE4. (See Table 6c.)

At low thermal forcing, the QG mean model state differs significantly from that of the PE. The QG $\overline{\sigma_0}$ is low by $5.2 \pm 1.3\%$ while $\overline{\Psi_1}$ is low by $45 \pm 9.6\%$ (relative to the PE results). The variances are similar except that those of the corner variables and the χ_I variables are significantly low. At high thermal forcing differences between QG and PE model statistics present at the lower forcing become more pronounced and other differences become evident. There are significant differences for all variables associated with the forced mode as well as a 37 ± 0.76 decrease in $\overline{\sigma_0}$. Most of the variances are different; relative to the PE variances the QG variances of the τ_I and θ_6 variables are higher while the variances of the other model variables especially the χ_I and ψ_6 variables are lower. Relative to run QG5, run BE4 is a much better simulation of run PE3. Comparing the mean states, only $\overline{\sigma_0}$, $\overline{\theta_0}$ and $\overline{\tau_1}$ are significantly different from the PE results and these differences are all smaller by a factor of two than the differences between the PE and QG mean model states. Although the F_{xy} statistics are significantly different from unity, the variances of runs BE4 and PE3 are in relatively good agreement.

The statistics of the energy variables are compared in Tables 7a-f. The residuals of the energy budgets (energy variables 13-16), are all very small except in the case of the filtered PE (which is discussed below). The major time averaged flow of energy in all the models is



The time mean conversion of zonal to eddy kinetic energy, $\overline{C_K}$, is significantly negative in the PE and BE runs indicating barotropic stability. $\overline{C_K}$ is negative, but not significantly so, for the QG model runs. The comparisons of the kinetic energies below also apply in a rough sense to the dissipations since the ratios of the means and standard deviations of total, zonal or eddy kinetic energy to the corresponding statistic

of the same component of dissipation are always in the range 39 to 65. Although not listed as separate variables in the tables, \bar{G} , \bar{C} and \bar{D} agree to within 10^{-6} for each of runs 1 through 5, excluding \bar{D} calculated from the filtered data of run PE3. The standard deviations of G and C for the same run always agree to within a factor of 2, but s_C is greater than s_D by factors of 3 and 7 for $\theta^* = 0.008$ and 0.032 respectively.

At $\theta^* = 0.008$ the QG simulation is energetically in agreement with the PE climate. The most important differences are that the QG \bar{K}_Z and \bar{K}_E are low by $16 \pm 2.0\%$ and $5.4 \pm 1.6\%$ respectively. At the higher thermal forcing it is again found that the differences present at low thermal forcing become magnified. Comparing the QG to PE results, \bar{K}_Z and \bar{K}_E are low by $57 \pm 1.2\%$ and $25 \pm 0.95\%$ respectively. Significant differences also exist for the conversions; \bar{C}_E and \bar{C}_Z are both low by about a third. \bar{A}_E is high by $35 \pm 1.4\%$. The variances of the energy variables are substantially different and generally lower, especially those of K_Z , C_Z , D_Z and C_K .

It seems that the key to the differences of the time mean energy variables at $\theta^* = 0.032$ is that the QG model is less efficient at converting A into K. Consider the major flow of energy through the system illustrated earlier. \bar{G}_Z is principally controlled by $(h \theta^* / \sigma_m)$. For the sake of argument assume \bar{G}_Z is fixed by external conditions. If \bar{G}_Z is fixed then so are \bar{A}_Z and \bar{C}_A . The initial effect of decreasing the efficiency of C_E is to increase \bar{A}_E and to decrease \bar{K}_E and \bar{C}_E . To balance the budgets \bar{D}_E should then decrease and $(-\bar{G}_E)$ increase. This argument properly predicts the signs of the observed

changes. In simpler QG models having constant σ_0 this complicated behavior could not occur - in particular, because of the thermal wind relationship, a small change in the mean model state associated with a decrease in \bar{K} would be expected to be associated with a decrease in \bar{A} . In our model K and σ_0 are correlated and σ_0 appears in the denominator of the definition of A , so a decrease in \bar{K} may actually be associated with an increase in \bar{A} .

Comparing the BE to PE energetics, the major differences are that $\overline{A_E}$ is high by $18 \pm 2.4\%$, $\overline{K_Z}$ is low by $11 \pm 2.3\%$ and the magnitude of $\overline{G_E}$ is too large by $19 \pm 2.5\%$. The differences between the energetics of the BE and PE models are much smaller than the differences between the QG and PE models. In terms of the metric defined by T^2 the QG simulated energies and energy flows are 33 times farther than are those of the BE from those of the PE.

The direct effects of gravity waves on the PE model climate are isolated by comparing the statistics obtained from filtered and unfiltered model variables. In the tables, results from the unfiltered data are labeled PE3*. As expected the means are unaffected. Filtering cannot cause an increase in the variance of the model variables and so must introduce a bias. The greatest decrease in variance is 75% for the χ_1 variables. However except for the τ_1 and χ_1 variables the changes in variances are the same size or smaller than the sampling uncertainty of the variances. Since the energy variables are not actually filtered but rather calculated from the filtered model variables, the mean "filtered" kinetic energies and dissipations are equal to weighted sums of the variances of the filtered model variables and are therefore smaller

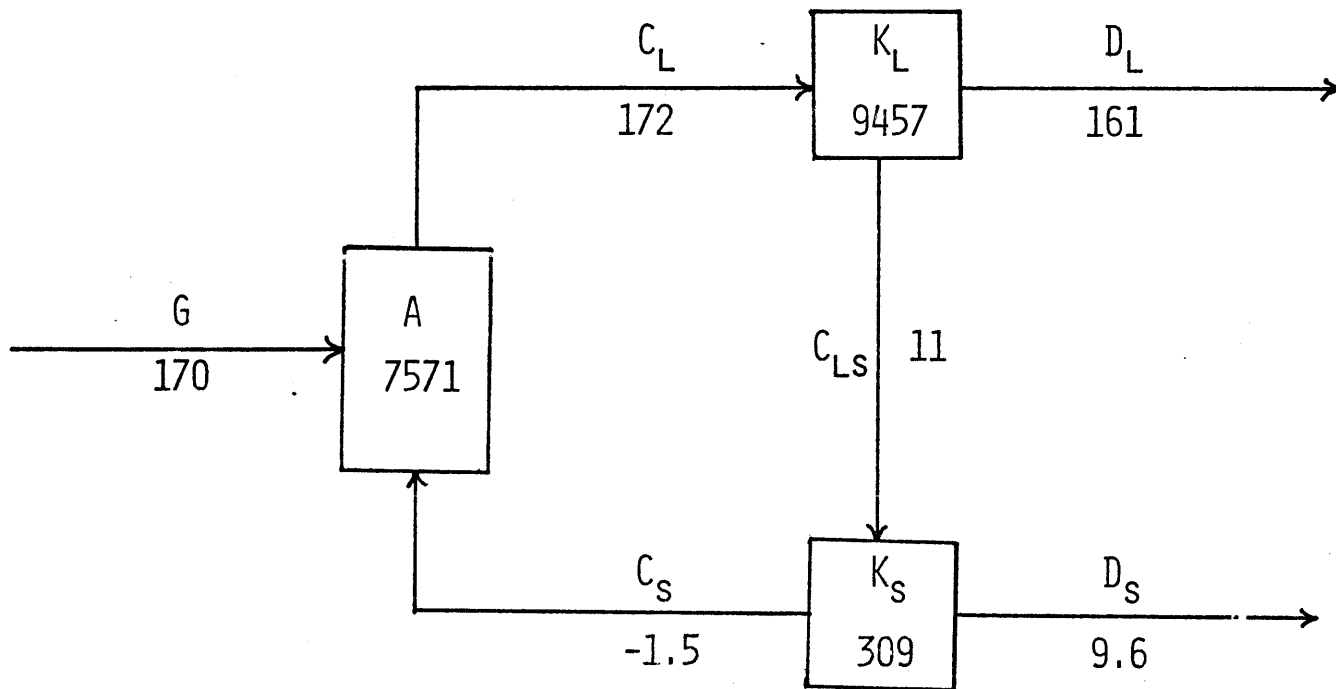


Figure 3. Energy budget ($\times 10^6$) of run PE3 decomposed into short (S) and long (L) time scales. Sample length is 200000 time units.

than the mean "unfiltered" kinetic energies and dissipations. As dissipation is underestimated by filtering the "filtered" energy budgets do not exactly balance. To separate the direct effects of the gravity waves on C, K and D, note that for a perfect low pass filter (\sim)

$$\overline{xy} = \overline{\tilde{x}\tilde{y}} + \overline{\hat{x}\hat{y}}$$

where \hat{x} , the high frequency component of x is $x - \tilde{x}$ and where x and y are continuous functions of time on a finite interval of time. This relationship is easily verified by expanding each of x and y in Fourier series. Thus any quadratic quantity may be resolved into long (L) and short (S) period components. Formally

$$\frac{d}{dt}K_L = C_L - D_L - C_{LS}$$

$$\frac{d}{dt}K_S = C_S - D_S + C_{LS}$$

where C_{LS} is the conversion from long to short period energy. Although explicit formulae for $\frac{d}{dt}K_L$, $\frac{d}{dt}K_S$ and C_{LS} are unknown, $\overline{C_{LS}}$ may be obtained as a residual. The results are summarized in Figure 3; $\overline{C_{LS}} = 11$, i.e., the gravity waves obtain their energy from the longer period waves. In the time mean sense the gravity waves act as an additional energy dissipation mechanism in the PE model, but have no net effect on the conversion of available into kinetic energy.

The budgets maintaining the time mean model state are obtained by

averaging the evolution equations in time. The invariance arguments apply to each term of the budgets, so only the budgets for the real parts of the zonal modes of the spectral variables are considered here. To the extent that the invariance arguments hold, the time mean continuous variables are of the form

$$\overline{z} = \overline{z}_0 + 2(\text{Re } \overline{z}_1 \cos 2y + \text{Re } \overline{z}_2 \cos 4y)$$

It is observed that $\text{Re } \overline{z}_2$ and the components of the budget of $\text{Re } \overline{z}_2$ are all approximately zero excluding the case $z = \psi$ for the PE and BE model runs.

The budget calculation results for the maintenance of $\text{Re } \psi_1$, $\text{Re } \tau_1$ and $\text{Re } \kappa_1$ are displayed in Table 8. These values are calculated directly from the first and second moment statistics. The same calculations were also performed for shorter samples; comparisons show the results are known to 1×10^{-6} for the low thermal forcing experiments. At high thermal forcing the uncertainty is larger; some of the PE statistics change by 10% when the sample length is doubled from 100000 to 200000. In Table 8 the fluxes are divided into transient eddy (TE) and mean meridional circulation (MMC) components. The decomposition of a typical nonlinear term of the evolution equations is

$$\sum_{J,K} \overline{z_J^{q_{IJK}} \tau_K} = \sum_{J,K} q_{IJK} \overline{z_J' \tau_K'} + \sum_{J,K} q_{IJK} \overline{z_J \tau_K}$$

Budget for	Terms in 3-D continuous PE ¹	Terms in two layer equations	PE1 1000	
			TE	MMC
Re Ψ_1	$-\underline{V}_2 \cdot \nabla \chi$ Advection	$-\mathcal{J}(\Psi, \nabla^2 \Psi)$ $-\mathcal{J}(\tau, \nabla^2 \tau)$	-24.33 10.58	0.02 0.00
	$-\nabla \cdot (\omega \frac{\partial}{\partial p} \underline{V} \times \underline{k})$ Twisting	$\nabla \cdot (\nabla^2 \chi \nabla \tau)$	-0.23	-0.16
	$-\underline{V}_3 \cdot \nabla \chi$ Advection	$\mathcal{J}(\chi, \nabla^2 \chi)$	-0.04	-0.00
	$-\chi \nabla \cdot \underline{V}$ Divergence	$\nabla \chi \cdot \nabla (\nabla^2 \tau)$	-4.58	-0.07
		$\nabla^2 \tau \nabla^2 \chi$	6.07	0.15
		Friction	$-k_0 (\nabla^2 \Psi - \nabla^2 \tau)$	
Re τ_1	$-\underline{f} \cdot \underline{V}$ Divergence	$\nabla^2 \chi$		28.11
	$-\underline{V}_2 \cdot \nabla \chi$ Advection	$-\mathcal{J}(\tau, \nabla^2 \Psi)$	458.34	0.12
	$-\underline{V}_3 \cdot \nabla \chi$ Advection	$-\mathcal{J}(\Psi, \nabla^2 \tau)$	-453.83	-0.10
	$-\chi \nabla \cdot \underline{V}$ Divergence	$\nabla \chi \cdot \nabla (\nabla^2 \Psi)$	6.52	0.30
		$\nabla^2 \Psi \nabla^2 \chi$	-7.54	-0.11
		Friction	$-k_1 \nabla^2 \tau + k_0 \nabla^2 \Psi$	
Re χ_1	$-g \nabla^2 z$ $-\nabla \cdot (\underline{f} \times \underline{V})$	$\nabla^2 \theta$ $-\nabla^2 \tau$		2327.30 -2399.66
	$-\nabla \cdot ((\underline{V} \cdot \nabla) \underline{V})$	$-\nabla \cdot (\nabla^2 \Psi \nabla \tau + \nabla^2 \tau \nabla \Psi)$	19.95	-7.10
		$\nabla^2 (\nabla \Psi \cdot \nabla \tau)$	18.69	7.09
		$-\mathcal{J}(\chi, \nabla^2 \Psi)$	43.96	0.00
		$-\nabla^2 (\mathcal{J}(\Psi, \chi))$	-9.78	0.00
		Friction	$-k_1 \nabla^2 \chi$	


Table 8. Budget calculations for the real part of the mode 1 spectral variables ($\times 10^6$).

¹Standard meteorological variables where \underline{V}_2 is the nondivergent wind and \underline{V}_3 is the irrotational wind. (See Lorenz (1960) for details.)

QG2 1000		PE3 2000		BE4 500	
TE	MMC	TE	MMC	TE	MMC
-28.69	0.00	-48.31	0.16	-49.45	0.80
13.37	0.00	15.42	-0.03	22.34	-0.19
		-27.65	-1.71	-23.55	-1.71
		-0.06	0.00		
		28.14	-0.14	9.56	0.31
		-2.49	1.20	16.33	0.84
	15.35		36.05		25.10
	29.37		153.19		91.25
457.47	0.04	2265.62	0.64	2241.31	4.49
-452.49	-0.03	-2276.34	-0.62	2220.55	-4.62
		273.36	7.75	213.17	5.41
		-335.07	-3.67	-262.64	-2.74
	-34.36		-84.72		-68.82
	2376.60		4781.38		4547.35
	2376.60		-6082.79		-4966.08
		274.42	-79.35	192.10	-74.82
		292.22	79.31	227.58	74.03
		957.78	0.07		
		-209.30	-0.02		
			-2.45		

Table 8 (cont.)

(Blank Page)



QG5 2000		TQG6 1000		PQG7 1000	
TE	MMC	TE	MMC	TE	MMC
-74.84	0.03	-165.44	-0.09	-44.06	0.15
53.36	-0.01	83.72	0.01	12.33	-0.01
	21.50		81.85		28.42
	-38.92		149.47		16.02
2341.49	0.27	2941.75	0.23	2411.10	0.63
-2251.71	-0.23	-2909.67	-0.22	-2410.97	-0.71
	-51.05		-181.37		-69.99
	3694.04		5114.10		5195.40
	-3694.04		-5114.10		-5195.40

Table 8 (cont.)

On the right hand side, the first term is the TE component and the second term is the sum of the standing eddy (SE) and the MMC components. In the table the columns headed MMC are actually this second term. The SE component should be close to zero if the averaging time is sufficiently long since the ensemble mean state is zonal. In Table 8 the rows are identified in the second and third columns by the terms in the original three dimensional PE and by the terms in the nondimensional two layer equations corresponding to the terms in the spectral equations whose time averages are displayed.

In the budget of $\text{Re } \overline{\tau}_1$, each of the two Jacobian terms are large in magnitude but they very nearly cancel. At low thermal forcing what remains is basically a balance between destruction of the vorticity of the time mean wind shear by friction and production by divergence. At high thermal forcing the net effect of the divergence term is negative for all three models. This effect plus friction balance the positive contributions from net advection.

The momentum lost by the baroclinic component due to friction between the two layers is gained by the barotropic component. Thus the frictional contribution to the budget of $\text{Re } \overline{\psi}_1$ may be positive, as is observed. The advection of "thermal" vorticity by the "thermal wind" - $J(\overline{\tau}, \nabla^2 \overline{\tau})$ - also provides a positive contribution to the budget of $\text{Re } \overline{\psi}_1$. These two effects are offset by the advection of mean vorticity by the mean wind - $J(\overline{\psi}, \nabla^2 \overline{\psi})$. The additional terms in the PE and BE budgets give only a small net contribution but individually all three of the terms involving $\overline{\tau}$ and $\overline{\chi}$ are important in the time mean budget. The budget for $\text{Re } \overline{\psi}_2$ (not shown) is less interesting since the Jacobian terms must be

zero. For the PE and BE runs, the budget of $\text{Re } \Psi_2$ is balanced by positive contributions from the twisting and divergence terms and by negative contributions from the advection term involving the divergent wind and the frictional term.

The budgets for $\text{Re } \chi_1$ describe how far the mean model state is from geostrophic balance. The mean PE model state at $\theta^* = 0.008$ is very nearly geostrophic while at $\theta^* = 0.032$ the mean state is considerably ageostrophic. The sum of the first four terms in the MMC column is the residual of the mean model state from the nonlinear balance condition. Of these four terms the two nonlinear terms must exactly cancel if the model state is zonal.

The θ_0 budget states that the net radiation must have zero average, yielding the constraint

$$\overline{\theta_0} - \theta_0^R = \overline{\sigma_0} - \sigma_0^R$$

The σ_0 budget states that radiation must balance conversion, that is

$$\bar{c} = h \overline{\sigma_0}$$

Combining these constraints with those obtained from the budgets of

θ_0^2 , σ_0^2 and $\theta_0 \sigma_0$ yields

$$\overline{\sigma_0' \theta_0'} = \overline{\theta_0'^2} \geq 0$$

$$\overline{\theta_0'c'} = h(2\overline{\theta_0'^2} - \overline{\sigma_0'^2})$$

and

$$\overline{\sigma_0'c'} = h(2\overline{\sigma_0'^2} - \overline{\theta_0'^2}) = h(\overline{\sigma_0'^2} + (\overline{\sigma_0' - \theta_0'})^2) \geq 0$$

where the prime indicates a deviation from the time average. The first of the three above equations may be written as

$$1 \geq \rho(\sigma_0, \theta_0) = (\overline{\theta_0'^2} / \overline{\sigma_0'^2})^{1/2} \geq 0$$

where $\rho(x,y)$ is the correlation of x and y . The constraint on $\overline{\sigma_0'c'}$ is fairly strong; it implies that

$$2(\overline{\sigma_0'^2} / \overline{c'^2})^{1/2} \geq h^{-1} \rho(\sigma_0, c) \geq (\overline{\sigma_0'^2} / \overline{c'^2})^{1/2} \geq 0$$

and therefore

$$\overline{c'^2} \geq h^2 \overline{\sigma_0'^2}$$

In the budget calculations for $\text{Re } \theta_1$ it is observed that the horizontal eddy heat flux $-J(\Psi, \theta)$ - balances radiation. The other terms are negligible; the vertical eddy heat flux is always less than 10^{-6} and the magnitude of the MMC term $(-4\overline{\sigma_0} \overline{\kappa_1})$ is approximately 1% the magnitude of the Jacobian term. Therefore since $\theta^* > \text{Re } \overline{\theta_1}$

for all the runs the time averaged contribution of the Jacobian term must be approximately equal to $-h \theta^*$. Thus the horizontal eddy heat flux is roughly the same for all model runs having the same values of h and θ^* .

6. Model tuning.

A rational method of tuning numerical models is proposed. The best choice of parameters is defined as that which minimizes the averaged squared forecast error. The QG model is tuned to the data from run PE3, and the climate of the tuned QG (TQG) model is examined.

6a. Tuning procedure.

Suppose a model of a real system is

$$(7) \quad \frac{d}{dt} \underline{X}(t; \underline{K}) = \underline{F}(t, \underline{X}; \underline{K})$$

where the model state vector \underline{X} contains observables of the real system and the vector \underline{K} contains adjustable parameters. We wish to minimize the sum of the squared short term prediction errors $S = \sum \underline{E}^T \underline{E}$, where the sum is over the available observations and where the error is

$$\underline{E}(\underline{K}) = \underline{X}^f - \underline{X}(T; \underline{K})$$

(Superscript T indicates matrix transposition.) Assume there is a set of pairs of observations $(\underline{X}^i, \underline{X}^f)$ in which each \underline{X}^i precedes the corresponding \underline{X}^f by a time lag T. $\underline{X}(T; \underline{K})$ is obtained by integrating (7) from initial conditions \underline{X}^i for a time interval T. We assume that observational errors are negligible and that \underline{X}^i may be used as initial conditions without any special initialization. Let $\underline{K} = \underline{K}_0$ be a first guess of the optimal value of \underline{K} . This defines a basic solution $\underline{X}_0 = \underline{X}(t; \underline{K}_0)$ for $t \in (0, T)$ and a sum of squared errors,

associated with the basic solution,

$$S_0 = \sum E(\underline{K}_0)^T E(\underline{K}_0)$$

Let $\underline{Y}(t; \underline{\delta K}) = \underline{X}(t; \underline{K}_0 + \underline{\delta K}) - \underline{X}(t; \underline{K}_0)$. For small $\underline{\delta K}$, \underline{Y} is approximately governed by the linear equation

$$(8) \quad \frac{d}{dt} \underline{Y}(t; \underline{\delta K}) = \underline{A}(t) \underline{Y}(t; \underline{\delta K}) + \underline{B}(t) \underline{\delta K}$$

The matrices \underline{A} and \underline{B} depend on the basic solution.

$$A_{ij}(t) = \left. \frac{\partial}{\partial x_j} F_i(t, \underline{X}; \underline{K}) \right|_{\underline{X}_0, \underline{K}_0}$$

$$B_{ij}(t) = \left. \frac{\partial}{\partial K_j} F_i(t, \underline{X}; \underline{K}) \right|_{\underline{X}_0, \underline{K}_0}$$

Consider any explicit time marching scheme approximating (8). If $\underline{Y}(n \Delta t; \underline{\delta K})$ is a linear combination of the $\underline{\delta K}_j$, then according to (8) $\underline{Y}((n+1) \Delta t; \underline{\delta K})$ will be also. The initial conditions for (8) - $\underline{Y}(0; \underline{\delta K}) = \underline{0}$ - are a linear combination of the $\underline{\delta K}_j$. By induction and taking the limit as $\Delta t \rightarrow 0$, we see that, to first order,

$$(9) \quad \underline{Y}(T; \underline{\delta K}) = \underline{C} \underline{\delta K}$$

where the matrix \underline{C} depends on the basic solution. Now

$$(10) \quad \underline{E}(\underline{K}_0 + \underline{\delta K}) = \underline{E}(\underline{K}_0) - \underline{Y}(T; \underline{\delta K}) = \underline{E}(\underline{K}_0) - \underline{C} \underline{\delta K}$$

The condition for an extremum of S may be written

$$\left(\sum (\underline{C}^T \underline{C}) \right) \underline{\hat{K}} = \sum \underline{C}^T \underline{E}(\underline{K}_0)$$

Let \hat{S} be the value of S corresponding to $\hat{\underline{K}} = \underline{K}_0 + \underline{\hat{K}}$, the optimal value of \underline{K} . Then the relative reduction of S due to $\underline{\hat{K}}$ is

$$R^2 = \frac{S_0 - \hat{S}}{S_0} = \frac{\underline{\hat{K}}^T \left(\sum \underline{C}^T \underline{C} \right) \underline{\hat{K}}}{S_0} = \frac{\sum \underline{Y}(T; \underline{\hat{K}})^T \underline{Y}(T; \underline{\hat{K}})}{\sum \underline{E}(\underline{K}_0)^T \underline{E}(\underline{K}_0)}$$

which is positive, implying that the extremum is a minimum. If $\underline{\hat{K}}$ is not small, then the linearization is not strictly valid and \underline{K}_0 should be replaced by $\underline{K}_0 + \underline{\hat{K}}$ and the process repeated. Convergence is not assured. Neither is it assured that the minimum found is the absolute minimum. As in all nonlinear least squares problems a good initial guess is desirable and helps to avoid these problems.

To calculate \underline{C} note that (9) is valid for any small $\underline{\delta K}$, and (7) may be used to calculate \underline{X} and therefore \underline{Y} for any $\underline{\delta K}$. If $\underline{\delta K} = \epsilon_i \underline{Z}^i$, where ϵ_i is a small number and \underline{Z}^i is a vector having all zero entries excluding the i (th) entry which is equal to one, then the calculated \underline{Y} is (to first order) equal to ϵ_i times the i (th) column of \underline{C} . The procedure is thus to perturb each adjustable parameter in turn by a small amount, integrate (7) and obtain $\underline{Y}(T; \epsilon_i \underline{Z}^i)$

by subtracting the basic solution. Then

$$\underline{C} = (\epsilon_1^{-1} \underline{y}(T; \epsilon_1 \underline{z}^1) \dots \epsilon_i^{-1} \underline{y}(T; \epsilon_i \underline{z}^i) \dots)$$

Note that it is only necessary to integrate the original model equation (7) with altered values of the adjustable parameters - the evolution of \underline{y} , governed by (8), need not be explicitly calculated. The numerical burden can be kept down by carefully choosing a representative ensemble of data, and using only a subset of this ensemble until the final iteration.

The choice of T is somewhat arbitrary and it is not necessary that T be the same for all pairs of observations. In general slightly different values of $\hat{\delta K}$ will be obtained when the model is tuned for different prediction times, T . T should be short enough so the linearized equations are valid, yet long enough to average over the time scales of the parameterized and/or subgrid scale processes. As $T \rightarrow 0$ the procedure becomes one for minimizing the sum of squared tendency errors. This is not recommended since the observational errors of tendencies are generally greater than those of initial and final states and if the tendencies are correctly observed they may contain contributions from processes omitted in the model. For example, in our particular case the presence of gravity waves in the PE solution makes it undesirable to minimize the tendency errors.

There are several possible extensions of the tuning method. The definition of S may include a constant symmetric weight matrix, \underline{W} . Then the extremum condition becomes

$$\left(\sum \underline{c}^T \underline{w} \underline{c} \right) \underline{\delta K} = \sum \underline{c}^T \underline{w} \underline{E}(\underline{K}_0)$$

Other definitions of \underline{E} are possible. Suppose

$$(11) \quad \underline{E}(\underline{K}) = \underline{D}(\underline{X}^f) - \underline{D}(\underline{X}(T; \underline{K}))$$

where \underline{D} is analytic; then (10) is replaced by

$$\underline{E}(\underline{K}_0 + \underline{\delta K}) = \underline{E}(\underline{K}_0) - \underline{c}' \underline{\delta K}$$

where

$$c'_{ij} = \sum_k c_{kj} \left. \frac{\partial D_i}{\partial X_k} \right|_{\underline{X}_0}$$

\underline{D} might transform the model variables into energy variables, for example.

The extremum condition is as before with \underline{c}' replacing \underline{c} . \underline{c}' may be obtained in a manner analogous to that described for \underline{c} by rewriting

(11) as

$$\underline{c}' \underline{\delta K} = \underline{D}(\underline{X}(T; \underline{K})) - \underline{D}(\underline{X}(T; \underline{K}_0))$$

The model climate itself may be tuned if it can be assumed that small changes in \underline{K} produce small changes in the model climate. (This must in fact be assumed if any form of the tuning procedure is applied to a simulation, as opposed to a prediction, model.) Then letting $\underline{E}(\underline{K})$

be the difference between the statistics of the observations and of the model data an equation like (11) holds but it is no longer possible to write an explicit formula for \underline{C}' . Now $S = \underline{E}^T \underline{E}$; the summation symbol no longer appears but the rest of the argument is unchanged.

When tuning a prediction model it is reasonable to assume that the ensemble of initial conditions is stationary. It may be necessary to remove diurnal and seasonal trends first (see Leith (1974b) for an example) or replace the adjustable parameters by new adjustable parameters multiplying functions of time. For example, to take into account seasonal surface changes - snow cover, deciduous trees, etc. - we might assume the drag coefficient in the skin friction formula, C_D , is of the form

$$C_D' (1 + a_1 \sin 2\pi t + b_1 \cos 2\pi t)$$

where t is measured in years, and then tune the constants C_D' , a_1 and b_1 . On the other hand when tuning a simulation model small changes in \underline{K} may result in a very different climate. It is well known that simple models may have surfaces in the space of their adjustable parameters separating different regimes of model behavior. Therefore the results of tuning a simulation model by the above procedure must be carefully checked.

6b. Tuning the QG model and results.

We have tuned the QG equations using the observations of run PE3, identifying \underline{K} as $(k, h, \theta^*)^T$ and \underline{x} as the vector of prognostic model variables (i.e., model variables 1-26). The low pass filtered

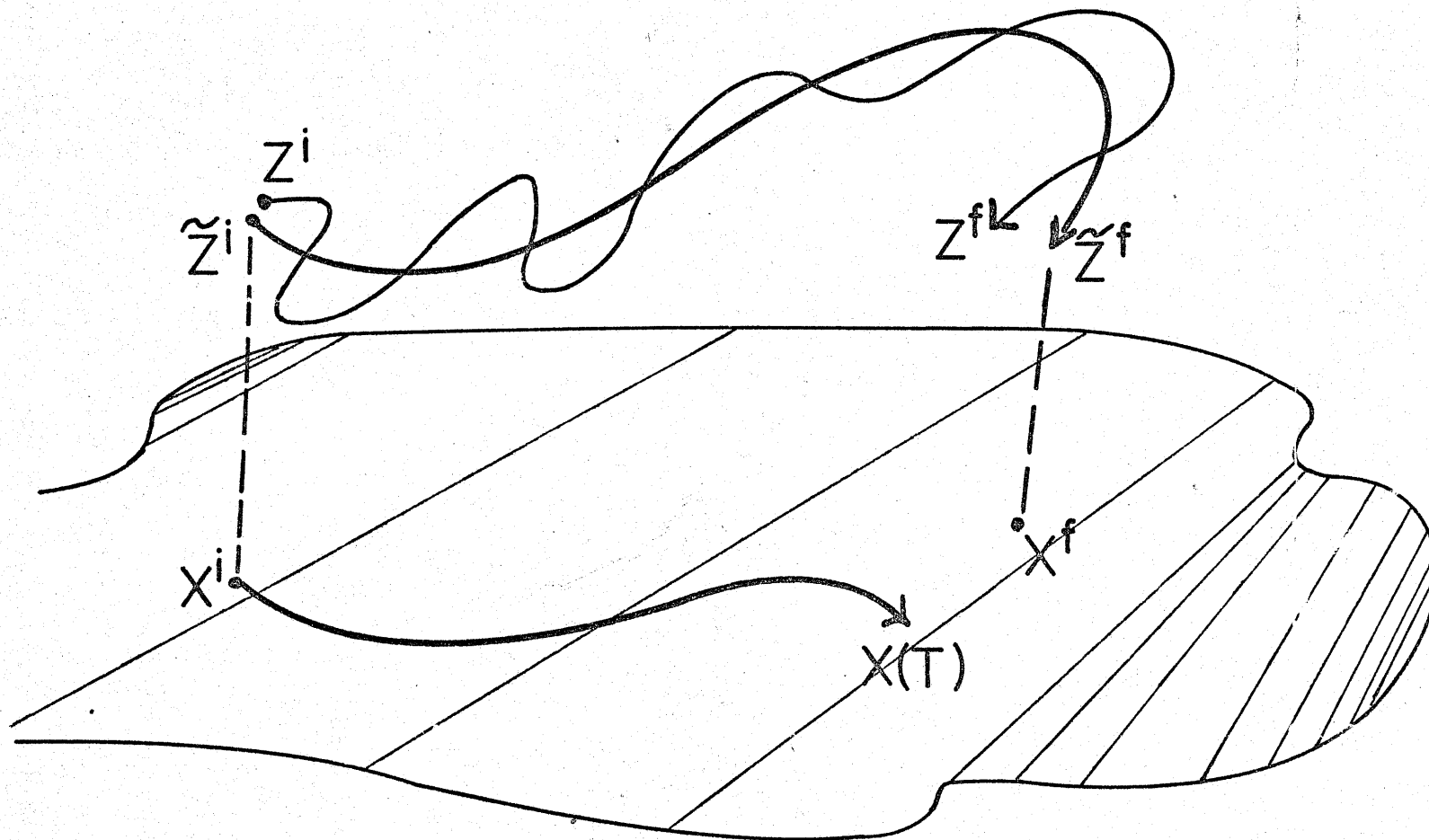


Figure 4. Schematic description of short term prediction error. The line $\underline{z}^i - \underline{z}^f$ represents the PE model evolution. The line $\underline{\tilde{z}}^i - \underline{\tilde{z}}^f$ is the low pass filtered PE model evolution. $\underline{\tilde{z}}^i$ and $\underline{\tilde{z}}^f$ are projected onto \underline{x}^i and \underline{x}^f in the QG manifold, represented by the ruled surface. The QG prediction from the initial conditions \underline{x}^i is $\underline{x}(T)$. The short term prediction error is $\underline{x}^f - \underline{x}(T)$.

PE observations are used to eliminate the presence of gravity waves which the QG model cannot simulate. (See Figure 4.) Hopefully this avoids initialization problems which might be caused by using only the prognostic model variables to initialize the QG forecast. An equally unsophisticated but perhaps better approach would be to initialize the QG model τ and θ fields to the average of the PE observed τ and θ fields and to evaluate the forecast error analogously.

\underline{W} is chosen to be the identity matrix so the squared error is equal to

$$\overline{(\delta\theta)^2} + \overline{(\delta\sigma)^2} + \frac{1}{2}\overline{(\delta\psi)^2} + \frac{1}{2}\overline{(\delta\tau)^2}$$

In this expression, the overbar is an areal average and $\delta\zeta$ is the error made in predicting ζ . 4000 pairs of observation vectors are used. $T = 5$ and successive \underline{x}^f 's are separated by 50 time units. The first choice of \underline{K}_0 is naturally the vector of parameters used in PE3. Two iterations of the tuning procedure are needed. The results are summarized in Table 9. The statistic F^* is defined by

$$F^* = \frac{N'-P}{P} \cdot \frac{S_0 - \hat{S}}{\hat{S}}$$

where N' is the effective number of sample pairs and P is the number of tuned parameters. If the model were truly linear and the errors were ideally distributed then F^* has an F distribution with P and $N'-P$ degrees of freedom under the hypothesis that $\underline{\hat{K}} = \underline{K}_0$. Note that the value of \hat{S} for the first iteration is approximately equal to the

Table 9. Tuning the QG model to the observations of run PE3.
Refer to text (Section 6) for definitions.

Iteration 1: $s_0 = 0.1790$ $R^2 = 0.053$
 $\hat{S} = 0.1695$ $F^* = 37.5$

<u>j</u>	<u>K_{0j}</u>	<u>ϵ_j</u>	<u>$\hat{\delta K}_j$</u>
1	0.0160	0.0004	0.0218
2	0.0180	0.0005	0.0063
3	0.0320	0.0010	0.0005

Iteration 2: $s_0 = 0.1715$ $R^2 = 0.012$
 $\hat{S} = 0.1694$ $F^* = 8.3$

<u>j</u>	<u>K_{0j}</u>	<u>ϵ_j</u>	<u>$\hat{\delta K}_j$</u>
1	0.0380	0.0010	0.000922
2	0.0240	0.0010	0.000342
3	0.0325	0.0010	-0.000465

value of S_0 for the second iteration. They would be equal if the linearization were exact.

In run TQG6 the parameter values $k = 0.03892$, $h = 0.02434$ and $\theta^* = 0.032035$ are used. (The TQG model is not a distinct model; it is simply the QG model with different constants.) The tuned values of k and h represent a marked increase in the strength of the dissipative processes. Qualitatively the solutions are similar to those of the high forcing experiments. However $(\overline{K-S})$ is negative ($= -3032 \times 10^{-6}$) and the distinctive high and low K regimes identified in the other runs are not evident.

The tuning resulted in a much better simulation of the PE model mean state. (See Table 6.) There are significant differences between the TQG and PE mean model states but these differences are considerably smaller than the differences between the QG and PE results. Relative to the PE mean model state the TQG $\overline{\sigma_0}$ is $5.1 \pm 0.9\%$ low, $\text{Re } \overline{\tau_1}$ is $16 \pm 2.5\%$ low and $\text{Re } \overline{\theta_1}$ is $7.0 \pm 2.7\%$ high. In the quasigeostrophic models τ_I must be equal to θ_I for all $I \neq 0$. If the PE mean model state is not in geostrophic balance then a QG model can do no better than to simulate a value of $\text{Re } \overline{\tau_1}$ and $\text{Re } \overline{\theta_1}$ in the interval between the values of $\text{Re } \overline{\tau_1}$ and $\text{Re } \overline{\theta_1}$ observed in the PE experiment.

The simulation of the energy cycle is not improved by the tuning. This is not surprising. Neglecting the kinetic energy of the divergent flow, if the same parameters are used, the governing equations for the conserved quantities - S-K, A+K and θ_0 - are the same in the QG and PE models, The same holds for the dissipation and generation terms in the energy budgets. Tuning the model must change the relationships between

statistical quantities constrained by the budgets. For example, since the TQG value of $\overline{\sigma_0}$ is approximately correct but h is larger than the value used in the PE model the budgets force the TQG values of \overline{C} , \overline{G} and \overline{D} to be larger than the PE values. (See Table 7a.) Although \overline{D} is larger, kinetic energies in TQG6 are even lower than those in QG5. The ratios $\overline{kK_Z/D_Z}$ and $\overline{kK_E/D_E}$ are approximately the same as in the other models.

Budget considerations also imply that the maintenance of the mean fields will be different in the TQG model. The dissipative terms in the budgets are all larger in magnitude. This forces the fluxes to be different. In particular the real part of the mode 1 component of the $-J(\psi, \theta)$ term is -650×10^{-6} for run TQG6, much larger in magnitude than the value of -485×10^{-6} observed in run PE3.

7. Monte Carlo simulation.

This section describes a Monte Carlo simulation experiment at the high level of the thermal forcing in which random perturbations are added to the QG model state every $5f^{-1}$. These perturbations are generated so that their statistics, other than those involving time lags, agree to a large extent with the statistics of the observed short term prediction errors. The perturbations are then adjusted so that the energy invariants of the system are conserved. The perturbed QG (PQG) model simulates the observed PE model climate nearly as well as does the BE model.

7a. Analysis of the short term prediction errors.

The short term prediction errors are calculated by the same procedure used in the tuning experiment. That is the initial and true final states are taken to be the low pass filtered observations of the PE prognostic model variables. The prediction interval is 5 time units and the 40000 such intervals in run PE3 from time 2000 to 202000 have been used. The first three columns of Table 10 display for model variables 1-26 the standard deviations of the PE model variables, of the short term ($5f^{-1}$) changes in the PE model variables and of the short term ($5f^{-1}$) prediction errors. The prediction errors of σ_0 , the τ_I variables and the ψ corner variables are relatively large while the prediction errors of θ_0 and the other ψ_I variables are relatively small.

First, some of the prediction error may be accounted for by a regression analysis in which the QG model variables are predictors. This part of the analysis could be used as the basis of a statistical correction procedure like those employed by Faller and coworkers (Faller and Lee,

1975; Faller and Schemm, 1977; Schemm and Faller, 1977). Good discussions of the problem of the statistical estimation of prediction errors can be found in their papers. A regression equation is found separately for each E_i , the prediction error of the i (th) prognostic model variable. The predictors in the regression are chosen from elements of the vector $\underline{X}(T)$, the current QG model state and the vector $\underline{X}(T) - \underline{X}(0)$, which is proportional to the average tendency over the prediction interval. Here \underline{X} is extended from the definition of the previous section to include the quasigeostrophically determined χ_I variables, which are expected to be dynamically significant. The least squares estimate of E_i is

$$(12) \quad \hat{E}_i = b_{0i} + \sum_1^J b_{ji} X_j(T) + \sum_1^J c_{ji} (X_j(T) - X_j(0))$$

where J is in this case 38. The stepwise regression procedure of Efroymsen (1960) is used to limit the number of predictors (and thus ensure the significance of the nonzero b_{ji} and c_{ji} .) In this procedure the predictors entering the final regression equation are chosen by considering the partial F statistics (F'_m) at each step and either adding or deleting a predictor. For large samples, if there are currently M predictors in the regression equation then

$$F'_m = N(r^{-2} - 1)$$

where r^2 is the additional reduction in variance caused by the m (th) predictor, given that the other $M-1$ predictors are in the regression equation. Under the hypothesis that the true coefficient of the m (th)

predictor is zero F'_m has an F distribution with 1 and N' degrees of freedom. During each step removal of the predictor currently in the regression equation associated with the smallest F'_m is considered first. This predictor is deleted if the smallest F'_m is less than F_{del} (a prespecified constant) and the next step begins. Otherwise adding the predictor currently not in the regression equation which would cause the largest reduction in variance is considered. This predictor is added if its value of F'_m is greater than F_{add} (another prespecified constant which must be at least as large as F_{del}) and the next step begins. Otherwise the stepwise procedure is complete. We have chosen $F_{add} = 2.0$ and $F_{del} = 1.5$. These values are smaller than normally chosen and take into account the fact that N' has been underestimated.

The reduction in variance due to the regression ranges from 1 to 53%. The b_{0i} are all small. Notably the terms involving the χ_I variables are important in several of the regression equations. The residuals, $E_i - \hat{E}_i$, are not normally distributed; compared to a normal distribution the distributions of the residuals are too highly peaked and have longer tails. It is found that the variances of the residuals and prediction errors are proportional to K^2 , the square of the kinetic energy of the current QG model state. This is not unexpected; K^2 is proportional to Ro^2 and we expect the QG approximation to cause larger prediction errors as Ro increases. In general, when the residual variance is not constant the least squares estimators of the regression coefficients are no longer minimum variance estimators. A suitable transformation which normalizes the residual variances is to divide everything by K . Allowing a constant term, the normalized regression equations are

$$(13) \hat{E}'_i = b_{0i}K^{-1} + \sum_1^J b_{ji}X'_j(T) + \sum_1^J c_{ji}(X'_j(T) - X'_j(0)) + d_i$$

where $X'_j = X_j/K$. Now the least squares estimate of \underline{E} is $\hat{\underline{E}} = K\hat{\underline{E}}'$. If (13) is multiplied through by K (12) is recovered with the additional term d_iK . The stepwise procedure is now constrained to always include K as a predictor of E_i but the constant term b_{0i} may be zero. The normalized residuals, $(E_i - \hat{E}_i)/K$, are found to be approximately normally distributed with zero mean and uniform variance. In those cases when the d_i are small, the actual regression equations are similar to the original equations obtained from (12). The d_i are not small for $i = 1, 5$ and 15 and the constant term is nonzero only for $i = 5$. The reduction in variance ranges from 1 to 52% in terms of the normalized variables and from 1 to 55% in terms of the original variables. (See Table 10 for details.) The number of nonzero constants in the regression equations excluding d_i ranges from 3 to 14.

The normalized residuals have a complicated covariance structure, i.e., the matrix \underline{C} , equal to the average over the sample of $K^{-2}(\underline{E} - \hat{\underline{E}})(\underline{E} - \hat{\underline{E}})^T$, has many off diagonal terms which are substantially nonzero. To generate perturbations with these statistics it is necessary to essentially perform an empirical orthogonal function analysis of the normalized residuals. Let $\underline{\Lambda}$ be the diagonal matrix of the square roots of the eigenvalues of \underline{C} and let \underline{P} be the matrix of the corresponding normalized eigenvectors of \underline{C} . Then $\underline{P}^T \underline{C} \underline{P} = \underline{\Lambda}^2$ and $\underline{P}^{-1} = \underline{P}^T$: If $K^{-1}(\underline{E} - \hat{\underline{E}}) = \underline{P} \underline{\Lambda} \underline{W}$, then the average of $\underline{W} \underline{W}^T$ is the

Table 10. Standard deviations ($\times 10^6$) of terms associated with regression equation (13). Column headed J_n is the number of nonzero coefficients, excluding d_i in the n (th) regression equation. Refer to text (Section 7) for other definitions. Sample length is 200000.

n	X_n^f	$X_n^f - X_n^i$	E_n	$E_n - \hat{E}_n$	E_n/K	$(E_n - \hat{E}_n)/K$	J_n
1	2691.26	1481.97	1250.90	966.30	92518.26	82516.58	9
2	1809.03	174.58	53.56	43.58	4113.67	3735.17	10
3	7264.26	3168.27	990.61	863.17	88247.24	78928.17	7
4	7945.94	3466.89	1046.56	936.83	91206.44	83068.77	7
5	2668.41	702.74	692.60	640.75	62424.96	58440.71	9
6	2941.98	705.21	695.82	628.43	63431.90	58287.61	8
7	6792.03	4730.64	1288.18	1074.40	107694.98	93459.47	10
8	6889.13	4825.06	1278.58	1066.25	107974.41	93395.45	12
9	6735.87	4843.56	1263.84	1082.48	104242.00	92379.83	8
10	6753.82	4831.66	1239.29	1066.94	103261.02	91849.27	8
11	6803.58	4536.21	963.72	829.97	82876.62	72554.95	12
12	6741.22	4417.46	952.57	819.38	82150.98	72078.62	12
13	2764.63	656.64	651.39	648.71	60745.60	60513.30	3
14	2838.22	658.44	653.17	650.42	60512.62	60246.81	3
15	4825.25	3368.75	2381.92	2229.35	219913.26	208849.38	11
16	4200.15	3209.77	2060.28	1983.77	190155.56	183357.28	7
17	3198.10	2709.05	1406.51	1343.13	133491.45	128948.12	7
18	3161.05	2696.27	1409.20	1341.22	134005.83	129208.10	6
19	3257.38	2924.43	1851.81	1255.77	163301.99	113810.54	14
20	3254.33	2902.45	1860.31	1254.96	163562.44	113868.67	14
21	3292.76	2879.80	1218.62	1093.68	110181.05	100724.55	7
22	3265.87	2855.56	1205.39	1074.63	109775.26	99973.16	10
23	3075.05	2099.43	1380.11	961.93	120711.14	92436.31	13
24	3082.82	2091.63	1387.63	970.13	122617.89	93487.15	12
25	2021.66	1415.35	1195.78	926.76	102314.92	86497.21	4
26	2020.71	1416.42	1188.95	920.54	101675.86	86180.33	4

identity matrix and each W_i has zero mean. The W_i are found to be approximately normally distributed. The eigenvalues of \underline{C} are all of the same order of magnitude, except for the smallest, whose associated eigenvector makes an insignificant contribution to the total variance. Using standard pseudo-random number generators, identically independently normally distributed numbers \hat{W}_i with zero mean and unit variance can be obtained. Then perturbations may be generated of the form

$$(14) \quad \underline{E}^* = \underline{K}\hat{\underline{E}}' + \underline{K}\underline{P} \underline{\Delta} \hat{\underline{W}}$$

where $\hat{\underline{E}}'$ is obtained from the normalized regression equation (13).

Although we do not take it into account when generating the perturbations the W_i have some nonzero time lagged correlations. The magnitudes of the correlations of $W_i(t)$ and $W_j(t+nT)$ are all less than 0.3 for $n=1$ and all less than 0.2 for $n=2$. The largest correlations are found for $n=1$ and $i=j$; therefore most of the structure of the second order time lagged statistics could be taken into account by modeling each W_i as a first order Markov process.

Excluding time lagged statistics, the \underline{E}^* are expected to have statistics similar to the observed error statistics. By construction each \hat{W}_i is approximately normally distributed. Each W_i is observed to be approximately normally distributed. Agreement in means and covariances implies agreement in all contemporaneous statistics for two populations which are normally distributed. Since $\underline{P}\underline{\Delta}\underline{W}$ and $\underline{P}\underline{\Delta}\hat{\underline{W}}$ are linear combinations of \underline{W} and $\hat{\underline{W}}$ the statistics of the normalized residuals and the random part of the normalized perturbations are

approximately the same. The regression procedure implies that the normalized residuals and the \hat{E}' are virtually uncorrelated. (If the same predictors were used in each regression equation then $\underline{P} \wedge \underline{W}$ and \hat{E}' would be uncorrelated.) $\underline{P} \wedge \hat{W}$ and \hat{E}' are uncorrelated by construction, therefore \underline{E}/K and \underline{E}^*/K have the same means and covariances, if the sample is unchanged. Since the X'_j are not all normally distributed it is not necessary that \underline{E}/K and \underline{E}^*/K agree in all statistics. In any case, when the \underline{E}^* are used in a Monte Carlo simulation the sample will generally be altered. The above discussion suggests but given no assurance that the \underline{E} and \underline{E}^* will have similar statistical properties. If no normalization were used the first and second moment statistics of \underline{E} and the perturbations would agree but the variances of the perturbations would be independent of K . We feel the dependence of the variances of the E_i on K is an important property which should be mimicked by the perturbations.

7b. Adjustment to conserve energy invariants.

Straightforward use of the above \underline{E}^* yields unbounded solutions, since higher values of K are associated with larger perturbations and the perturbations may be a source of energy. In the experiments described below the perturbation procedure is forced to conserve the energy invariants. Besides yielding bounded solutions this is desirable since both PE and QG models nearly conserve the energy invariants for short prediction times. However, the error in predicting the energy invariants is not small because with the simple projection procedure used here, the path of the projection on the QG manifold of an adiabatic inviscid PE integration in general does not conserve the energy invariants.

However the error in predicting the changes in the energy invariants is relatively small and if a different projection procedure were used the error in predicting the energy invariants might also be small. Moreover, forcing the perturbations to conserve the energy invariants assures the correct qualitative behavior in the adiabatic inviscid limit.

In order to conserve the energy invariants it is sufficient to conserve three of them - in this case, K-S, σ_m^2 and θ_0 . First, the initial values $(K-S)_i$, $(\sigma_m^2)_i$ and $(\theta_0)_i$ are calculated. Then the model state is perturbed by adding \underline{E}^* to the model state vector. Now we seek the model state closest to the perturbed model state which has values of K-S, σ_m^2 and θ_0 identical to $(K-S)_i$, $(\sigma_m^2)_i$ and $(\theta_0)_i$ respectively. θ_0 is set equal to $(\theta_0)_i$; that is, θ_0 is not perturbed. We assume the perturbed value of σ_0 is correct and seek small adjustments, $\delta\psi_I$ and $\delta\tau_I$, to the perturbed variables, ψ_I and τ_I . That is, the adjusted model state prognostic vector is $(\sigma_0, (\theta_0)_i, \psi_I + \delta\psi_I, \tau_I + \delta\tau_I)^T$.

Now to minimize

$$D^2 \equiv \sum_I |\delta\psi_I|^2 + |\delta\tau_I|^2$$

subject to the constraints

$$G \equiv \frac{1}{2} \sum_I a_I^2 (|\psi_I + \delta\psi_I|^2 + |\tau_I + \delta\tau_I|^2) - \sigma_0 - (K-S)_i = 0$$

$$H \equiv \sum_I |\tau_I + \delta\tau_I|^2 + \sigma_0^2 - (\sigma_m^2)_i = 0$$

introduce the Lagrangian multipliers λ_1 and λ_2 and minimize $D^2 + \lambda_1 G + \lambda_2 H$. The conditions for an extremum are

$$2 \delta\psi_I + \lambda_1 a_I^2 (\psi_I + \delta\psi_I) = 0$$

$$2 \delta\tau_I + \lambda_1 a_I^2 (\tau_I + \delta\tau_I) + 2\lambda_2 (\tau_I + \delta\tau_I) = 0$$

Thus

$$\psi_I + \delta\psi_I = \psi_I (1 + \frac{\lambda_1}{2} a_I^2)^{-1} = \psi_I (1 - \frac{\lambda_1}{2} a_I^2 + O(\lambda_1^2))$$

$$(15) \quad \tau_I + \delta\tau_I = \tau_I (1 + \frac{\lambda_1}{2} a_I^2 + \lambda_2)^{-1} = \tau_I (1 - \frac{\lambda_1}{2} a_I^2 - \lambda_2 + O(\lambda_1^2, \lambda_1 \lambda_2, \lambda_2^2))$$

If the adjustments, $\delta\psi_I$ and $\delta\tau_I$, are small relative to ψ_I and τ_I then $\lambda_1 a_I^2/2$ and λ_2 must be small and the expressions for G and H may be linearized. This yields

$$\frac{1}{2} \lambda_1 \sum_I (a_I^2)^2 (|\psi_I|^2 + |\tau_I|^2) + \lambda_2 \sum_I a_I^2 |\tau_I|^2 = (K-S)_p - (K-S)_i$$

$$\lambda_1 \sum_I a_I^2 |\tau_I|^2 + 2 \lambda_2 \sum_I |\tau_I|^2 = (\sigma_m^2)_p - (\sigma_m^2)_i$$

where $(\sigma_m^2)_p$ and $(K-S)_p$ are the values of σ_m^2 and K-S for the perturbed model state. Solving these two linear equations gives an

approximate solution for λ_1 and λ_2 . Then (15) gives the adjusted model state. If λ_1 and λ_2 are small but not very small the procedure can be iterated replacing the perturbed model state by the adjusted model state just calculated. This will assure conservation of the energy invariants to any degree of accuracy and the final adjusted model state will be close (but not necessarily as close as possible) to the original perturbed model state. Since the perturbations are randomly generated anyway, this final adjusted model state is acceptable if the values of λ_1 and λ_2 obtained during the first iteration are small. If λ_1 and λ_2 are not small we conclude no model state having the correct energy invariants is close to the perturbed model state, discard the original perturbation as being dynamically improbable, generate a new perturbation and begin the adjustment procedure again.

7c. Perturbing the QG model and results.

In run PQG7 perturbations of the form (14) are added to the model state every $5f^{-1}$; the perturbed model state is then adjusted according to the above procedure. The perturbed model state is accepted if $|\lambda_2| \leq 0.2$ and the final adjusted model state is accepted if $|\lambda_2| \leq 0.002$. The size of λ_1 is not checked since in test cases it is always smaller than λ_2 by an order of magnitude or more. Of the perturbed model states generated during run PQG7 about 80% are acceptable; an average of 2.5 iterations are required to conserve the energy invariants. (There were never as many as 8 iterations of the adjustment process. 10^{-6} is the typical magnitude of the change in energy invariants caused by the perturbation procedure; very occasionally

changes of $O(10^{-5})$ are observed.) A test of the adiabatic inviscid form of the PQG model shows that this model conserves the energy invariants as well as does the PE model.

After the perturbations are adjusted the adjusted \hat{W}_i may be obtained by solving (14) with the adjusted perturbation replacing \underline{E}^* . It is found that the adjustment process does not appreciably alter the statistics of the \hat{W}_i , except for \hat{W}_1 and \hat{W}_{26} , associated with the largest and smallest eigenvalues respectively. Changes in the statistics of \hat{W}_{26} are presumably unimportant. The mean of the adjusted \hat{W}_1 is slightly negative and its variance is reduced by about 50%. The eigenvector associated with the largest eigenvalue is very nearly parallel to the $\text{Re } \tau_1$ axis. Since the regression equation for the prediction error of $\text{Re } \tau_1$ includes the term $+0.107K$, a plausible explanation of this phenomenon is that the adjustment process tends to cancel this additional forcing term.

Run PQG7 is actually divided into 6 segments. At the start of each segment the initial conditions are obtained from the final model state of the previous segment; the pseudo-random number generator is initialized with a number constructed from the time of day and the date. One segment ended abnormally when too many (15 in this case) perturbations were rejected for a single model state. The last part (approximately 2000 time units long) of this segment was discarded. The final model state of the retained part of this segment was used as the initial conditions for the next segment. No further difficulties occurred. As in the other runs, before statistics are collected the digital filter is applied to the data. At the times during the model run when perturbations are added, the model state is not uniquely defined. For the purpose of

continuing the integration the model state must be defined as the final adjusted model state. Throughout the calculations reported here this definition has been used. However, for the purpose of calculating time averages this is not the best choice and introduces errors in the averages of those quantities which on the average are increased or decreased substantially by the perturbation procedure.

On the basis of the T^2 and F^2 statistics the PQG model climate is much closer than the QG and TQG model climates to the PE model climate. The PQG model is nearly as successful as the BE model at simulating the PE climate. Comparing the statistics of run PQG7 to the statistics of run PE3, the most significant differences between the mean model states are that σ_0 and θ_0 are low by $15 \pm 0.9\%$ and $0.39 \pm 0.014\%$ respectively. Variances of σ_0 , θ_0 and the χ_I variables are too small roughly by a factor of two. The variances of the other model variables are in good agreement with the PE observations, considering that in the QG models θ and T are identical.

The agreement between the mean energy variables of runs PQG7 and PE3 is much better than the agreement of runs QG5 and PE3. However, there are still significant differences in the means of all the energy variables. Compared to the results of run PE3, the worst defects of the energetics of run PQG7 are that $\overline{A_Z}$ and $\overline{A_E}$ are too high by $32 \pm 2.7\%$ and $23 \pm 1.9\%$ respectively. As in the other comparisons this is principally because $\overline{\sigma_0}$ is too low and also because the variances of the θ_I variables are too high. The variances of the energy variables are somewhat improved relative to the unperturbed model.

For any budget calculation using PQG7 data the time averaged residual is $(-5f^{-1})$ times the average perturbation of the quantity for

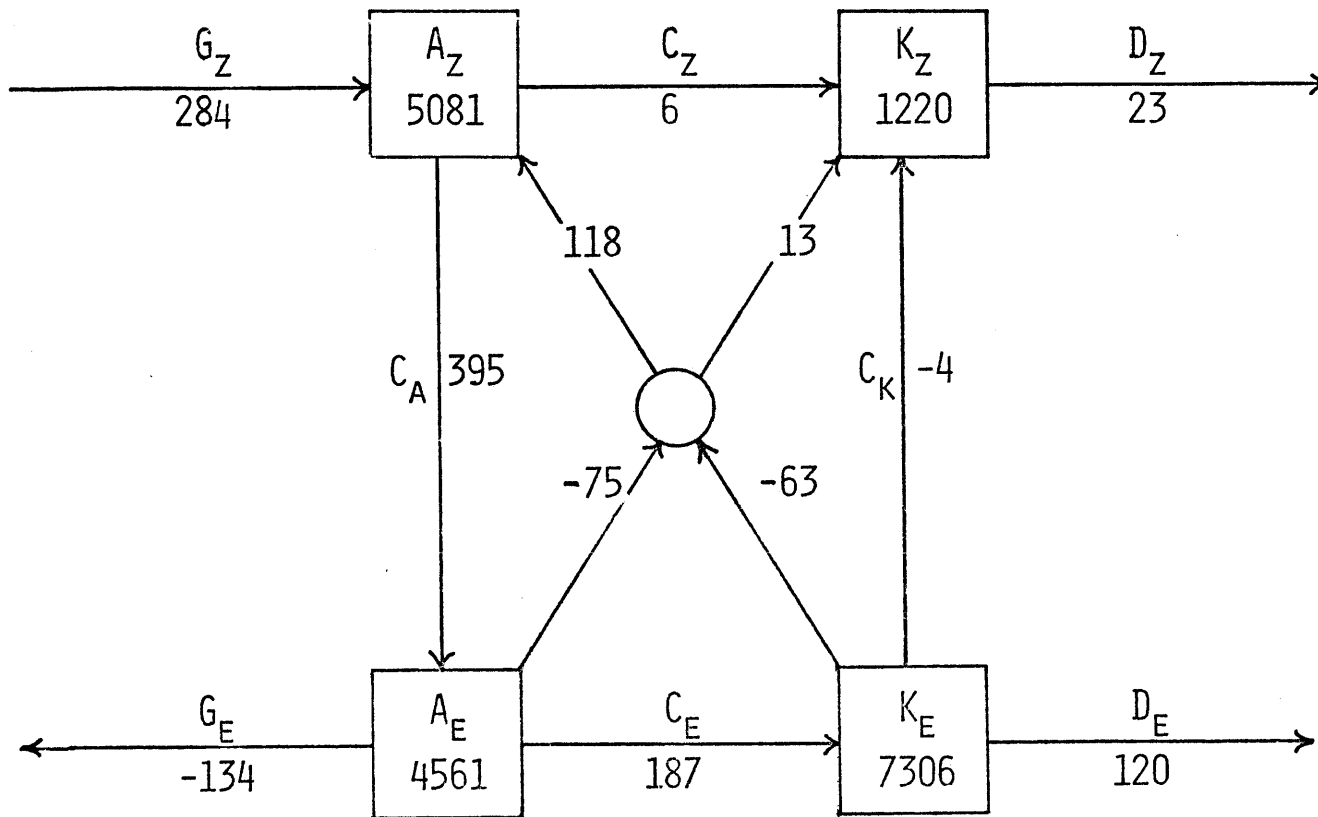


Figure 5. Energy budget ($\times 10^6$) of run PQG7. Sample length is 100000 time units.

which the budget is being calculated, neglecting the effects of sampling, filtering and the end points. By construction the perturbations do not affect $A+K$; therefore \bar{D} should be equal to \bar{G} and the effects of the perturbations may be thought of as conversions between the various forms of energy. The energy budget is displayed in Figure 5; the arrows in the center of the diagram represent the energy conversions due to the perturbations. In the mean the perturbations act to convert eddy to zonal and kinetic to available forms of energy. Presumably the net residual occurs because the averaged dissipation has been underestimated due to the way the model state has been defined at times during the model run when perturbations are added. If we force \bar{D} to be equal to \bar{G} the net residual is $O(10^{-6})$.

For the PQG model most of the budget constraints of Section 5 do not hold. In the budget for $\text{Re } \theta_1$ the radiation component is correct to within 2% of the PE value but the mean Jacobian term is 9% larger in magnitude than the PE value. The difference between these two terms balances the forcing by the perturbations. In the budgets for $\text{Re } \psi_1$ and $\text{Re } \tau_1$ the frictional terms are roughly 20% smaller in magnitude than the corresponding terms in the PE budgets. The transport terms are correct to roughly 10% of the PE values but the divergence term in the $\text{Re } \tau_1$ budget is too small by an order of magnitude.

8. Summary and concluding remarks.

We have examined the properties of several simple numerical models of the atmosphere, based on Lorenz's (1960) energy preserving model. The basic model is a two layer spectral PE model. The BE model is identical in all respects to the PE model except that the nonlinear balance assumption is made. The QG model is also identical to the PE model except that the linear balance assumption is made. Because the models are otherwise identical the effects of the balance assumptions are isolated.

For the sake of efficiency several compromises were made in developing these models. These compromises or approximations must be regarded as model deficiencies which inhibit the application of the results of this study to more complex systems. The model deficiencies are the simplified geometry, the low vertical resolution, the low horizontal resolution, the unrealistic vertical boundary conditions, the simplified friction and simplified zonal heating, the absence of horizontal variations of static stability and (in runs 3-7) the high thermal forcing. It is not claimed that these simple models are adequate representations of the real atmosphere; they are only prototypes for study. However the approximations are well motivated and internally consistent. Considering the model geometry, there are three plausible choices - a sphere, an infinite plane and a channel. We were unable to formulate (and do not believe there exists) a single set of energy preserving boundary conditions for all three systems of equations; therefore using any bounded domain would require differences in boundary conditions as well as differences in governing equations. More importantly the real atmosphere is unbounded. Spherical geometry is

rejected since the QG model is not valid at the equator. Thus the appropriate choice of geometry for comparing the different governing equations without extraneous influences is an infinite f-plane. Since Phillips' (1956) early experiment it has been known that two layer models can reproduce the basic features of the general circulation. If a two layer model is acceptable then a low order spectral model is sufficient because it is known that two layer models misrepresent the short waves. Given the low resolution the simplest physics seems reasonable. To a first approximation the real atmosphere is zonally heated. The use of a single independent variable to represent the static stability is a compromise between using a constant static stability and allowing the static stability to vary horizontally. A constant static stability would greatly change the system's energetics. Use of a temporally and horizontally varying static stability would require a parameterization of convection. In a few test cases where horizontal variations of static stability are allowed the model invariably develops a convectively unstable region near the equator (i.e., near $y = 0$). The high forcing yields a Rossby number which is not small, but this allows differences between the models to be more easily detected. On the one hand it is possible that the simplifications act to constrain the models' behavior so that their climates are necessarily similar. On the other hand it is possible that more complicated models with more degrees of freedom might be free to evolve to the same statistical state. That is, there is no doubt the simplifications constrain the models, but it is debatable whether the simplifications constrain the models to be more or less alike.

The models' evolutions are good prototypes of atmospheric behavior. The solutions are complex and aperiodic for appropriate choices of the

constants. For the nominal parameter values, two regimes which differ energetically may be identified. This is a type of almost intransitivity, since these regimes have long persistence times. As energies are integral quantities this behavior may be independent of horizontal resolution.

At low forcing ($\theta^* = 0.003$, $Ro \sim 0.11$) internal gravity waves in the PE solutions are present only as initial transient disturbances. At high forcing ($\theta^* = 0.032$, $Ro \sim 0.33$) internal gravity waves are always present in the PE solutions. (The Rossby number for this model may be defined by $Ro = 3.6 K^{\frac{1}{2}}$, where the typical wave number is taken to be 4.) Gravity waves cannot be forced by topography, by fronts, or by cumulus or meso scale processes, as these phenomena do not exist in the model. In the time mean sense the gravity waves obtain their energy from the synoptic scale waves and are frictionally dissipated.

We compared the climates of the models in terms of the first and second order statistics. Transports are reasonably well simulated by the QG model at both forcing levels. At the low level of forcing the QG model and at the high level of forcing the BE model are successful at simulating the PE mean states and energy cycles. At high forcing the QG model gives only a qualitatively correct simulation of the PE mean state and energy cycle. The filtered equations always tend to underestimate the time mean gross static stability observed in the PE model runs. The time mean energy flows are also underestimated as must be the case since for any given model run the energy flows are all constrained to be (approximately) proportional to the gross static stability. Since kinetic energy is observed to be roughly proportional to dissipation the time mean kinetic energy is also underestimated.

It is somewhat surprising that the QG model is so successful at the low level of forcing (which corresponds approximately to the level of forcing found in the earth's atmosphere). This may be due to one or more of the model deficiencies listed earlier. The other possibility is that the QG assumption is actually adequate for climate research but other effects limit current QG models in their ability to simulate the climate. Perhaps a QG model with comparable physics and resolution may give as good a simulation of the climate as current global circulation models. If for some purpose, low resolution and simplified physics are not objectionable serious consideration should be given to QG models.

At the high level of forcing we made two attempts to get better simulations of the PE climate within the QG framework - the tuned and perturbed quasigeostrophic models. These models are both more successful than the original QG model at simulating the PE climate.

Both the tuning procedure and the perturbation procedure require some knowledge of the short term ($5f^{-1}$) prediction errors caused by the QG assumption. One might argue that tuning models for the purpose of simulation studies is a futile exercise since any procedure based on observations is strictly valid only for present "external" conditions. However, current observations, especially considering seasonal variations, span different "external" conditions. Second "external" is nearly equivalent in meaning to "having a large scale separation" (Leith, 1978b); if the process causing errors has short time or space scales current observations do embrace a variety of external conditions. Third, objective comparisons of different models must be based on their ability to reproduce current conditions. To be fair, the models should first be optimally tuned. The first two points also apply to perturbing models.

As far as the perturbation procedure is concerned we may in some situations have theoretical knowledge of the order of the magnitudes of the errors involved over the short time scale. These theoretical estimates will in general depend on the external parameters and we may use this knowledge for other than current conditions.

In the experiments reported here although the observing system is perfect the initialization and forecast verification procedures used in determining the prediction errors are open to question. In brief, gravity waves are eliminated by low pass filtering and then each PE observation is projected onto the QG solution space by replacing the values of θ and χ by their geostrophically determined diagnostic values. Filtering is justified since the QG and BE models cannot simulate gravity waves. The projection procedure is arbitrary.

The tuning procedure described in Section 6 is quite general; it is actually a particular form of least squares estimation. We have tuned the QG model to minimize the average squared short term ($5f^{-1}$) prediction errors. (This criterion is somewhat arbitrary; other criteria defining the optimal QG model might be considered.) The tuned QG model is better than the untuned version at simulating the PE time mean model state, but the simulated energy cycle and the budgets maintaining the mean state are not improved at all.

In the perturbed QG model randomly generated perturbations are added to the model state every $5f^{-1}$. These perturbations are designed so that their statistics, other than those involving time lags, are very similar to the statistics of the observed prediction errors. An important statistical feature of both perturbations and prediction errors is that their variances are proportional to the square of the model's kinetic energy.

The perturbations are adjusted to conserve the energy invariants of the system thereby ensuring bounded solutions. The perturbed QG model is nearly as successful as the BE model at simulating the PE climate. This procedure is economical; once the statistics of the errors are known the additional computer time needed to generate the perturbations is small relative to the computer time necessary for the time marching procedure.

Although we are concerned here with climate simulation models the tuning and perturbation procedures can be applied to numerical weather prediction models. The tuning procedure offers an objective way of choosing empirical constants once a scoring rule is defined. Tuning of operational models is probably possible with currently available data. If one chooses just a subset of the observations which are truly independent then the computations should not be too burdensome and would only have to be done once for each model (modification). The major stumbling block is that current initialization procedures depend on the previous forecast so that several forecast analysis cycles would be needed prior to each "initial" condition. The perturbation technique can easily be incorporated into a Monte Carlo stochastic dynamical prediction model. (Fleming (1972) and Pitcher (1977) have already accomplished the more difficult task of incorporating stochastic forcing into stochastic dynamical prediction models which directly forecast the statistical moments.) It seems however that as computer resources increase the complexity of numerical models increases apace, so that operational Monte Carlo prediction models may never be economical.

REFERENCES

- Charney, J. G., 1947: The dynamics of long waves in a baroclinic westerly current. J. Meteorol., 4, 135-162.
- Charney, J. G., 1948: On the scale of atmospheric motions. Geofysiske Publikasjoner (Norway), 18, No. 2, 17 pp.
- Derome, J., and C. L. Dolph, 1970: Three-dimensional non-geostrophic disturbances in a baroclinic zonal flow. Geophys. Fluid Dyn., 1, 91-122.
- Efroymsen, M. A., 1960: Multiple regression analysis. In Mathematical Methods for Digital Computers, A. Ralston and H. S. Wilf, editors, John Wiley & Sons, New York, 191-203.
- Faller, A. J. and D. K. Lee, 1975: Statistical corrections to numerical prediction equations. Mon. Weather Rev., 103, 845-855.
- Faller, A. J., and C. E. Schemm, 1977: Statistical corrections to numerical prediction equations. II. Mon. Weather Rev., 105, 37-56.
- Fleming, R. J., 1972: Predictability with and without the influence of random external forces. J. Appl. Meteorol., 11, 1155-1163.
- Flierl, G. R., 1978: Models of vertical structure and the calibration of two-layer models. Dyn. Atmos. Oceans, 2, 341-381.
- Fraedrich, K., 1978: Structural and stochastic analysis of a zero-dimensional climate system. Q. J. R. Meteorol. Soc., 104, 461-474.
- Frankignoul, C. and K. Hasselmann, 1977: Stochastic climate models, part 2. Application to sea surface temperature anomalies and thermocline variability. Tellus, 29, 289-305.
- Frankignoul, C. and P. Müller, 1979: Quasi-geostrophic response of an infinite β -plane ocean to stochastic forcing by the atmosphere. J. Phys. Oceanogr., 9, 104-127.
- Fullmer, J. W. A., 1979: The baroclinic instability of simple and highly structured one-dimensional basic states. Ph.D. dissertation, M.I.T., Cambridge, Mass., 236 pp.
- Gall, R. L., 1976a: A comparison of linear baroclinic instability theory with the eddy statistics of a general circulation model. J. Atmos. Sci., 33, 349-373.

- Gall, R. L., 1976b: Structural changes of growing baroclinic waves. J. Atmos. Sci., 33, 374-390.
- Gall, R., 1976c: The effects of released latent heat in growing baroclinic waves. J. Atmos. Sci., 33, 1686-1701.
- Gall, R., 1977: Some non-quasigeostrophic effects in linear baroclinic waves. Mon. Weather Rev., 105, 1039-1051.
- Gall, R. and R. Blakeslee, 1977: Comments on "A note on the wavelength of maximum growth rate for baroclinic instability." J. Atmos. Sci., 34, 1479-1480.
- Geisler, J. E. and R. R. Garcia, 1977: Baroclinic instability at long wavelengths on a β -plane. J. Atmos. Sci., 34, 311-321.
- Haltiner, G. J. and R. T. Williams, 1975: Some recent advances in numerical weather prediction. Mon. Weather Rev., 103, 571-590.
- Hartjenstein, G., and J. Egger, 1979: Linear parameterization of large-scale eddy transports. Tellus, 31, 89-101.
- Hasselmann, K., 1976: Stochastic climate models, part 1. Theory. Tellus, 28, 473-485.
- Heck, W. J., 1979: An observational test of the quasi-geostrophic relation between eddy momentum flux convergence and eddy fluxes of potential vorticity and potential temperature. J. Atmos. Sci., 36, 785-791.
- Hollingsworth, A., 1975: Baroclinic instability of a simple flow on the sphere. Q. J. R. Meteorol. Soc., 101, 495-528.
- Kaiser, J. F., 1974: Nonrecursive digital filter design using the I_0 -sinh window function. Proc. 1974 IEEE Int. Symp. on Circuits and Syst., April 22-25, 1974, 20-23. (This paper is reprinted in Selected Papers in Digital Signal Processing, II, IEEE Digital Signal Processing Committee, 1976, pp 123-126.)
- Klein, W. H., and H. R. Glahn, 1974: Forecasting local weather by means of model output statistics. Bull. Am. Meteorol. Soc., 55, 1217-1227.
- Laurmann, J. A., and W. L. Gates, 1977: Statistical considerations in the evaluation of climatic experiments with atmospheric general circulation models. J. Atmos. Sci., 34, 1187-1199.
- Leith, C. E., 1974a: Theoretical skill of Monte Carlo forecasts. Mon. Weather Rev., 102, 409-418.

- Leith, C. E., 1974b: Spectral statistical-dynamical forecast experiments. In Report of the International Symposium on Spectral Methods in Numerical Weather Prediction, Copenhagen, 12-16 August 1974. GARP Working Group on Numerical Experimentation, Report no. 7, December 1974, 445-467.
- Leith, C. E., 1975: Numerical weather prediction. Rev. Geophys. Space Phys., 13, 681-684, 799-800.
- Leith, C. E., 1978a: Objective methods for weather prediction. Annu. Rev. Fluid Mech., 10, 107-128.
- Leith, C. E., 1978b: Predictability of climate. Nature, 276, 352-355.
- Lemke, P., 1977: Stochastic climate models, part 3. Application to zonally averaged energy models. Tellus, 29, 385-392.
- Lorenz, E. N., 1951: Computations of the balance of angular momentum and the poleward transport of heat. Sci. Report No. 6, M.I.T. General Circulation Project, Contract No. AF19(122)-53. (Reprinted in Starr, V. P., and B. Saltzman, compilers, 1966: Observational studies of the atmospheric general circulation, Sci. Report No. 2, Planetary Circulations Project, M.I.T., Cambridge, Mass., pp 32-65.)
- Lorenz, E. N., 1960: Energy and numerical weather prediction. Tellus, 12, 364-373.
- Lorenz, E. N., 1962: Simplified dynamic equations applied to the rotating-basin experiments. J. Atmos. Sci., 19, 39-51.
- Lorenz, E. N., 1963a: Simplified dynamical equations and their use in the study of atmospheric predictability. Final report, Statistical Forecasting Project M.I.T., Cambridge, Mass., Contract No. AF19(604)-4969, 121 pp.
- Lorenz, E. N., 1963b: The mechanics of vacillation. J. Atmos. Sci., 20, 448-464.
- Lorenz, E. N., 1970: Climatic change as a mathematical problem. J. Appl. Meteorol., 9, 325-329.
- Lorenz, E. N., 1971: An N-cycle time-differencing scheme for stepwise numerical integration. Mon. Weather Rev., 99, 644-648.
- Lorenz, E. N., 1977: An experiment in nonlinear statistical weather forecasting. Mon. Weather Rev., 105, 590-602.

- Mak, M., 1977: On the nongeostrophic baroclinic instability problem. J. Atmos. Sci., 34, 991-1006.
- Manabe, S., J. Smagorinsky, J. L. Holloway, Jr., and H. M. Stone, 1970: Simulated climatology of a general circulation model with a hydrological cycle: III. Effects of increased horizontal computational resolution. Mon. Weather Rev., 98, 175-212.
- Manabe, S. and T. B. Terpstra, 1974: The effects of mountains on the general circulation of the atmosphere as identified by numerical experiments. J. Atmos. Sci., 31, 3-42.
- Manabe, S., and R. T. Wetherald, 1975: The effects of doubling the CO₂ concentration on the climate of a general circulation model. J. Atmos. Sci., 32, 3-15.
- Olbers, D. J., P. Müller and J. Willebrand, 1976: Inverse technique analysis of a large data set. Phys. Earth Planet. Inter., 12, 248-252.
- Oort, A. H., 1964: On estimates of the atmospheric energy cycle. Mon. Weather Rev., 92, 483-493.
- Phillips, N. A., 1956: The general circulation of the atmosphere: a numerical experiment. Q. J. R. Meteorol. Soc., 82, 123-164.
- Phillips, N. A., 1963: Geostrophic motion. Rev. Geophys., 1, 123-176.
- Pitcher, E. J., 1977: Application of stochastic dynamic prediction to real data. J. Atmos. Sci., 34, 3-21.
- Reynolds, R. W., 1978: Sea surface temperature anomalies in the North Pacific Ocean. Tellus, 30, 97-103.
- Robock, A., 1978: Internally and externally caused climate change. J. Atmos. Sci., 35, 1111-1122.
- Saltzman, B., and C-M. Tang, 1975: Analytical study of the evolution of an amplifying baroclinic wave: part II. Vertical motions and transport properties. J. Atmos. Sci., 32, 243-259.
- Schemm, C. E., and A. J. Faller, 1977: A note on the statistical correction of prediction equations. Mon. Weather Rev., 105, 1473-1477.
- Sellers, W. D., 1973: A new global climatic model. J. Appl. Meteorol., 12, 241-254.
- Semtner, A. J., and W. R. Holland, 1978: Intercomparison of quasigeostrophic simulations of the western North Atlantic circulation with primitive equations results. J. Phys. Oceanogr., 8, 735-754.

- Simmons, A. J. and B. J. Hoskins, 1976: Baroclinic instability on the sphere: normal modes of the primitive and quasi-geostrophic equations. J. Atmos. Sci., 33, 1454-1477.
- Simmons, A. J., and B. J. Hoskins, 1977a: Baroclinic instability on the sphere: solutions with a more realistic tropopause. J. Atmos. Sci., 34, 581-588.
- Simmons, A. J., and B. J. Hoskins, 1977b: A note on the wavelength of maximum growth rate for baroclinic instability. J. Atmos. Sci., 34, 1477-1478.
- Simmons, A. J., and B. J. Hoskins, 1978: The life cycles of some nonlinear baroclinic waves. J. Atmos. Sci., 35, 414-432.
- Simons, T. J., 1972: The nonlinear dynamics of cyclone waves. J. Atmos. Sci., 29, 38-52.
- Staley, D. O., and R. L. Gall, 1977: On the wavelength of maximum baroclinic instability. J. Atmos. Sci., 34, 1679-1688.
- Stone, P. H., 1972: On non-geostrophic baroclinic instability, part III. The momentum and heat transports. J. Atmos. Sci., 29, 419-426.
- Stone, P. H., 1978: Baroclinic adjustment. J. Atmos. Sci., 35, 561-571.
- Thompson, P. D., 1957: Uncertainty of initial state as a factor in the predictability of large scale atmospheric flow patterns. Tellus, 9, 275-295.
- Trenberth, K. E., and A. A. Neale, 1977: Numerical weather prediction in New Zealand. Mon. Weather Rev., 105, 817-825.
- Warn, H., 1976: Baroclinically unstable modes of a two-layer model on the sphere. J. Atmos. Sci., 33, 1478-1498.
- Wetherald, R. T., and S. Manabe, 1975: The effects of changing the solar constant on the climate of a general circulation model. J. Atmos. Sci., 32, 2044-2059.
- Williams, G. P., 1978: Planetary circulations: 1. Barotropic representation of Jovian and terrestrial turbulence. J. Atmos. Sci., 35, 1399-1426.

Acknowledgments.

I thank Professor Lorenz for his help and encouragement during the course of this work. I am indebted to previous workers, many of whom are listed in the references; I have been particularly influenced by the writings of R. Gall, C. E. Leith and E. N. Lorenz.

This work was supported by National Science Foundation Grant NSF-g 77 10093ATM.

Production: This manuscript was typed by V. I. Mills. The figures were drafted by J. Hoffman.